Combined use of Sentinel 1 and Sentinel 2 for urban land cover mapping using Google Earth Engine in the case of Adama City, Ethiopia.

Taresa Chamada Mulata

Thesis submitted to the Department of Architecture

College of Civil Engineering and Architecture (SOCEA),

Office of Graduate Studies

Adama Science and Technology University

June, 2025

Adama, Ethiopia

Combined use of Sentinel 1 and Sentinel 2 for urban land cover mapping using Google Earth Engine in the case of Adama City, Ethiopia.

Taresa Chamada Mulata

Under the Supervision of

Temesgen Abraham (Phd)

Thesis submitted to the Department of Architecture

College of Civil Engineering and Architecture (SOCEA),

Office of Graduate Studies

Adama Science and Technology University

June, 2025

Adama, Ethiopia

DECLARATION

I hereby declare that this research entitled "**Combined use of Sentinel 1 and Sentinel 2 for Urban Land Cover Mapping using Google Earth Engine in the Case of Adama City, Ethiopia."** is my original work. That is, it has not been submitted to any other university. All materials used for this thesis have been duly acknowledged through citation.

Taresa Chamada Mulata ______________________ _______________

Name of student Signature Date

RECOMMENDATION

I, the advisor of this thesis, hereby certify that I have read this thesis entitled "**Combined use of Sentinel 1 and Sentinel 2 for urban land cover mapping using Google Earth Engine in the case of Adama City, Ethiopia."** prepared under my guidance by Taresa Chamada Mulata. Therefore, I recommend the submission to the department following the applicable procedures.

Temesgen Abraham (PhD)	________________	________________
Name of Major Advisor	Signature	Date

APPROVAL PAGE OF THE THESIS

I, the advisor of this thesis entitled "**Combined use of Sentinel 1 and Sentinel 2 for Urban Land Cover Mapping using Google Earth Engine in the Case of Adama City, Ethiopia.**" developed by Taresa Chamada Mulata hereby certify that the recommendation and suggestions made by the board of examiners are appropriately incorporated into the final version of the thesis.

____________________	____________________	____________________
Major Advisor	Signature	Date

We, the undersigned, members of the Board of Examiners of the thesis by Taresa Chamada Mulata have read and evaluated the thesis entitled "**Combined use of Sentinel 1 and Sentinel 2 for Urban Land Cover Mapping using Google Earth Engine in the Case of Adama City, Ethiopia.**" and examined the candidate during open defense. This is, therefore, to certify that the thesis is accepted for public defence.

____________________	____________________	____________________
Chairperson	Signature	Date
____________________	____________________	____________________
Reviewer 1	Signature	Date
____________________	____________________	____________________
Reviewer 2	Signature	Date

Final approval and acceptance of the thesis is contingent upon submission of its final copy to the Office of Postgraduate Studies (OPGS) through the Department Graduate Council (DGC) and College Graduate Committee (CGC).

____________________	____________________	____________________
Department Head	Signature	Date
____________________	____________________	____________________
College Dean	Signature	Date
____________________	____________________	____________________
Office of Postgraduate Studies, Dean	Signature	Date

Table of Contents

LIST OF TABLES

LIST OF FIGURES

ACRONYMS AND ABBREVIATION

Acronym	Meaning
SAR	Synthetic Aperture Radar
MSI	Multispectral Instrument
GEE	Google Earth Engine
RF	Random Forest
SVM	Support Vector Machine
NDVI	Normalized Difference Vegetation Index
NDBI	Normalized Difference Built-Up Index
OA	Overall Accuracy
PA	Producer's Accuracy
UA	User Accuracy
ETB	Ethiopian Birr
SWIR	Short-Wave Infrared
NIR	Near-Infrared
OBIA	Object-Based Image Analysis
CNNs	Convolutional Neural Networks
DCD	Differential Change Detection
DEMs	Digital Elevation Models

Abstract

Urban land cover mapping plays a vital role in understanding urbanization patterns and their associated environmental consequences. This study investigated the effectiveness of combining Sentinel-1 Synthetic Aperture Radar (SAR) and Sentinel-2 Multispectral Instrument (MSI) satellite data for urban land cover classification in Adama City, Ethiopia, utilizing the capabilities of Google Earth Engine (GEE). The primary objectives included classifying urban land cover types, detecting changes in land cover between 2015 and 2025, and assessing the classification performance of two machine learning algorithms Support Vector Machine (SVM) and Random Forest (RF). The study employed GEE for efficient data access, preprocessing, and analysis. Preprocessing procedures included radiometric and geometric corrections, cloud masking, and image stacking. Classification was conducted using SVM and RF, and a subsequent change detection analysis was carried out to track land cover transformation over the ten-year period. Results indicated substantial land cover changes in Adama City. Built-up areas expanded by 219.37%, growing from 1,679.38 hectares in 2015 to 5,364.57 hectares in 2025, reflecting rapid urban development. Agricultural land experienced a slight decline of 2.33%, decreasing from 21,742.77 hectares to 21,235.69 hectares, likely due to conversion into urban zones. Forest areas saw a significant reduction of 50.61%, dropping from 5,201.93 hectares to 2,569.65 hectares, pointing to accelerated deforestation. Similarly, shrubland decreased by 32.75%, while bareland increased dramatically by 346.18%, rising from 87.58 hectares to 390.83 hectares. In terms of classification accuracy, the SVM algorithm yielded better results for Sentinel-2 MSI data, achieving an overall accuracy (OA) of 83% and a Kappa coefficient of 0.78, compared to RF's OA of 74% and Kappa of 0.67. For Sentinel-1 SAR, RF outperformed SVM with an OA of 85% and a Kappa of 0.81, while SVM reached an OA of 75% and Kappa of 0.68. When the datasets were combined, RF again showed stronger performance (OA = 83%) compared to SVM (OA = 77%), illustrating the benefits of data fusion for urban land cover classification. These findings demonstrate the potential of integrating radar and optical satellite data for enhanced urban monitoring and planning. The study recommends incorporating additional data sources and employing more advanced machine learning methods to further improve classification precision and support sustainable urban development in rapidly expanding cities.

Keywords: Sentinel-1, Sentinel-2, Google Earth Engine, Random Forest, Support Vector Machine.

CHAPTER ONE

1. INTRODUCTION

1.1.Background of the study

Urban land cover mapping is essential to effective urban planning (Lv et al., 2015; Van de Voorde et al., 2011). The information is essential to city planners in decision-making on zoning, infrastructure development, and resource allocation (Faehnle et al., 2014; Grêt-Regamey et al., 2017). Land cover maps may be applied to identify land appropriate for residential, commercial, industrial, and recreational purposes and thereby facilitate planned urban development as well as prevention against urban sprawl (Avelar et al., 2009; Herold et al., 2003a; Maclachlan et al., 2017). Urban land cover mapping plays a significant role in environmental management as it makes it possible to monitor and manage the impacts of urbanization on natural resources (Bajocco et al., 2012; Yin et al., 2011). Sound land cover maps can be used to estimate urban green cover, water bodies, and imperviousness, which are also important factors in mitigating urban heat islands, flood hazard, and biodiversity conservation (Gunawardena et al., 2017; Morabito et al., 2021; Weng, 2012a). They also need to track land cover changes over time because this is where the ability to detect trends and possible environmental issues comes in (Gong et al., 2013; Hansen & Loveland, 2012; Li & Shao, 2014).

Urban land cover mapping provides data that can be used to evaluate whether urbanization is sustainable (Dewan & Yamaguchi, 2009a; Schneider, 2012a). Depending on the area and diversity of land cover, policymakers can develop policies for supporting effective, green, and resilient cities (Abass et al., 2019; Carter et al., 2015). These include promoting green infrastructure development, improving public transport infrastructure, and urban natural ecosystems conservation (Seto et al., 2012). Traditional urban land cover mapping procedures such as field surveys and aerial photograph manual interpretation take a lot of time and involve much labor (Cleve et al., 2008; Y. Hu et al., 2018; Mboga et al., 2020). These methods are time-intensive and require significant human effort and capability to obtain, inspect, and interpret data and are thus inefficient for big or dynamically changing maps (Ma et al., 2015; Schadt et al., 2010; Sivarajah et al., 2017). Manual mapping also has the risk of producing different and subjective maps due to the different interpretations made by diverse analysts (Diesing et al., 2014; Singh & Frazier, 2018). This discrepancy can have an effect on the reliability and precision of the land cover maps and therefore, by extension, urban planning and environment management choices (Grafius et al., 2016; Olofsson & Ohman, 2006; Verburg et al., 2011).

Remote sensing, or gathering data on an object without coming into contact with it, is a critical component in the study of cities as it is able to make repeated measurements timely and accurately across extensive areas (Wurm et al., 2011; Esch et al., 2020). Remote sensing supports urban planning, environmental surveillance, and disaster management through the capacity to generate precise maps, identify changes, and measure environmental characteristics (Boulos et al., 2011; Khan et al., 2017). Remote sensing has historically developed from its nascent stages using aerial photography to the launch of Landsat satellites in the 1970s to provide the first persistent world record of the Earth's surface (Goetz, 2009). There has been improvement in satellites with high resolution, multispectral and hyperspectral imaging, as well as Synthetic Aperture Radar (SAR) technology, which collects data regardless of weather (Ottinger & Kuenzer, 2020; Ouma, 2016). Harmonization of remote sensing data and Geographic Information Systems (GIS) and cloud computing platforms like Google Earth Engine has also revolutionized urban analysis to become less time-consuming and more accessible (Gorelick et al., 2017; Parece & Campbell, 2015; Richards, 2009).

Google Earth Engine (GEE) is a cloud-based geospatial big computing platform with access to a vast repository of remote sensing data and large computation (Tamiminia et al., 2020; Wang et al., 2020). With the use of the cloud infrastructure provided by Google, GEE processes and analyzes big data sets like time-series analysis, environmental monitoring, and urban planning effectively (Amani et al., 2020; Cao et al., 2020). The infrastructure provides an interactive code editor that is JavaScript and Python-supported, thus simplifying complex workflow development (Yang et al., 2022). GEE provides reproducible, collaborative research through script and dataset sharing and is readily compatible with other Google products for enhanced data management and analysis (Gorelick et al., 2017). GEE has a cost-effective, open solution for intricate geospatial analysis. Hence, the primary goal of this research work is to analyze land cover dynamics change in Adama city by integrating sentinel 1 and sentinel 2 imagery in GEE cloud computing platform.

1.2.Statement of the problem

Sentinel-1 and Sentinel-2 satellite images have been valuable assets to many fields of science due to their widespread uses. Sentinel-2 MSI imagery, for example, has been applied in large-scale research such as detection of burnt areas, hydrothermal alteration mapping caused by mineralization, landslide hazard mapping, and mangrove cover demarcation (Hu et al., 2018; Huang et al., 2016; Roteta et al., 2019; Wang et al., 2018). These optical data have also been utilized to map urban land cover. One among the modern-day challenges, however, is that dark impervious surfaces and water are spectrally indistinguishable from one another in spectral imagery and therefore readily confused. This confusion has been as cities' cover such as asphalt roadways or rooftops incorrectly being classified as water (Zhang et al., 2018).

In contrast, Sentinel-1 SAR data are useful in a variety of applications including land use maps, flood maps, estimation of soil moisture content, and estimation of crop yields for crops like rice (Balzter et al., 2015; Bao et al., 2018; Ruzza et al., 2019). Since SAR data are not affected by atmospheric conditions like fog or cloud, it can be a suitable backup in case Sentinel-2 optical data are unavailable or highly degraded. Despite this advantage, cities offer classification challenges due to structural heterogeneity and complex surface materials. In attempting to improve mapping accuracy, researchers have increasingly relied on data fusion methods that merge Sentinel-1 SAR and Sentinel-2 MSI, which results in higher performance in specific applications such as detection of vegetation type, mangrove biomass quantification, and burned area identification (Castillo et al., 2017; Colson et al., 2018; Erinjery et al., 2018). The complementarity of the data optical and radar is that greater understanding of the terrain is provided, to the degree that that builds confidence in analysis results (Mahdianpari et al., 2019).

Empirical observation has already observed that a combination of SAR and optical images tends to generate greater classification accuracy in land cover maps (Walker et al., 2010; Weng, 2012b). Urban areas—and by extension their peculiar problems—have not, nonetheless, dominated the focus of most fusion-based studies. Particularly, there is scant in-depth research evaluating Sentinel-1 and Sentinel-2 mosaicking performance for urban land cover mapping. Examining this Sentinel-1 and Sentinel-2 mosaicking under the urban environment, where traditional methods do not work, can be highly enlightening and lead to stronger and more accurate mapping techniques.

Google Earth Engine (GEE) is now a strong cloud platform to process large-area images, merge, classify, and visualize remote sensing images like Sentinel-1 and Sentinel-2 data (Vizzari, 2022). With GEE, users have a convenient means to conduct such fundamental preprocessing operations like noise reduction, geometric correction, and radiometric normalization for large data. Its ability to combine radar and optical imagery gives the user a broader view of surface features, which offsets the constraints that result from the use of one data source (Tassi & Vizzari, 2020). Besides, the comprehensive support by GEE for various classification algorithms makes advanced applications such as change detection, land cover mapping, and time-series analysis much easier, thus making it an incredibly valuable tool for scientists studying environment and urban dynamics (Gomes et al., 2020).

Random Forest (RF) and Support Vector Machine (SVM) machine learning algorithms are conventional methods being used for image classification operations in typical desktop environments (Pal et al., 2013a). Executing the algorithms on the GEE platform is an approach toward handling large datasets in an efficient way with reduced processing time and scalability. But their performance in deriving persistent urban land cover maps from Sentinel-1 and Sentinel-2 data fusion, particularly in the case of Adama City, Ethiopia, remains to be rigorously evaluated.

While some potential has been exhibited in using the fusion of satellite optical and radar data to enhance environmental classification accuracy in different applications, there is an unclear research gap in how it can enable improved urban land cover mapping. This is particularly crucial in complex urban environments, where misclassificiation issues like confusing water bodies with dark surfaces are typical. Aside from this, an analysis of SVM and RF functionality in the GEE platform for such a purpose remains to be done. This study intends to fill this gap by assessing the potential of Sentinel-1 and Sentinel-2 data fusion enhanced with machine learning algorithms in enhancing Adama City urban land cover mapping.

1.3.Objective

1.3.1. General Objective

The main objective of this study is to develop an accurate and efficient urban land cover mapping for Adama City, Ethiopia, by integrating Sentinel 1 (SAR) and Sentinel 2 (optical) satellite data using Google Earth Engine.

1.3.2. Specific objectives

This research was aspired to answer the following specific objectives;

This research aims to achieve the following specific objectives:

- Perform urban land cover classification using Sentinel-2 and Sentinel-1A data with RF and SVM algorithms.
- Integrate and classify fused Sentinel-2 and Sentinel-1A data for improved mapping.
- Compare the performance of RF and SVM using optical, radar, and fused datasets.
- To analyze land cover changes in Adama City over a ten-year period, between 2015 and 2025.

1.4.Research questions

- How accurately can Sentinel-2 MSI and Sentinel-1A SAR data independently classify urban land cover using Random Forest (RF) and Support Vector Machine (SVM) algorithms?
- What is the impact of fusing Sentinel-2 MSI and Sentinel-1A SAR data on urban land cover classification accuracy?
- How do the RF and SVM algorithms perform individually and in combination when applied to optical, radar, and fused datasets for urban land cover classification?
- What are the major land cover changes that occurred in Adama City between 2015 and 2025?

1.5.Significance of the study

This research is of high relevance in that it seeks to enhance urban land cover mapping in Adama City, Ethiopia, through the synergistic advantage of Sentinel-1 SAR and Sentinel-2 MSI satellite imagery in the Google Earth Engine (GEE) platform. Through the implementation of RF and SVM this study aims at determining the best technique to classify urban land cover from radar and optical data. The outcomes are expected to aid in the derivation of stronger remote sensing techniques and aid in efficient decision-making for urban planning settings.

1.6.Organization of the Thesis

There are five chapters in the thesis, and all utilize the Google Earth Engine platform to synchronize Sentinel-1 (SAR) and Sentinel-2 (optical) satellite data to provide an accurate and effective urban land cover mapping technique for Adama City, Ethiopia.

Introduction to the history of the study, research problem, objectives, significance, scope, and methods is given in Chapter One. An outline of the structure of the thesis is also given. In order to present the theoretical and empirical background for the current work, Chapter Two is devoted to literature review, where research on land cover classification, use of SAR and optical satellite imagery, data fusion techniques, and cloud-based remote sensing platforms is addressed.

Chapter Three introduces the study materials and techniques. It involves a detailed description of the study site, character of the satellite imagery (Sentinel-1 and Sentinel-2), data preprocessing process, the adopted classification approach in Google Earth Engine, and accuracy assessment techniques.

Chapter Four provides the result of the classification of urban land cover and presents a detailed description of the result. This includes quantifying the accuracy of the classification, the impact of the SAR and optical data combination, and comparison with the result of previous studies. Chapter Five concludes the thesis by expounding the key findings, reflecting on the research objectives, and proposing recommendations in urban land management and future research papers.

1.7.Operational terms of definition

Urban Land Cover Mapping: Detection and classification of various land cover elements of an urban site, such as buildings, roads, plants, and water bodies, using satellite information and classification methods (Zhang et al., 2018; Mahdianpari et al., 2019).

Data Fusion: Fusing Sentinel-1 SAR and Sentinel-2 MSI data to take advantage of their complementing strengths. In order to boost the precision of land cover classification, SAR is used for structural and textural details and MSI for spectral details (Walker et al., 2010; Weng, 2012b).

Google Earth Engine (GEE): Cloud-based software for processing and analyzing satellite images of large-scale images is provided. Sentinel-1 and Sentinel-2 data were merged, preprocessed, classified, and visualized using GEE to map urban land cover (Gomes et al., 2020; Tassi & Vizzari, 2020).

Support Vector Machine (SVM): For classification issues, a supervised machine learning method is applied. It works by seeking the best hyperplane within the feature space to distinguish among multiple classes (Pal et al., 2013a).

Random Forest (RF): A supervised learning algorithm using an ensemble of decision trees to classify data. It is renowned for its accuracy and stability when dealing with high-dimensional data, e.g., satellite images (Pal et al., 2013a).

Classification Accuracy: A comparison measure between reference and the classification algorithm (SVM or RF) accuracy in identifying land cover classes. Performance was evaluated using metrics such as the Kappa coefficient, user and producer accuracy, and overall accuracy (Mahdianpari et al., 2019).

Dark Impervious Surfaces: Difficult-to-classify urban structures include asphalt roads and light-absorbing rooftops that are optically confusing with water in optical images (H. Zhang et al., 2018).

CHAPTER TWO

2. LITERATURE REVIEW

2.1.Introduction to urban land cover mapping

Urban land cover mapping is a critical tool for understanding and management of urbanisation trends (Solórzano et al., 2021a). As urban populations expand exponentially, mainly in the Third World, there is mounting pressure for prudent land cover data to guide sustainable urban planning (Dewan & Yamaguchi, 2009b; Hassan, 2017a). Urban land use maps enable planners and municipalities to make effective decisions that affect land use, transportation, infrastructure planning, and environmental preservation (Herold et al., 2002). Unmanaged urban growth causes issues like urban sprawl, vegetation land loss, surface runoff, and heat islands. Accurate data on urban land cover evades these impacts through enabling sustainable land use patterns that balance development with the conservation of the environment (Seto et al., 2011). In addition, global agencies like the United Nations Sustainable Development Goals (SDGs) are highly interested in urban land cover mapping as core towards achieving sustainable cities and communities (UN, 2015). Land cover change monitoring shows how cities are expanding and transforming, thus playing a direct role in fulfilling the SDG 11.3 of sustainable urbanization. Land cover change monitoring also plays a vital role in urban climate action plans because cities produce a huge percentage of greenhouse gas emissions and are vulnerable to climate hazards (McPhearson et al., 2014).

Urban land cover mapping has several significant uses (Yin et al., 2021). Second, it is important for tracking urbanization, a phenomenon with horizontal growth of urban land, often at the expense of natural environment (Z. Chen & Zhao, 2022). Land cover mapping quantifies the pace, trends, and causes of urban sprawl, especially in the rapidly expanding cities (Fu et al., 2020). It helps planners manage growth and promote compact, efficient cities (El Garouani et al., 2017). Second, urban land cover maps are key to monitoring environmental changes. Urbanization results in natural land cover being converted to impervious surfaces, increasing surface runoff, reducing water infiltration, and elevating flood risk (Tang et al., 2024). The urban land cover maps monitor the changes and supply data regarding water resource planning, flood mitigation, and climate adaptation (Wheater & Evans, 2009). Studies have established that places with elevated impervious cover levels are warmer and therefore end up causing urban heat islands (Voogt & Oke, 2003). Urban land cover change mapping assists in the identification of the heat zones and guides initiatives such as incorporation of green areas in an effort to prevent urban warming (Bowler et al., 2010). Urban land cover data are key to guiding policy formulation. Decision makers utilize this data for prioritizing conservation, zoning laws, and resource allocation in a well-planned manner (Arsanjani et al., 2013). Multi-temporal land cover data can inform decision makers whether or not their policies are effective and help lead them to change rules based on urban development as well as the needs of the environment (Bengston et al., 2004).

Urban land cover classification is not devoid of numerous challenges and intricacies (Y. Li et al., 2024). Urban regions are extremely heterogeneous, where heterogeneously distributed surface classes like buildings, roads, parks, and water bodies occur near one another (Ban & Jacob, 2013). Spatial heterogeneity is a challenging situation where land cover well may not be appropriately classified due to the inability of normal methods to differentiate easily spaced and spectrally similar surfaces (Blaschke et al., 2014). Further, uncertainty in the spectral domain over urban and other land cover types such as bare soil complicates classification in cities (Lu & Weng, 2006). Mixed land cover classes are another issue (Verburg et al., 2011). In urban areas with high population densities, a pixel of remote sensing information may hold more than one land cover, especially where the buildings are compact, roads are narrow, and the vegetation is patchy (Heiden et al., 2012). Mixed pixels cause misclassification and reduce map accuracy, particularly with the use of medium- to low-resolution satellite images (Busetto, 2008). This is addressed with high-resolution images and advanced classification techniques like object-based image analysis (OBIA), but at higher cost and generally more computationally demanding (Amiri et al., 2021).

Temporal and spectral complications also complicate urban land cover mapping (Schneider, 2012b). Urban landscapes are highly dynamic with continuous activity in the form of construction, demolition, and yearly green phenology cycles, and therefore it is difficult to take quality images with sparsely temporal satellite data (Weng, 2012c). The composite spectral properties of urban materials like asphalt, concrete, and metal can lead to spectral mixing, i.e., misclassification (Herold et al., 2004). Current remote sensing progress in data fusion techniques and machine learning systems foretells solutions, but computing requirements and access are constraints for some urban applications (Pu et al., 2021). Urban land cover mapping remains pivotal to sustainable urban development, as it can be used for managing land use, environmental footprint, and urban policymaking (Myneni et al., 2002).

2.2.Role of Remote Sensing in Urban Land Cover Mapping

Remote sensing has transformed urban land cover mapping from basic aerial photography to complex satellite sensors with high spatial and varied data (Yin et al., 2021). Urban research initially relied on aerial photography, which, while adequate for local mapping, was marred by the much-too-prohibitive cost of procurement and ambiguity in data coverage (Schumann et al., 2011). The advent of satellite imagery during the 1970s with the initiatives like Landsat introduced the capability to obtain persistent, repeatable, and large-scale observations of cities (Weng, 2012c). Advances over the past decades in satellite technology, processing of data, and in analytical approaches have enabled the capability for more sophisticated urban analysis, rendering remote sensing a corner stone tool for urban land cover change research (Hassan, 2017b).

The advantages of satellite imagery for application in urban land cover mapping are worth while (Saadat et al., 2011). Satellite imagery is of high spatial resolution with which the features of cities can be mapped in a detailed manner, e.g., buildings, roads, and vegetation (Herold et al., 2003b, 2004). Temporal coverage is also a value added because satellite missions like Landsat, MODIS, and Sentinel have systematic revisits that allow researchers to monitor the temporal dynamics of city change over time with seasonal and long-term trends (Gómez-Limón et al., 2020). Multi-spectral data also facilitate urban studies by measuring data through different wavelengths, required to separate more than one land cover class, for example, vegetation, water, and built-up (Ban & Jacob, 2013). Spectral data allow for the calculation of indices such as Normalized Difference Vegetation Index (NDVI), a common parameter in the computation of vegetation cover in an urban environment (Gascon et al., 2016).

Some of these remote sensing sensors and platforms widely used in mapping urban land cover have distinct characteristics suitable for specific use (Alexander, 2020). Landsat has been operational since 1972 with an imaging capability at medium resolution (30 meters) that has greatly contributed to the investigation of urban growth due to its large temporal record (Wulder et al., 2012). MODIS offers lower resolution data (250 to 1,000 meters) but with high temporal frequency and is worth utilizing in monitoring trends in big cities, especially in large cities (Mertes et al., 2015). European Space Agency's Copernicus program Sentinel-2 offers multispectral high-resolution data (10 meters), allowing finer details on urban mapping (Drusch et al., 2012). Sentinel-1, being a synthetic aperture radar (SAR) sensor, possesses the unique ability to acquire data regardless of clouds and lighting and is optimally suitable for cloudy area mapping and nighttime mapping (Torres et al., 2012). SAR data would prove highly useful for urban area mapping and infrastructure mapping because it is sensitive to the roughness of the surface, which would be complementary to optical data from other sensors (Cerbelaud et al., 2021).

2.3.Sentinel 1 and Sentinel 2 in Urban Studies

Sentinel-1 and Sentinel-2, the two pioneers of the satellites of the European Space Agency's Copernicus program, have been leading urban studies based on remote sensing (Shelestov et al., 2017). Both offer complementary data for city maps, where Sentinel-1 offers synthetic aperture radar (SAR) and Sentinel-2 offers optical multispectral images (Hafner et al., 2022). The combination of these data sources supports high-resolution observation of cities even under adverse weather conditions such as cloud cover or darkness (Bibri, 2018). Sentinel-1 SAR and Sentinel-2 multispectral data have been most effective in monitoring different characteristics of urban land cover, ranging from urbanization to vegetation cover and water features, that would be beneficial for urban planning and environmental management (Haas & Ban, 2017).

Sentinel-1 uses synthetic aperture radar (SAR), radiating microwaves and sensing their return after bouncing off the Earth's surface (Liang et al., 2021). SAR can penetrate cloud and smoke, unlike optical sensors, and even during nighttime hours, making it therefore an immensely dependable source for certain urban mapping (Torres et al., 2012). It is particularly useful in areas of high cloud cover or atmospheric humidity, where optical sensors are inefficient (C. W. Huang et al., 2018). SAR backscatter from surface roughness must be used to distinguish between urban structures: built-up area complexity backscatters more strongly than natural land use and holds information on urban infrastructure and building density (Ban & Jacob, 2013). Besides, SAR data can also acquire textural and structural information, which is a major factor in impervious surface cover mapping like pavement areas, roofs, and roads typical of urban environments (Cai et al., 2017).

Sentinel-1 SAR data have been found to be very useful for built-up facility and building detection and classification due to data sensitivity to surface structure and texture change (Fibæk et al., 2021). Sentinel-1 trials for urban uses have been discovered to be capable of distinguishing between highly populated urbanized areas and other areas like fields and forests through the radar backscatter signals that are contingent upon the surface roughness and structure (Z. Chen & Zhao, 2022). Sentinel-1 has been applied to monitor urbanization in cities globally, providing real-time data which can be used to inform urban development and zoning policy update (Plank, 2014). Moreover, the sensitivity of SAR to minimal surface movement makes it well-suited to function well in monitoring subsidence and structural evolution in city infrastructures, a primary driving force for urban resilience and disaster preparedness (J. Liu et al., 2024).

Sentinel-2 also has a high-resolution multispectral sensor with the capacity to monitor 13 spectral bands, thus being even more appropriate for analyzing urban areas in comparison to delineating vegetation, water features, and surfaces of non-pervious material (Hunt et al., 2019). Compared to SAR, Sentinel-2 operates based on weather- and sunlight-limited visible imagery but provides high-resolution, spectrally diversified visible, near-infrared, and short-wave infrared observations (Schulz & Siriwardane, 2016). Such spectral heterogeneity enables Sentinel-2 to map many dissimilar urban land covers with precision, and it is highly well-suited for the identification and monitoring of vegetation, water bodies, and impervious surfaces in urban areas (Drusch et al., 2012). Visible and near-infrared bands are optimally utilized for the detection of vegetation, while short-wave infrared bands assist in the discrimination of impervious surfaces from other land covers (Liu & Yang, 2015).

Sentinel-2 has a spatial resolution (10 meters for the central bands) and can map fine-scale detail across urban landscapes, such as small parks, individual trees, and narrow water courses, which would be lost with coarser sensors (Johnson, 2013). Along with that, Sentinel-2's relatively high temporal frequency in the form of 5-day revisit times coupled with its twin Sentinel-2B provides uninterrupted time series observation of temporal urban processes (Ienco et al., 2019). Temporal frequency is best suited to observe dynamic changing seasonally changing plant patterns and to detect rapid urbanization or land cover change (Kabisch et al., 2019). Sentinel-2 data have also been widely utilized to monitor the urban heat island by mapping the impervious surfaces that cause heat retention and thus establish their position in urban greening initiatives reducing temperature increase in densely populated urban cities (M. S. Chowdhury, 2024; S. Chowdhury et al., 2021).

Multispectral nature of Sentinel-2 offers a significant benefit in assessing urban land cover classes (Izakovičová et al., 2017). It, being multi-bands, can also calculate vegetation indices like the Normalized Difference Vegetation Index (NDVI) and water indices, which are important in green and blue space monitoring of the urban area (Deng & Wu, 2013). Such indices allow one to quantify vegetation status, water status, and degree of imperviousness, providing essential data for environmental quality mapping and urban sustainability (Villeneuve et al., 2018). By combining Sentinel-2 optical information and Sentinel-1 SAR information, researchers and urban planners are able to gain more comprehensive and more accurate understandings of city spaces, even further ensuring the reliability and correctness of urban land cover mapping (X. Zhang et al., 2023).

2.4.Integrated Use of Sentinel 1 and Sentinel 2 for Enhanced Urban Land Cover Mapping

The complementary synergy of Sentinel-1 (SAR) and Sentinel-2 (optical) data has been of immense utility in sharing urban land cover mapping due to their complementary potential (Steinhausen et al., 2018). SAR and optical data collect various characteristics of cities: SAR collects structural data by feeling surface ruggedness and physical properties (Hu et al., 2018), while optical data can feel spectral information pertinent to separating land covers like vegetation, water bodies, and impervious surfaces (Ban & Jacob, 2013). This fusion takes advantage of the structural and spectral data, yielding more accurate and specific information on cities, especially in hilly areas where developed land, water bodies, and forests have intimate proximal relationships with one another (Li et al., 2023).

Sentinel-1 SAR data also possesses its own strengths in mapping urban land cover because it can identify surface roughness and pass through unfavorable weather conditions such as cloud and haze (Li et al., 2018). SAR data is particularly useful where there is frequent cloud cover, as optical sensors can be impaired (Torres et al., 2012). Sensitivity of SAR to structural characteristics like building density, road network, and other man-made features allows for precise mapping of urban built-up land (Jiang & Eastman, 2000). This is significant in urban expansion and high-density area mapping since radar backscatter intensity varies greatly between urban and other land surfaces (Majidi Nezhad et al., 2021). Aside from this, SAR can also detect subtle deformation of the surface and change in infrastructure, which can be employed to track natural disaster resilience and urban sprawl (Liu et al., 2020).

Multispectral imaging capability of Sentinel-2, on the other hand, provides high spectral resolution across multiple bands and maintains vegetation, water, and hard surfaces' respective spectral signatures (Pahlevan et al., 2017). This spectral information facilitates the detection and monitoring of blue and green regions, which are required in the estimation of urban environmental quality (Drusch et al., 2012). Optical imagery facilitates the calculation of values such as NDVI, which can be used in sensing vegetation cover and estimation of urban vegetation health (Deng & Wu, 2013). Sentinel-2's 10-meter spatial resolution and moderate repeat cycle enable temporal change capture in urban landscapes, from season vegetative change to new developments of construction (Shrestha et al., 2020).

Combined, Sentinel-1 and Sentinel-2 imagery provide a solid basis for urban land cover mapping (Schulz & Siriwardane, 2016). The SAR data help to outline structural features and the optical data help to classify land cover by distinguishing spectrally mixed features that would be alike-looking features in SAR imagery by itself (Laurin et al., 2013). For example, the integration of Sentinel-2 spectral observations with SAR backscatter observation can allow for improved differentiation between urban cover and bare soil, both of which are classification challenges since they are so similar in radar reflectance and spectral properties (Johnson, 2013). The integration of these data types has enabled more detailed urban mapping results, with the promise of acquiring more accurate land use identification along with that of urban spatial structure (Y. Liu et al., 2017). It is particularly useful in rapidly expanding urban areas, where timely and homogenous information is required for sustainable planning, infrastructure management, and environmental monitoring objectives (Herold et al., 2004).

Integration of Sentinel-1 and Sentinel-2 data through urban mapping has been applied successfully in a number of case studies across the world (B. Hu et al., 2021). Techniques for image fusion allow researchers to leverage the unique advantage of each type of sensor in order to reach maximum levels of classification accuracy, monitoring urban processes, and guiding sustainable city planning (Lau et al., 2019). Most of the studies have been capable of distinguishing intricate urban details with Sentinel-1 SAR and Sentinel-2 optical data fusion (Fakhri & Gkanatsios, 2021). Case studies prefer to prove the advantage of fusing SAR's structural information with the wealth of optical information in the spectrum for a composite description of the urban environment (Tsokas et al., 2022).

For example, scientists used a combination of Sentinel-1 and Sentinel-2 data in a Southeast Asian case study to monitor five years of urban sprawl and land cover change. The research demonstrated that it was indeed possible to successfully monitor rapid urbanization and map peri-urban and urban areas from SAR and optical imagery. Having access to both datasets allowed the study to analyze cloud cover, which is prevalent in the tropics because SAR data can penetrate cloud cover and offer eternal temporal cover (Shrestha et al., 2020). In addition, for cities in Europe, Sentinel-1 and Sentinel-2 synergies were used for persistent mapping of urban hard surfaces, water bodies, and urban green cover for enabling urban planning intervention to prevent urban heat island and enhance green infrastructure (Lehmler et al., 2023).

2.5.Fusion Techniques: Pixel-based vs. Object-based Classification

Sentinel-1 and Sentinel-2 fusion, to a significant degree, is a matter of the classification approaches employed (Chakhar et al., 2021). Two general methods in common use are pixel-based and object-based classification: pixel-based and object-based classification. Pixel-based classification operates directly with individual pixels, each being assigned a specific land cover based on its backscatter or spectrum (Demers et al., 2015). While useful for high-resolution images, pixel-based methods risk being limited in mixed urban regions with dominance of mixed pixels (e.g., vegetation and urban). This can cause ambiguity of spectral data and lower accuracy in classification, especially in highly urbanized regions (Yan et al., 2016).

Object-based classification separates pixels into meaningful, or "segments," based on spatial, spectral, and textural similarity (Myint et al., 2011). It is more accurate in simulating real land cover classes in modeling spatial context and boundary definition and is best applied to high-resolution imagery (Blaschke, 2010). Object-based classification is better suited for urban mapping as it eliminates confusion between aggregate land cover classes, and promotes the identification of built-up land, scattered vegetation, and bodies of water. Most of the recent studies operating with Sentinel-1 and Sentinel-2 data have all concurred that object-oriented approaches are more precise when applied for urban mapping purposes, especially utilizing SAR's structural information and optical richness (Haas & Ban, 2017).

2.6.Machine Learning Algorithms in Data Fusion

Advanced machine learning algorithms are commonly applied to conduct data fusion for Sentinel-1 and Sentinel-2 urban land cover mapping. Methods like Random Forest (RF) and Support Vector

Machine (SVM) have been shown to excel at classifying complex urban land cover classes at high levels of accuracy. Random Forest, which is an ensemble algorithm based on decision trees, is especially popular since it is stable and highly accurate in the handling of vast, multispectral data. RF's capacity for handling non-linear relations and preventing overfitting makes it a perfect algorithm for SAR and optical data fusion since it can efficiently fuse spectral, textural, and structural knowledge (Belgiu & Drăgu, 2016).

Support Vector Machine (SVM) is another supervised learning method which is among the most widely applied algorithms, which works on binary as well as multi-class classification tasks on urban mapping. SVM works especially effectively on discrimination of overlapping spectral features classes such as peri-urban and urban. SVM analysis with Sentinel-1 and Sentinel-2 data fusion has also achieved high levels of classification accuracy, especially to separate impervious surfaces, vegetation, and water bodies in cities (Y. Hu et al., 2018). Both SVM and RF have both been utilized to great effect for numerous urban uses, and accuracy tends to be enhanced with the incorporation of ancillary data, e.g., DEMs, in an effort to enhance sophistication for classifications.

There are other types of fusion that have been suggested, including deep learning architectures such as convolutional neural networks (CNNs), which have the potential to detect sophisticated spatial and spectral relationships in high-resolution urban imagery (Liu et al., 2017). CNNs have the ability to learn from huge data sets independently and mitigate the need for rigid pre-processing. Despite their computational complexity, CNNs have already proved efficacious for urban land cover mapping based on fused Sentinel data, particularly in mega cities that have very diversified landscape (Shrestha et al., 2020). With evolving machine learning and data fusion techniques, they will inherently improve the accuracy of urban mapping towards more enlightened urban planning and sustainable development plans.

2.7.Google Earth Engine (GEE) as a Platform for Urban Land Cover Mapping

Google Earth Engine (GEE) is currently an advanced cloud-computing platform for urban land cover mapping with phenomenal capability in managing large geospatial data sets, performing computationally intensive operations, and providing scalability (Ghosh et al., 2022). GEE is a global scale platform created by Google that allows scientists to access petabytes of satellite imagery and geospatial data and the computational resources necessary to process these data in an efficient way (Tamiminia et al., 2020b). It is especially useful for urban studies due to the fact that fast urbanization and environmental change must be measured using multi-temporal and high-resolution data (Gorelick et al., 2017).

One of the significant advantages of GEE is that it works with enormous data sets without any additional hardware or large storage capacity (Waleed & Sajjad, 2023). Unlike other GIS and remote sensing applications whose natural bias is to have users download and cache huge volumes of data onto their own computers, GEE allows users immediate access to a big data storehouse of satellite images and data (Sidhu et al., 2018). These are Landsat, Sentinel, and MODIS images, which are used in critical functions to map cities. It is possible for users to perform data fusion, change detection, and classification of a global scale under one platform, and therefore GEE is the most suitable tool of preference for researchers dealing with urban studies where there is a requirement of homogeneous data over large areas or long durations (Azzari & Lobell, 2017).

GEE cloud computing facilitates fast processing of bulk data to facilitate high-resolution urban land cover mapping with spatial and temporal accuracy (Mahdianpari et al., 2019). Parallel processing allows GEE to conduct computationally intensive tasks like image classification, object detection, and time series analysis at hitherto unprecedented scales. This is a capability needed by city researchers mandated to track trends of changing land cover and urban sprawl over decades. For example, urban sprawl studies using decades-long time series analysis may be greatly benefited by GEE's ability to carry out such tasks on such scales and scales so easily that researchers may produce results in far fewer hours than would be required using traditional software (Ines et al., 2013).

The two major strengths of GEE are adaptability and scalability, which enable city-level study to continent-scale examination in urban mapping research at different scales. One can model and run models over large geography with little modification, and that itself is an flexible method of applying GEE in examining urbanization processes in different areas. GEE scalability is further supported by JavaScript and Python programming, allowing users to automate workflow, personalize analysis, and make reproducible methods. GEE has thus been a go-to site for urban land cover mapping and other big environmental monitoring tasks due to its enabling of collaborative science, replicability, and ease in study sharing (Gorelick et al., 2017).

Google Earth Engine (GEE) is becoming more used in city mapping, as most studies have validated GEE's capability to analyze complex urban complexity through its big data catalog, e.g., Sentinel imagery being easily available, and robust analysis capability. GEE's data catalog is robust, whereby users can tap into petabytes of satellite images, such as high-resolution and multi-temporal Landsat, MODIS, Sentinel-1, and Sentinel-2 sensor imagery. Such data are key to urban mapping in that it makes it possible for researchers to track changes in urban growth, land cover, and environmental diversity in a spatiotemporal manner, which is of significant concern in rapidly developing cities like Adama City in Ethiopia (Gorelick et al., 2017). With the access that it offers to both synthetic aperture radar (SAR) and multispectral data through Sentinel-1 and Sentinel-2, respectively, GEE offers urban researchers the innovative benefit of combining the structural and the spectral data for higher urban classification, particularly in cloud-prone areas where SAR's penetration ability through cloud is an added advantage (Azzari & Lobell, 2017).

2.8.Current Methodologies for Urban Land Cover Classification

Urban land cover mapping is required for tracking urbanization, tracking environmental degradation, and land use planning, and recent advances in remote sensing, particularly with Sentinel data, have offered new techniques to make this task easier (Schneider, 2012b). Sentinel-1 (SAR) and Sentinel-2 (optical) supply complementary data that can be used independently or fused for improved classification accuracy (Vanacker et al., 2007). Past methods of Sentinel-based urban land cover classification include supervised and unsupervised classification, time-series analysis, and change detection, each of which has some merits and demerits (Talukdar et al., 2020).

Supervised classification has also been largely utilized in urban land cover mapping since it will be more precise when trained on sample data representative of the area (L. Ma et al., 2017). Supervised classifiers, such as Random Forest (RF), Support Vector Machine (SVM), and Decision Trees, are typically employed on Sentinel-2 data because of the discriminative capacity with various forms of urban land cover, i.e., built-up, vegetation, and water, thanks to the multispectral ability of the sensor (Belgiu & Drăgu, 2016). These methods are particularly useful in urban research with accessible training data from easily obtainable land cover classes and develop highly calibrated classification models with adequate stability against modifying the Sentinel-2 data's spectral properties (Peng et al., 2024).

Unsupervised classification, however, depends not on any existing training samples but groups the pixels based on their inherent spectral similarity and thus relies where no labeled data are available (Wambugu, 2021). Techniques like K-means and ISODATA are routine processes in unsupervised classifications. Nevertheless, although unsupervised classification can deliver valuable information in initial urban analysis, it does not perform as well in cities with high-level land covers and spectral ambiguity (Neyns, 2024). Lack of adequate training data for unsupervised techniques might lead to misclassification in nuanced scenarios where different developed, vegetation, and bare land might have similar spectral behavior in certain bands (Pandey et al., 2021).

Time-series analysis was even more significant for the land cover mapping of cities because temporal changes, urban sprawl, land use change, and environmental impacts can even be monitored (Wang et al., 2022). Due to its revisit time, Sentinel-2 is best fit for time-series analysis so that researchers can see season and yearly urban changes. With time-series data, scientists are able to determine vegetation loss change, sprawl, and impervious surface change, and even data on direction and pace of urbanization (Wulder et al., 2012).

Detection of change in urban land cover is usually performed through change detection methods such as image differencing, thresholding, and post-classification comparison (Chen et al., 2016). Sentinel-1 SAR is also an appropriate option for change detection as it can penetrate cloud and provide continuous temporal information under all weather conditions. Sentinel-1 and Sentinel-2 have been experimented and tested for change detection and proved to provide high accuracy in the detection of growth in urban regions, deforestation, and water body modifications in urban regions (Billah et al., 2023). These methods form the core of the detection of urbanization processes and the assessment of their environmental impacts, though with the constraints of obtaining high temporal continuity and meeting data storage demands for long-term time-series studies (R. Wang et al., 2024).

Urban accuracy classification remains challenging due to the spectral heterogeneity of the urban landscape. Issues such as mixed pixels, shadowing, and heterogeneity of reflectance characteristics among buildings, vegetation, and roads may interfere with the accuracy of classification. Spatial and spectral high resolution of Sentinel-2 contribute to some alleviation of these effects, but spectral contamination among neighboring classes of land cover, i.e., urban and bare soil, contributes further to lowering accuracy. Furthermore, Sentinel-1 SAR data, although useful in structuring, is introducing speckle noise that requires preprocessing to improve the quality of urban classification (Schneider, 2012b).

Best practices for improving classification accuracy in urban studies are through the use of data fusion techniques that integrate Sentinel-1 SAR and Sentinel-2 optical data, and machine learning algorithms capable of managing the characteristic complex data behavior of urban environments (Becker et al., 2021). Object-based classification where the pixels are clumped together into meaningful image salient has managed to restrict misclassification via using spatial context, particularly in high-density urban areas where a single pixel is too limiting to be effective for classification (Whiteside et al., 2011). Accuracy measure criteria like the Kappa coefficient and F1-score perform similarly while evaluating Sentinel-1, Sentinel-2, and their fusion for urban land use mapping under different schemes (Blaschke, 2010).

Others compare Sentinel-1, Sentinel-2, and their fusion for comparing accuracy and limitations under different classification schemes (Solórzano et al., 2021a). For instance, integration of Sentinel-2 and Sentinel-1 data and machine classifiers like SVM and Random Forest in Asian and European urban city studies has led to more accurate urban land-use classification, i.e., industrial, residential, and green (Gong et al., 2013). There are still some limitations, though, like the inability to classify high-albedo surfaces like soil and concrete and high-quality ground truth requirements in order to be able to perform successful supervised classifications.

Data fusion methods, which combine SAR structure data with optical variation of data in the spectral, do comparatively better than mono-sensor methods, particularly in heavily heterogeneous urban environments. But SAR and optical processing requires pre-processing and geo-referencing data skills, as well as selecting good algorithms that will be able to cope with the high data complexity. Notwithstanding such challenges, joint application of Sentinel-1 and Sentinel-2 has been a best practice for urban land cover mapping, especially for cloud-covered areas, with SAR complementing data filling gaps and data continuity (Gorelick et al., 2017).

2.9.Empirical literature review

Several studies point out the potential of Sentinel data in urban mapping because of its revisit time and resolution. Sentinel-2, for instance, is widely utilized in empirical studies in urban land cover mapping with its heterogenous land use classes. While conducting research on urban expansion in

Addis Ababa, Ethiopia, researchers found Sentinel-2 multispectral ability enabled effective discrimination between built-up and non-built-up areas, revealing patterns of urban sprawl and their impacts on landscape environments (Gashu et al., 2022). This is corroborated by studies in other African cities, including Kampala, Uganda, where Sentinel-2 resolution was employed to closely monitor green cover and impervious surface deterioration, yielding valuable information for urban policymaking (Musoke et al., 2021).

Sentinel-1, a radar sensor, has also proved handy in urban studies, especially in areas with persistent cloud cover. Sentinel-1 synthetic aperture radar (SAR) can penetrate clouds and measure ground structural information and is applicable for mapping tropical urban regions. Sentinel-1 was used in Mumbai, India, where the study of urban flood risk integrated Sentinel-1 imagery and digital elevation models in the mapping of flood risk zones and mapping impacted urban infrastructure. SAR data precisely delineates man-made features and provided essential structure information for urban planning and hazard mapping (Paul et al., 2020). Such findings identify the use of Sentinel-1 in data acquisition under unfavorable weather and where structure information is needed.

Charles et al. (2020) also show further, in their empirical work, that integrating Sentinel-1 and Sentinel-2 data is useful in its capacity to improve accuracy in urban land cover classification. The combination of SAR and optical data provides spectral and structural information and mitigates the constraints in individual use of each sensor. Scholars in research in Shanghai, China, combined Sentinel-1 and Sentinel-2 data and achieved more than 90% classification accuracy in discriminating built-up, vegetation, and water. Fusion improved class precision with urban regions by reducing spectral misclassification among similar land cover classes, i.e., bare soil and concrete, as well as textural information that facilitated segmentation of highly developed regions more successful (Li et al., 2020). Furthermore, an investigation of the accelerated urban expansion in Lagos, Nigeria, revealed that data fusion improved the classification accuracy and facilitated monitoring of the urban expansion in time-series form, which was convenient in densely populated urban areas (Akinyemi & Yekinni, 2021).

A second comparative empirical evaluation of object-based vs. pixel-based classification approaches on fused Sentinel imagery confirmed that OBIA outperformed pixel-based approaches in small-scale urban feature mapping and minimizing misclassification within mixed land use patches. Such is specific relevance in urban settings with complex urban morphology, where application of traditional pixel-based approaches might be unable to discriminate urban boundaries (Blaschke et al., 2014). These findings show the effectiveness of data fusion and advanced classification methods in addressing heterogeneity challenge in cities and enhancing the accuracy of land cover maps.

While Sentinel data have advanced urban mapping, empirical studies also foresee limits in data processing, accuracy of classification, as well as spectral ambiguity in cities with heterogeneity. For example, spectral mixture confusion between urban elements, i.e., built-up and bare land, will lead to misclassification, especially in highly developed regions with equivalent reflectance values. In Jakarta, Indonesia, a research found that the use of Sentinel-2 data alone always misclassified bare soil as built-up areas due to spectral similarities, overstating the pace of urban growth. This issue was relieved with Sentinel-1 data that provided an additional structural information to distinguish these classes (Wijaya et al., 2019). Data fusion comes with preprocessing and SAR and optical data matching know-how and makes the classifying process more challenging.

High-resolution classifications are also predominantly constrained by the processing and storage capacity, particularly in time-series analysis. For large studies, for instance, research on Southeast Asian urbanization trends, scientists were not able to cope with the volume of Sentinel data, which required enormous cloud storage and supercomputing to analyze. The emphasis of this research was on the significance of platforms such as Google Earth Engine (GEE) in addressing these challenges through the availability of cloud computing and access, thereby making time-series analysis and data integration relatively easy (Chen et al., 2021).

Empirical results also show that machine learning algorithms such as Random Forest (RF) and Support Vector Machine (SVM) are among the highest-performing models for urban land cover mapping using Sentinel data. The two models are highly sensitive to detailed datasets and are capable of dealing with the high-dimensionality of cities. In São Paulo, Brazil, urban growth research, RF was applied to Sentinel-1 and Sentinel-2 merged data and had 88% correct classification attainment in urban built-up area, vegetation, and water body mapping. The study highlights the application of RF in addressing urban heterogeneity and achieving accurate classification with large ground truth data training (Moreira et al., 2020).

The comparison of RF, SVM, and traditional classification methods in cities arrived at the conclusion that the machine learning methods outperformed the traditional methods in accuracy as well as processing time and hence are increasingly popular day by day in city land cover mapping (Xu et al., 2019). The machine learning methods also rely on high-quality training data and could be parameter-sensitive, and rigorous tuning and validation are needed for best performance.

2.10. Scientific Knowledge Gaps

Despite the advances in the use of Sentinel-1 and Sentinel-2 data in the mapping of urban land cover, there are still some gaps in scientific research. These include, among others, the limited studies on the fusion of Sentinel-1 and Sentinel-2 data to map urban regions, particularly highly heterogeneous urban regions. While data fusion exhibited increased accuracy of classification, there is as yet no satisfactory full-scale investigation of its use in situations where mixed land cover patches and complex urban morphologies render accurate classification challenging.

The other serious issue is the issue of spectral confusion among alike land cover classes, for instance, bare soil and urban. Even though data fusion alleviates this issue to a certain degree, further studies on advanced methods of managing spectral overlaps are necessary. In addition, preprocessing and registration of the SAR and optical imagery require huge amounts of time and skills. The absence of properly engineered, automated workflows for the integration of these datasets remains an impediment to efficient urban mapping processes.

Scalability of high-resolution classification is another important gap. While some of the computational and storage challenges are mitigated by systems like Google Earth Engine (GEE), more research is needed to optimize computational workflows for time-series and large-area analysis. Besides, although machine learning algorithms like Support Vector Machine (SVM) and Random Forest (RF) have been successful, there is limited work on more recent state-of-the-art methods, e.g., Convolutional Neural Networks (CNNs), that may further improve the performance of urban land cover classification.

Good quality ground truth data is another necessity. Current research has the limitation of generating or obtaining large and accurate training datasets, especially for urban areas where land cover diversity and heterogeneity are prevalent. This consequently becomes the limiting factor in supervised classification procedures' reliability and resulting land cover maps' accuracy.

Geographical representation in research is also insufficient. While the majority of studies do focus on big cities in well-studied regions like Shanghai, Lagos, and São Paulo, much research is aimed at smaller cities or less studied regions, particularly in the developing world, where urbanization in general takes a very different form.

Last but not least, time-series Sentinel-1 and Sentinel-2 analysis remains unexploited. The combination of temporal trends with urban land cover mapping and change detection has yet to be exploited to its fullest. These types of analyses can provide valuable information on the dynamic dynamics of urban areas and help improve monitoring and management of urban growth and associated environmental effects. Filling these knowledge gaps was to enhance the accuracy, efficiency, and applicability of urban land cover mapping approaches, particularly in complex and less-researched urban environments.

CHAPTER THREE

3. MATERIALS AND METHODS

3.1.Description of the study area

Adama City is a city located in the central part of Ethiopia in the Oromia Regional State. The city is geographically situated between latitudes 8° 27′ 0″N and 8°39′ 0″N and longitudes 39° 9′ 0″E and 39° 21′ 0″E. The Adama City is located in the Great Rift Valley approximately 100 kilometers southeast of Addis Ababa, the capital city of Ethiopia. Adama is a significant urban area with infrastructural and economic strategic importance, serving as a transport node linking the capital to the eastern and southern parts of the nation. The city is surrounded by a mixture of peri-urban and rural areas, and therefore the city is an appropriate location for observing the urban land cover change and pattern of spread.

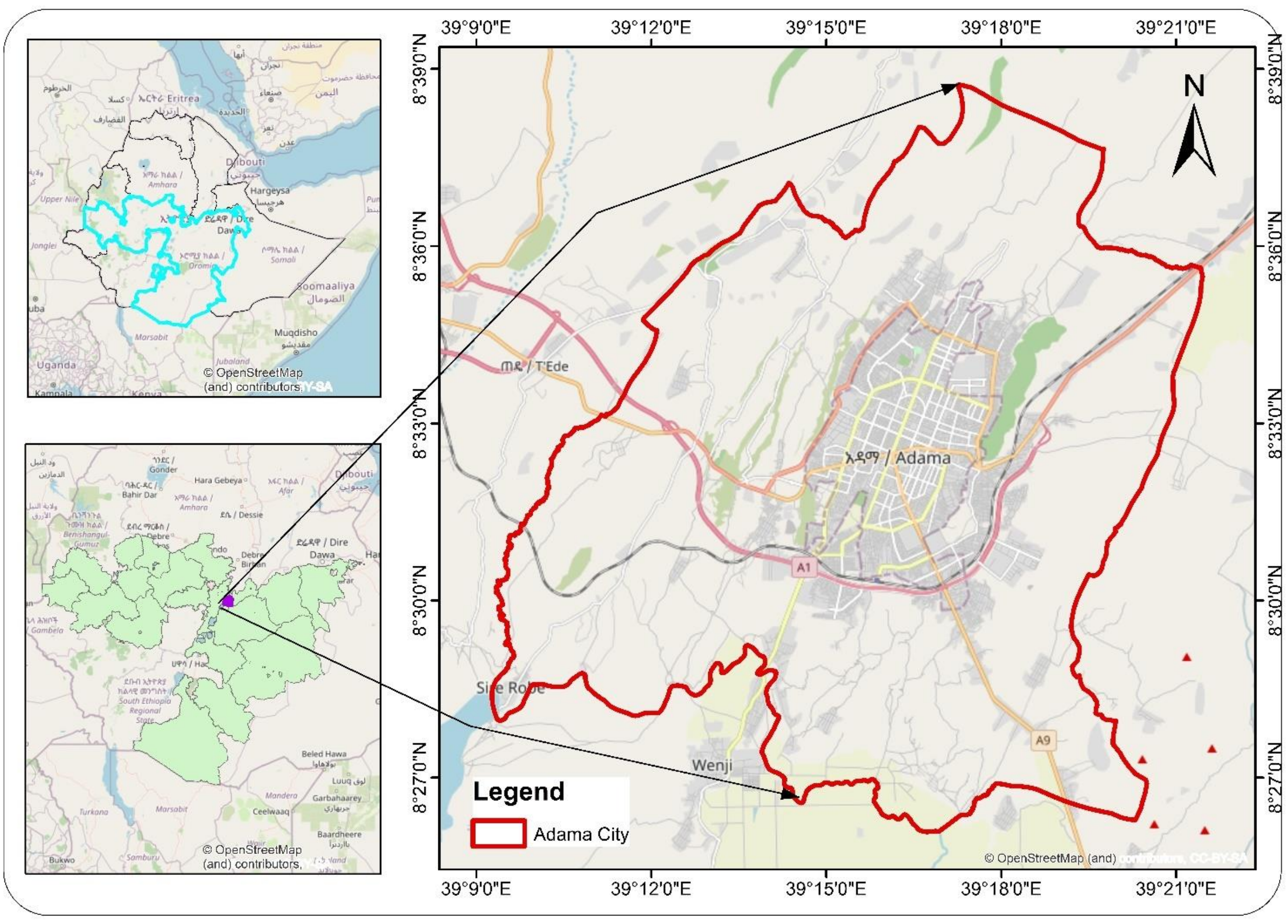

Figure 3-1: Location map of the study area

3.2.Data source

Satellite data for this study were supplied by the Copernicus Open Access Hub, and Sentinel-2 MSI and Sentinel-1 SAR images were utilized in specific cases. For areas of typical cloud cover or adverse weather conditions, Sentinel-1 SAR is especially effective because it offers radar imaging that is able to penetrate cloud cover and yield high-resolution data that is appropriate for metropolitan analysis (Bousbih et al., 2017). In contrast, Sentinel-2 MSI offers high spatial resolution multispectral data that allows for expansive examination of different land covers (Pahlevan et al., 2017). Both Sentinel-1 SAR and Sentinel-2 MSI were acquired for the years 2015–2025 since Sentinel imagery came on stream in 2015. A robust time series analysis is made possible by the 10-year window, capturing the dynamics of urban land cover and shedding light on change over nine distinct years within this time period.

Table 3-1: Sentinel 2 MSI available bands, spatial and spectral resolution

Band	Name	Central Wavelength (nm)	Resolution (m)	Application
Band 1	Coastal aerosol	443	60	Coastal and aerosol studies
Band 2	Blue	490	10	Vegetation, water, and soil discrimination
Band 3	Green	560	10	Vegetation monitoring
Band 4	Red	665	10	Vegetation discrimination
Band 5	Red Edge 1	705	20	Vegetation chlorophyll content
Band 6	Red Edge 2	740	20	Vegetation classification
Band 7	Red Edge 3	783	20	Vegetation and biomass
Band 8	Near Infrared (NIR)	842	10	Biomass and water content
Band 8A	Narrow NIR (Red Edge NIR)	865	20	Vegetation structure
Band 9	Water vapor	945	60	Atmospheric correction
Band 10	SWIR – Cirrus detection	1375	60	Cirrus cloud screening
Band 11	SWIR 1	1610	20	Soil and moisture content
Band 12	SWIR 2	2190	20	Vegetation and mineral detection

Source: ESA, 2021

Table 3-2: Spectral characteristics of SAR image

Attribute	Details
Frequency Band	C-band
Wavelength	~5.6 cm (corresponds to ~5.405 GHz frequency)
Polarization Modes	VV, VH, HH, HV (Sentinel-1 typically uses VV and VH in IW
Acquisition Modes	Interferometric Wide Swath (IW), Extra Wide Swath (EW),
Resolution	~10 m (Ground Range Detected for IW mode)
Data Type	Amplitude and/or phase of backscatter (intensity or complex values)
Spectral Range	Microwave (C-band: ~4–8 GHz, Sentinel-1 uses ~5.405 GHz)

3.3.Limitations of Sentinel 1 and Sentinel 2 data

Sentinel-1 is an active radar satellite and relies upon synthetic aperture radar (SAR) technology, which struggles to differentiate between similar urban land coverages. SAR data also tends to be speckle-noisy, and because of this, it becomes problematic to classify urban areas correctly (Zhu et al., 2017). The spatial resolution of Sentinel-1, typically 10 meters, also prevents it from capturing finer urban features, such as individual buildings or minute infrastructure components, which also makes land cover classification more complex (Kuppusamy et al., 2021). Sentinel-2 possesses higher spatial resolution optical imagery (up to 10 meters maximum) and higher spectral bands and is therefore well-suited for land cover classification in urban areas. However, Sentinel-2's optical information is susceptible to the weather conditions such as cloud cover, haze, or fog, which hide urban features and reduce the accuracy of classification, especially over areas with high cloud cover frequencies (Gómez et al., 2018).

3.4.Reference data

To validate satellite-based urban land cover mapping, stratified random sampling approach was used to guide field data collection such that every land cover class (e.g., urban, vegetation, exposed soil) detected would be well represented. Ground control points (GCPs) were obtained from high-resolution Google Earth imagery, providing precise coordinates to be used to refer to pixels on a satellite image.

Systematic observations, photographs, and land cover attributes (e.g., type, density, and purpose) were taken at every sample point. The field data collection was planned as close to the satellite image acquisition as feasible to minimize seasonal variation. After collection, the field data were aggregated into a GIS database to compare and refine on classification accuracy by cross-validating ground observations against satellite classifications.

3.5.Software

Table 3-3 is a breakdown of software used in this research, which played a specific role in the process. Google Earth Engine (GEE) was utilized for change detection, classification, and preprocessing of data for effective processing of satellite images. Spatial analysis and visualization were conducted using ArcGIS, which aided the interpretation of geographic data and its presentation in a meaningful way. Statistical analysis and modeling were covered by RStudio, which featured powerful analytical processing as well as data manipulation tools. Google Earth was used as a tool for field data collection and mapping, namely for obtaining high-resolution ground control points (GCPs). Microsoft Excel was finally used for data management and processing, allowing for data organization and basic analysis before further processing.

Table 3-3: Software's used in this research

Software	Purpose
Google Earth Engine (GEE)	Data preprocessing, classification, and change detection
ArcGIS	Spatial analysis, and visualization
RStudio	Statistical analysis and modeling
Google Earth	Field data collection and mapping
Microsoft Excel	Data management and analysis

3.6.Methods of data processing

3.6.1. Data Preprocessing

GEE API was utilized in this study to acquire the Sentinel 1 SAR and Sentinel 2 MSI datasets that were recorded from the Copernicus. All the Sentinel images were imported, visualized, and mosaiced via the JavaScript API. The border and training and validation sample data of Adama City were initially uploaded to the GEE platform.

Preprocessing that is crucial was conducted, such as filter mosaicking to merge the imagery from distinct path/row acquisitions, filtering data by entering the dates, cloud masking to provide cloud-free images, and clipping to the edge of the study region. Images with cloud cover of less than 10% are suitable for land cover mapping using Sentinel data (Sano et al., 2007). In order to make sure that Sentinels with lower than 10% cloud cover were used in this study, the GEE cloud masking algorithm was used.

3.6.2. Feature selection

Feature selection A variety of features for all satellite sensors are chosen to capture distinctive features of many land covers in attempting to classify land cover effectively using Sentinel-1 and Sentinel-2 data, improving classification robustness and accuracy. Synthetic Aperture Radar (SAR) data, offered by Sentinel-1, is very useful since it can penetrate through clouds and offer stable imagery in any weather conditions. Two notable features of Sentinel-1 are vertical-horizontal (VH) and vertical-vertical (VV) polarizations, which show differential backscatter features and enable the differentiation between vegetation, water bodies, and urban areas.

Moreover, backscatter coefficients of the strength of radar returns from surfaces can be used to distinguish smoother surfaces like water bodies (which are of lower backscatter) and rough surfaces like urban regions (which are of higher backscatter). SAR-derived texture statistics like contrast and entropy are useful for distinguishing more homogeneous natural surfaces like water from highly populated urban regions since they have the capability of offering more surface heterogeneity and roughness information. With the visible, near-infrared (NIR), and short-wave infrared (SWIR) bands imaged, Sentinel-2's multispectral imagery enhances the SAR information and gives complete information on the properties of land cover. Since vegetation is highly reflective in the NIR wavelength, the visible (Red, Green, and Blue) and NIR bands are especially useful to differentiate areas with and without vegetation. Red edge bands, designed to track vegetation chlorophyll fluctuations, are strongly sensitive to species differences and plant health and can be used to differentiate among different types and conditions of vegetation. The SWIR bands also help in the discrimination of natural ground cover from urban surfaces (such as concrete and asphalt) and determining the amount of water in soils and vegetation, helping in proper land classification cover in various environments.

3.6.3. Land use/cover classification

Land use/cover classification was done after feature selection and preprocessing for separating the satellite images into various classes. To achieve this classification, the GEE platform used machine learning methods, RF and SVM. These methods were used because they are robust and precise when used with complicated classification issues and big data (Breiman, 2001; Cutler, 2012;

Goldstein et al., 2010). In order to classify the images into the different land use/cover classes, the models were trained using the ROI that was gathered.

3.6.4. Change detection

Satellite images from Sentinel-1 and Sentinel-2 were utilized to determine the alterations from the year 2015 to 2025. To ensure that both pairs of images are spatially consistent, the data is first preprocessed with radiometric calibration and image co-registration. The backscatter elements of significant backscatter coefficients and spectral indicators like NDVI and NDBI from Sentinel-1 and Sentinel-2 data were used to map the land cover for 2015 and 2024. Various methods were employed to detect changes. For the detection of transition regions like vegetation loss or urban growth, post-classification comparison was employed by comparing the land cover classes of the two years. In order to identify changes in surface features, Sentinel-1 SAR data was subjected to differential change detection (DCD), which compares intensity of backscattering between the two time periods. Sentinel-2 identified locations with high vegetation and urban change by using spectral change detection on indices such as NDVI and NDBI.

3.6.5. Classification algorithms

Random forest (RF)

Owing to the many strengths of Random Forest (RF), especially in handling complex, high-dimensional datasets, it is usually favored over other machine learning algorithms in land cover classification. Among the many advantages of RF is that it can prevent overfitting, a problem prevalent in the use of simpler models like Decision Trees. Decision trees tend to overfit because they can memorize the training data and do not generalize well to new data, particularly when the trees are deep and complex (Breiman, 2001). In order to improve its robustness and generalization ability, RF averages out a collection of decision trees' predictions by building an ensemble of trees on random subsets of data and features (Liaw & Wiener, 2002). In land cover classification, where the data may be noisy, unbalanced, or incomplete, this ensemble technique improves the model's accuracy and stability (Cutler et al., 2007). RF can handle continuous and categorical variables, making it amenable to complicated datasets like those commonly utilized in remote sensing research (Strobl et al., 2007). They may consist of various features like vegetation, urban areas, and water bodies.

The RF encoder builds an ensemble of regression trees in training (Sahin, 2020). The ensemble method improves accuracy and stability by aggregating the predictions of a collection of independent decision trees (Shelestov et al., 2017). To account for differences in the training sets, bootstrap samples are randomly chosen first from the dataset. For every bootstrap sample, a decision tree is grown in a random subspace of the features available. Recursive binary splitting of the data in line with feature thresholds that minimize impurity—usually in terms of entropy or Gini impurity—is the manner in which these trees are grown (Cutler, 2012; Goldstein et al., 2010). Repeating this process creates a forest of decision trees. A new instance is classified by pushing it down all the decision trees. For classification problems, the mode, or most frequent class, of the ensemble's predictions is the final prediction, as shown in Eq. 3-1. All these ideas are embodied in the design of RF, making it more powerful on a wide range of machine learning problems.

$$y_{RF}(x) = Mode(y_{tree}^{1}(x), y_{tree}^{2}(x), \ldots\ldots y_{tree}^{n}(x)) \qquad (3\text{-}1)$$

where $y_{RF}(x)$ is the random forest prediction for sample x and where $y_{tree}^{i}(x)$ is the prediction of the ith decision tree for sample x.

Support Vector Machine (SVM)

Because of its capacity to efficiently handle high-dimensional data and classify intricate, non-linear relationships, Support Vector Machines (SVM) is usually chosen for land cover classification. SVM improves generalization and robustness, particularly in handling small or unbalanced datasets, through the identification of the optimal hyperplane that maximizes the margin among classes (Cortes & Vapnik, 1995). As the data tends to be high-dimensional and the land cover classes (e.g., urban, vegetation, and water bodies) are not necessarily linearly separable, this point is especially relevant for remote sensing applications (Müller et al., 2001). Even when the dataset is noisy or the classes overlap, SVM will not overfit as much as simpler models like K-Nearest Neighbors (KNN) (Cortes & Vapnik, 1995). Besides, SVM is extremely appropriate for complex remote sensing data as it can use the kernel method to map non-linearly separable data onto higher-dimensional space where linear separation can be obtained (Schölkopf et al., 2001).

The rigorous theoretical foundations of SVM that are geared towards margin optimization and minimization of the classification error give it an advantage compared to other models like Decision Trees. This results in more stable predictions, particularly in high-dimensional space

(Vapnik, 1995). In contrast to other models like Random Forest (RF), which need huge quantities of data to attain optimum performance, SVM has been demonstrated to perform effectively in situations when small quantities of labeled data are available for training (Müller et al., 2001). SVM is an attractive option for remote sensing land cover classification because it performs highly in high-dimensional space and can handle non-linear separations, although it can be computationally demanding because of having to solve difficult optimization problems.

In remote sensing and other classification problems, the SVM algorithm is a high achiever (Maulik & Chakraborty, 2017). Determining the correct surface to divide subclasses is how SVM works. To make it more robust and generalize to unknown data, it seeks to maximize the margin among data points of various features that are nearest to one another (Muñoz-Marí et al., 2010). Let us consider xi as attribute vectors and yi as class names (either -1 or 1 for binary classification) in the original data {(x1, y1), (x2, y2)., (xn, yn)}. For linearly separable data sets (Eqs. 3-2 and 3-3):

$$Minimize \frac{1}{2} \|w\|^2 \tag{3-2}$$

subject to:

$$y_i(w * x_i + b) \geq 1 \;\; for\ all\ i \tag{3-3}$$

In order to convert nonlinearly separable datasets into a higher-dimensional space that permits linear separation, SVM uses the kernel approach (Eqs. 3-4 and 3-5). The optimization issue turns into:

$$Minimize \frac{1}{2} \|w\|^2 + C \sum_{i}^{n} \xi_i \tag{3-4}$$

subject to:

$$y_i(w * \phi(x_i) + b) \geq 1 - \xi_i \tag{3-5}$$

The kernel algorithm is represented by (, -i.), the regularization parameter is C, and the slack factor is (, -i.) that permits misclassification. In the event that the optimal hyperplane constants w and b are determined, the following criteria should be used to classify a new sample x (Eq. 3-6):

$$f(x) = sign(w * \ \phi(x) + b) \tag{3-6}$$

SVMs are renowned for handling complex relationships and high-dimensional data and are thus suited to many types of classification issues, e.g., land cover classification in remote sensing (RS) applications.

3.6.6. Accuracy assessments

Overall accuracy (OA): OA measures the number of correctly classified samples in the entire data set (Pal et al., 2013b). Equation 3-7 gives a summary measure of the accuracy of classification. The "error matrix" object, which is a byproduct of the confusion matrix, is used in the GEE to calculate the OA. We calculated the total number of correctly classified samples for each feature by adding the diagonal members of this matrix. The percentage of samples correctly classified, or the OA, is determined by dividing this sum by the total number of samples in the dataset.

$$OA = \frac{Sum\ of\ correctly\ classified\ pixel\ in\ the\ diagonal}{Total\ number\ of\ pixel} * 100 \qquad (3\text{-}7)$$

Producer's accuracy (PA): The "error matrix" object, a by-product of the confusion matrix that holds data on correctly and incorrectly classified items by class, is used in the GEE to calculate the PA (Becker et al., 2021). PA is computed by dividing the number of correctly classified pixels by the sum of the row totals, and then multiplying by 100 (Eq. 3-8).

$$PA = \frac{Correctly\ classified\ pixel}{Row\ total} * 100 \qquad (3\text{-}8)$$

User accuracy (UA): The second vital measurement for validation of the classification task is the UA. It calculates the percentage of correctly classified samples of a specific class among all the samples that the classifier has determined to be of that class. The number of pixels in a column of a specific class of the confusion matrix and the number of pixels correctly classified in each column (true positives) are multiplied by 100 to get the UA for the class (Eq. 3-9).

$$UA = \frac{Correctly\ classified\ pixel}{Column\ total} * 100 \qquad (3\text{-}9)$$

Kappa Coefficient (K): A numerical measure of interrater agreement that corrects for chance is the kappa statistic. Observed accuracy of classification is contrasted with the accuracy expected by mere chance. Equation 3-10 presents the kappa coefficient (κ) formula:

$$K = \frac{OA - EA}{1 - EX} \tag{3-10}$$

where the expected accuracy (EA) is the percent chance agreement expected, and OA is the percent of correctly classified samples in our overall dataset. Under GEE, the kappa coefficient is calculated by first ascertaining the OA and then ascertaining the EA based on the minimum likelihood of the confusion array.

3.7.Method of data analysis

The flowchart utilizes both Sentinel-2 MSI and Sentinel-1 SAR data to represent the methodological process for classifying urban land use. The starting point of the process is the preprocessing of Sentinel-1 and Sentinel-2 raw data so that it becomes of an appropriate quality for analysis. Preprocessing entails processes such as radiometric calibration, geometric correction, and normalization to remove any distortions or noise from the data (Figure 3-2).

Following processing, the data is split into two main branches: a training and a validation branch. Both branches make use of the processed Sentinel-1 and Sentinel-2 data to train the model and validate its accuracy, respectively. While the validation data is used to guarantee the model's accuracy and reliability in categorization, the training data is employed to build the model.

Fusion is the subsequent process, which combines the preprocessed data from both satellite sources with a view to augmenting the accuracy and completeness of the classification. Following fusion, machine learning algorithms—more particularly, Support Vector Machines (SVM) and Random Forest (RF)—are applied to the fused data with a perspective to classifying the urban land use. These algorithms are employed in order to classify various categories of land cover and detect patterns.

Following classification, the success of the classification process is assessed using an accuracy assessment. To establish the validity and reliability of the classification result, this step compares the classified output with reference ground truth data. The final output of the methodology is the production of the urban land use map that presents a complete picture of the urban land cover as determined by the classification process.

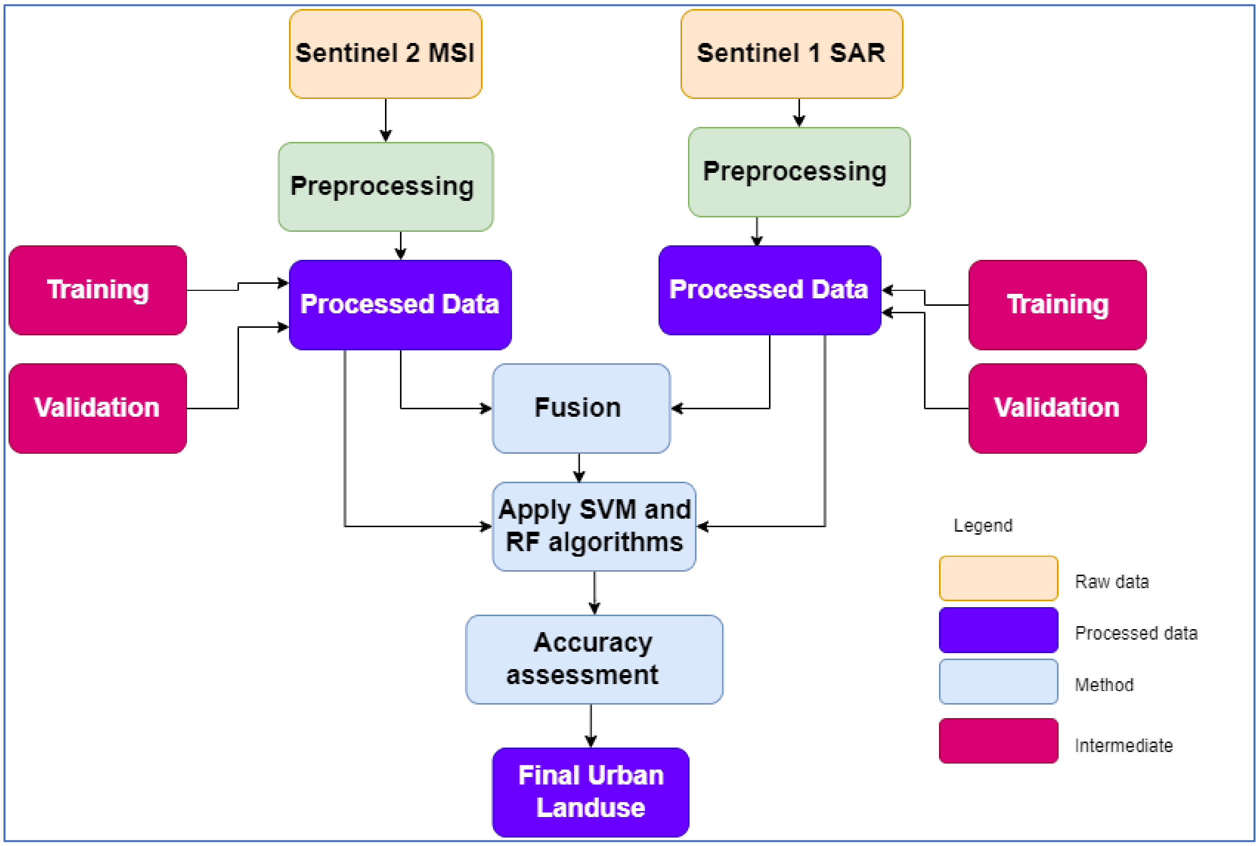

Figure 3-2: Methodological flowchart

CHAPTER FOUR

4. RESULT AND DESCUSSION

4.1.Introduction

The chapter offers a detailed analysis, interpretation, and discussion of the research results. The results are organized with respect to the specific research goals. First, it was necessary to conduct individual land cover classifications using Sentinel-2 MSI and Sentinel-1A SAR datasets. Each dataset was classified using two machine learning models, i.e., Random Forest (RF) and Support Vector Machine (SVM). The classified results were compared to assess land cover area estimates and validate the differences in performance between the two algorithms.

Phase two of the study involved the investigation of Sentinel-1 and Sentinel-2 dataset fusion. Classification of the fused dataset was performed using RF and SVM, and comparative area estimate assessment was carried out to determine the influence of multi-sensor data fusion on classification.

The third stage of analysis compared comparative performance assessment between RF and SVM between three scenarios: Sentinel-2 MSI only, Sentinel-1 SAR only, and the fused data. Classification performance was examined using confusion matrices, overall accuracy measures, and the Kappa coefficient to determine the performance of each algorithm and dataset pairing.

The final section of the chapter is a land cover change detection between 2015 and 2025. The detection is carried out based on the best classification results, as determined from the prior accuracy assessments, and provides details of the urban growth dynamics and land cover changes in Adama City.

4.2.Sentinel 2 MSI classifications

4.2.1. Sentinel 2 MSI classification using SVM

The Support Vector Machine (SVM) algorithm classification result using Sentinel-2 MSI data did well in classifying five primary land use and land cover (LULC) classes, as shown from the study area: Built-up, Agriculture, Forest, Shrubland, and Bareland, represented by Figure 4-1. The spatial arrangement of the classes signifies the pattern of the landscape of the region. The city's core area is primarily classified as Built-up, e.g., high-density urban settlements, areas adjacent to major roads, and settlements along dense road networks. The outer boundary of the city is primarily classified as Agricultural land, which holds the highest percentage of the study area. Forests are primarily fragmented along ridges and mountain slopes, and Shrublands tend to be found surrounding these patches of forests as a transition buffer zone. Bareland occupies a minute portion of the whole area, present as patches scattered throughout the landscape. Table 4-1 illustrates that SVM classification result reveals that Agricultural land is the dominant class, occupying 21,235.69 hectares (67.84%) of study area, followed by Built-up areas at 5,364.57 hectares (17.14%). The Forest category possesses 2,569.65 hectares (8.21%), Shrubland possesses 1,743.46 hectares (5.57%), and Bareland possesses the lowest at 390.83 hectares (1.25%).

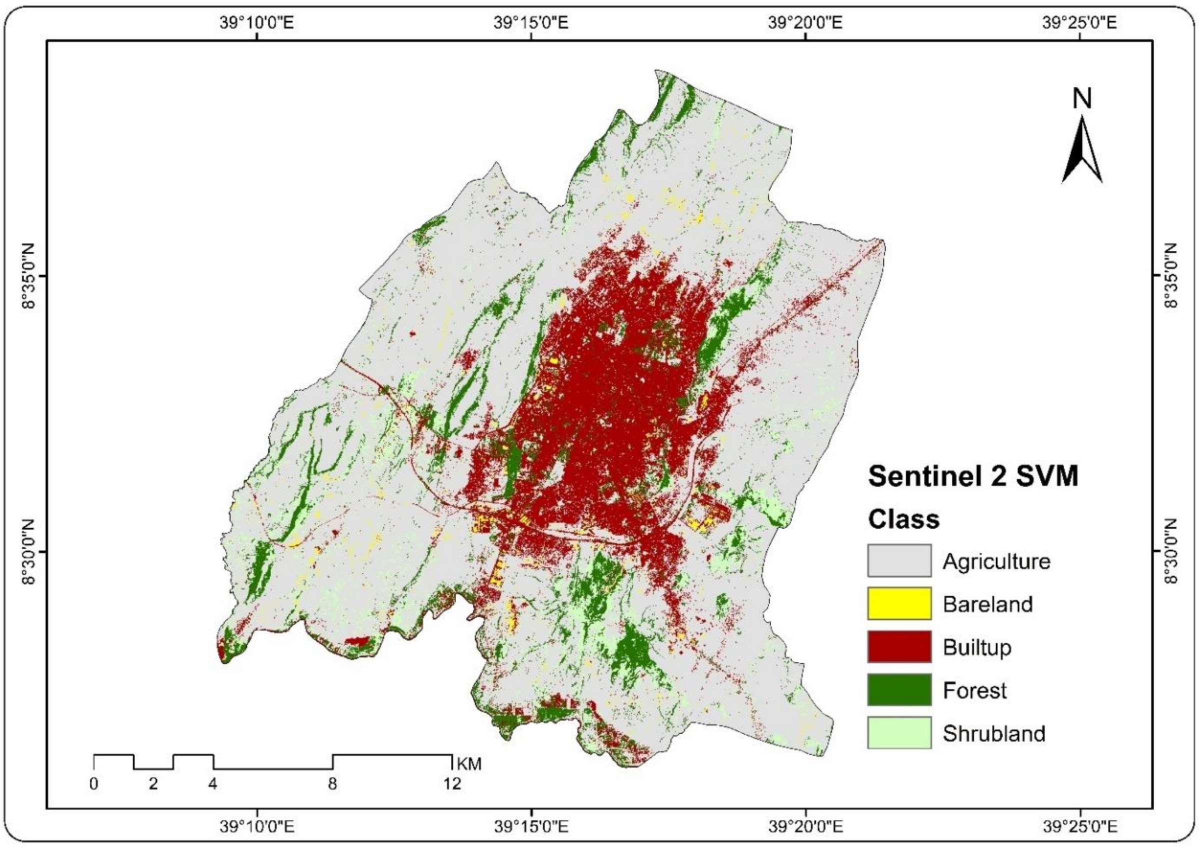

Figure 4-1: Sentinel 2 MSI land use land cover classification using SVM algorithm

4.2.2. Sentinel 2 MSI classification using RF

Random Forest (RF) algorithm is also demonstrated to produce a classification result for Sentinel-2 MSI data that generally follows patterns under the SVM model but with major deviations in the areal distribution of land cover classes (Figure 4-2). As shown in Table 4-1, RF classifier assigned the Built-up class a larger area of 5,492.34 hectares (17.55%) compared to SVM, which signifies a very slightly more liberal classification of urban features and impervious surfaces. Agriculture, on the other hand, was assigned a less area (19,833.66 hectares, 63.36%) compared to SVM since RF tagged some agriculture patches as Built-up or Forest. The Forest category grew significantly in RF classification, which had an area of 3,462.57 hectares (11.06%), whereas in SVM, it was 2,569.65 hectares (8.21%). The Shrubland was slightly higher in RF output (1,914.25 hectares, 6.11%) than in SVM output. Bareland also expanded to 601.38 hectares (1.92%), which was much larger than the area allotted by SVM for this category.

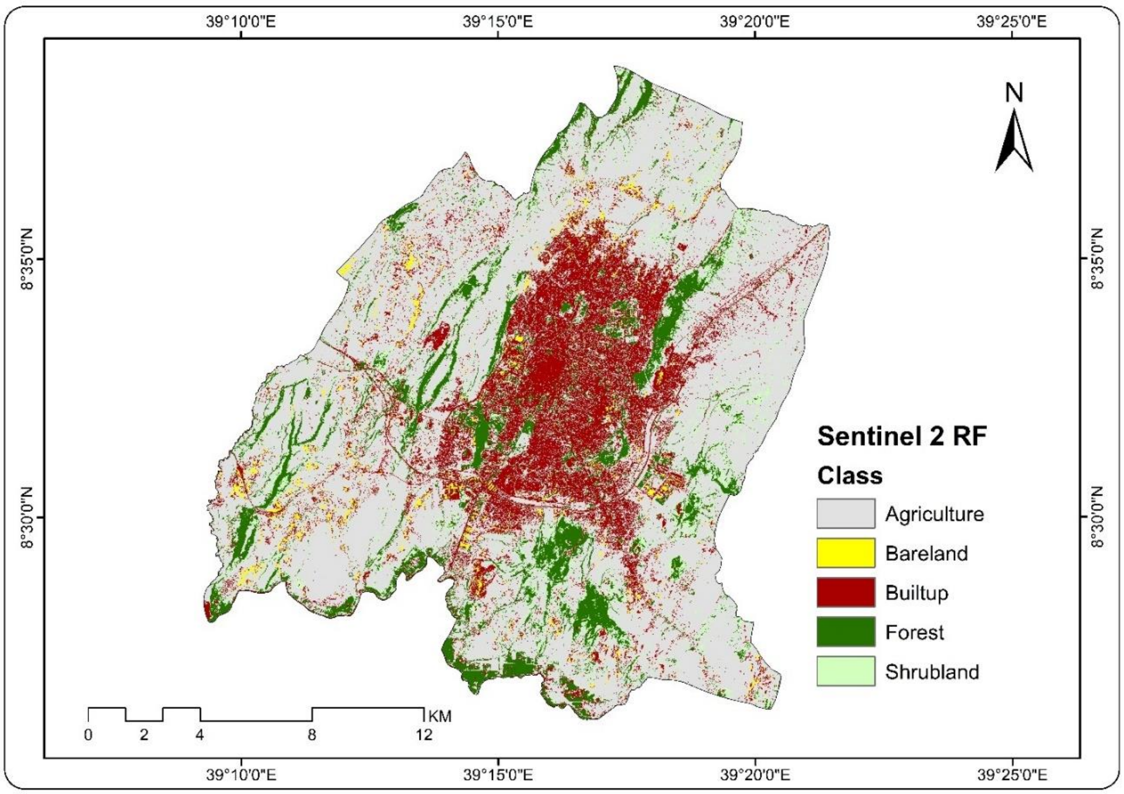

Figure 4-2: Sentinel 2 MSI land use land cover classification using RF algorithm

SVM and RF class results of Sentinel-2 MSI data comparison reveals noteworthy variations in the distribution of land cover classes. Built-up and Bareland were classified with a comparatively larger area by Random Forest (RF) algorithm than Support Vector Machine (SVM), reflecting RF's higher responsiveness to urban and open soil features. Conversely, SVM gave more room to Agriculture, and RF reallocated patches of cultivated land to Forest and Shrubland, which is an indication of RF's larger ability to predict vegetation diversity and canopy dynamics. The Forest and Shrubland classes were especially mapped more extensively by RF, likely due to its ensemble decision-tree structure that handles spectral variability more readily than SVM's boundary-based approach.

Table 4-1: Classification Area difference between the two algorithms for Sentinel 2 MSI

	SVM		RF	
Class	Area	Percentage	Area	Percentage
Builtup	5364.57	17.14	5492.34	17.55
Agriculture	21235.69	67.84	19833.66	63.36
Forest	2569.65	8.21	3462.57	11.06
Shrubland	1743.46	5.57	1914.25	6.11
Bareland	390.83	1.25	601.38	1.92
Total	31304.2	100	31304.2	100

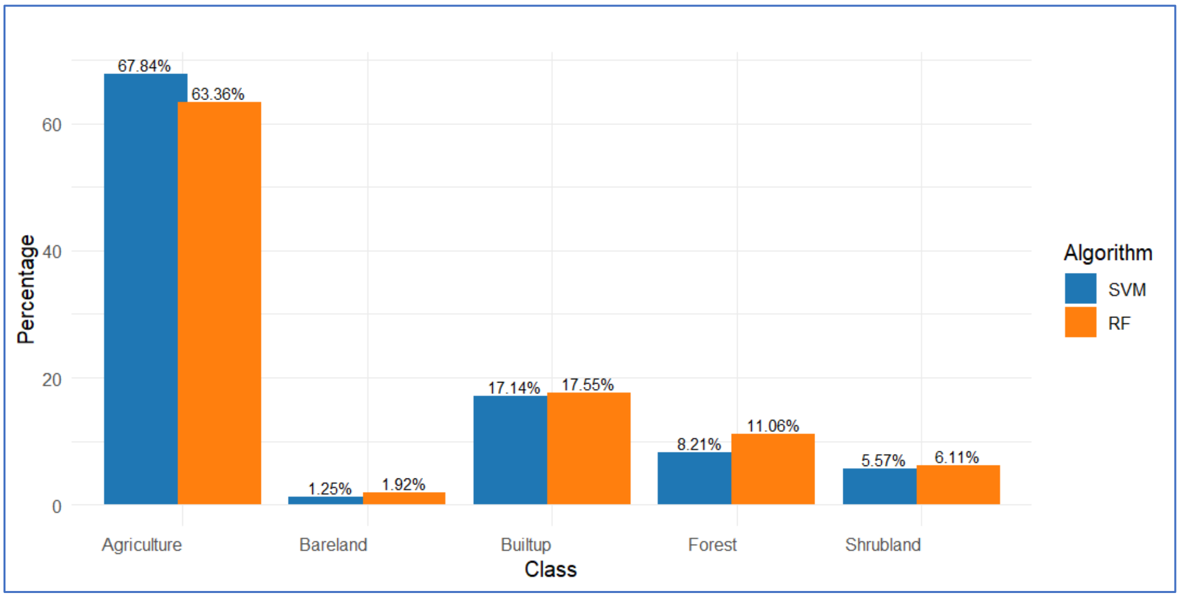

Figure 4-3: RF and SVM algorithms Land cover classification difference for Sentinel 2 MSI data

4.2.3. Accuracy assessment Sentinel 2 RF and SVM

As shown in Table 4-2, the Sentinel-2 MSI classification using the Support Vector Machine (SVM) algorithm produced a very high overall accuracy (OA) of 83% and a Kappa index of 0.78 showing high agreement between the classified land cover map and the reference ground truth data. Of the five land cover classes, the Built-up class boasted the best producer's accuracy (PA) of 89.74%, indicating that the majority of the actual built-up areas were accurately classified, and its user's accuracy (UA) was also high at 87.50%, indicating most of the pixels classified as Built-up were correct.

Similarly, the Agriculture class was also good with PA of 88.89% and UA of 86.49%, which was such that the classifier could distinguish between cultivated lands correctly. The Forest and Shrubland classes both recorded fair performances with PA values of 78.79% and 75.76% and slightly lesser UA values of 70.27% and 86.21%, respectively. The Bareland class, although with fewer samples, recorded fair accuracies with PA of 76.92% and UA of 83.33%. Overall, the SVM classifier was satisfactory in its classification performance, particularly for the two common classes Built-up and Agriculture and handled the class separability of the remaining land cover classes well, demonstrating that SVM is a suitable algorithm for land cover mapping based on Sentinel-2 MSI.

Table 4-2: Sentinel 2 MSI SVM classification accuracy assessment result

	Built-up	Agriculture	Forest	Shrubland	Bareland	Total	PA
Built-up	35	2	0	2	0	39	89.74
Agriculture	0	32	2	1	1	36	88.89
Forest	2	1	26	1	3	33	78.79
Shrubland	3	0	5	25	0	33	75.76
Bareland	0	2	4	0	20	26	76.92
Total	40	37	37	29	24	167	
UA	87.50	86.49	70.27	86.21	83.33		
OA	0.83						
Kappa	0.78						

From Table 4-3, it can be observed that RF classification of Sentinel-2 MSI yielded slightly lower total accuracy at 74% as well as Kappa value of 0.67, indicating moderate agreement between classified output and reference. Upon close examination, the Built-up class had a PA of 77.14% and a UA of 75.00%, both of which were far lower than for SVM, suggesting that RF did slightly poorly in identifying the urban areas.

For the Agriculture class, RF had a PA of 74.36% and a UA of 78.38%, both of which were good but also somewhat inferior to those of SVM. Shrubland and Forest classes were corrected with PA accuracies of 76.67% and 68.42%, and UA accuracies of 67.65% and 76.47%, respectively. The Bareland class, being disposed to the signatures of sparse or uncertain pixel classes, was 72.00% PA and 69.23% UA, reflecting some cross-classification confusion with those similarly low-vegetation land covers. Overall, while RF algorithm proved capable of dealing with heterogeneous and heterogeneous land covers, its classification performance was less consistent than SVM, particularly for minority or scattered classes like Bareland and Shrubland.

Table 4-3: Sentinel 2 MSI RF classification accuracy assessment result

	Built-up	Agriculture	Forest	Shrubland	Bareland	Total	PA
Built-up	27	2	0	2	4	35	77.14
Agriculture	4	29	2	3	1	39	74.36
Forest	2	1	23	1	3	30	76.67
Shrubland	3	3	6	26	0	38	68.42
Bareland	0	2	3	2	18	25	72.00
Total	36	37	34	34	26	167	
UA	75.00	78.38	67.65	76.47	69.23		
OA	0.74						
Kappa	0.67						

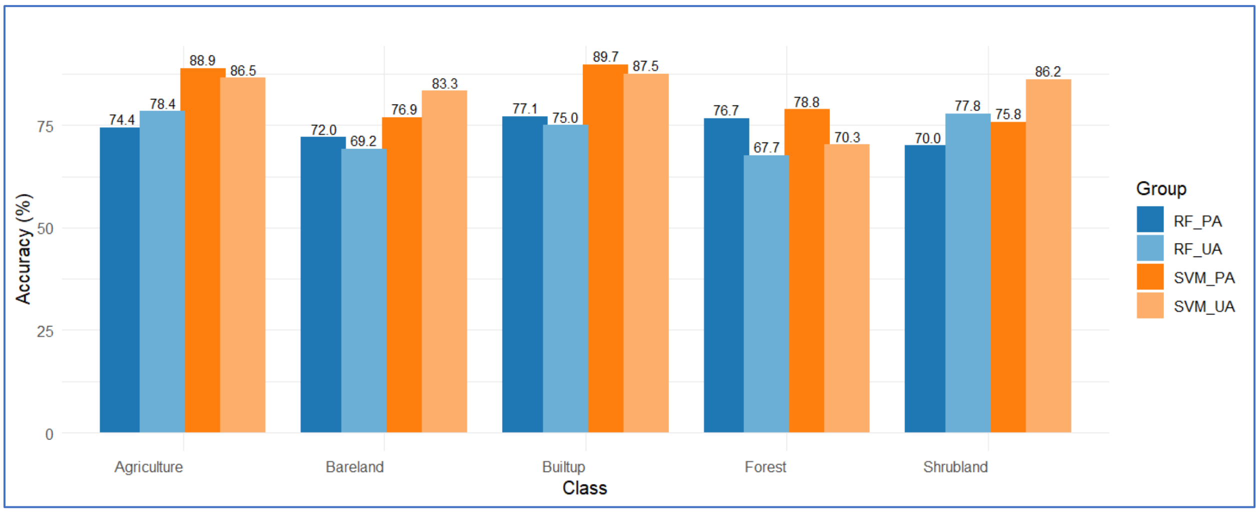

Figure 4-4: Accuracy assessments comparison between SVM and RF classifications for Sentinel 2 MSI

4.3.Sentinel 1A SAR classifications

4.3.1. Sentinel 1A SAR SVM classification

Sentinel-1A SAR classification with the Support Vector Machine (SVM) algorithm illustrates (Table 4-4) that the algorithm can classify and differentiate among the five land cover classes with unique spatial patterns. The Built-up areas accounted for 5,417.89 hectares or 17.31% of the total landscape, which supports SVM was highly successful in detecting the high-density urban texture and the associated radar backscatter signatures typical of built-up environments. Agricultural class dominated the regional coverage, occupying 19,810.27 hectares or 63.28% of the area, which implied that SVM effectively discriminated fields because of their comparative homogeneity of texture and backscatter profiles in radar images. Forest cover patches occupied 3,362.42 hectares (10.74%) and Shrubland occupied 2,322.7 hectares (7.42%), showing how efficiently the algorithm does vegetative land cover classes even where discrimination by radar data limitations of fine vegetation patterns are well defined. Bareland occupied 390.92 hectares (1.25%), showing SVM's ability to discriminate unvegetated open surfaces even in the case of backscatter-affected SAR data. Overall, SVM performed well, and in Built-up and Agricultural area classification, it was excellent, showing its strength in dealing with the complex scattering effects which are characteristic of radar imagery.

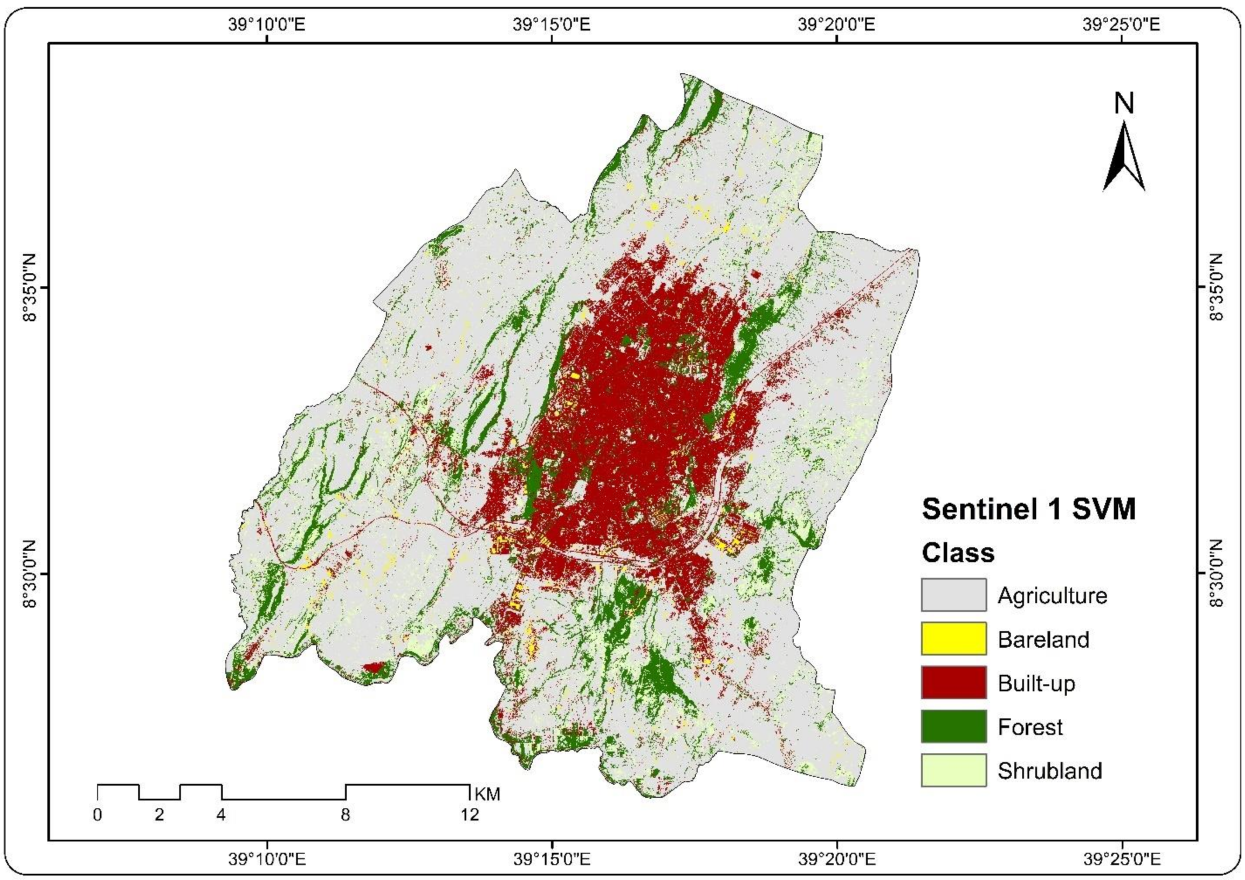

Figure 4-5: Sentinel 1 land use land cover classification using SVM algorithm

4.3.2. Sentinel 1A SAR RF classification

The RF classification output of Sentinel-1A SAR data, as evident from Table 4-4, reflected enormous discrepancies from SVM, especially in the spatial arrangement of the land cover classes over the study area. The Built-up class rose to 5,757.74 hectares (18.39%) using RF classification, i.e., RF sometimes overestimated urban extents perhaps due to confusing spectrally comparable surfaces such as compacted exposed soils or road networks as Built-up. The agriculture class consisted of 18,939.14 hectares (60.50%), which was slightly lower than was classified by SVM, and this could mean that RF may have redistributed some percentage of this class to neighboring classes such as Forest or Bareland.

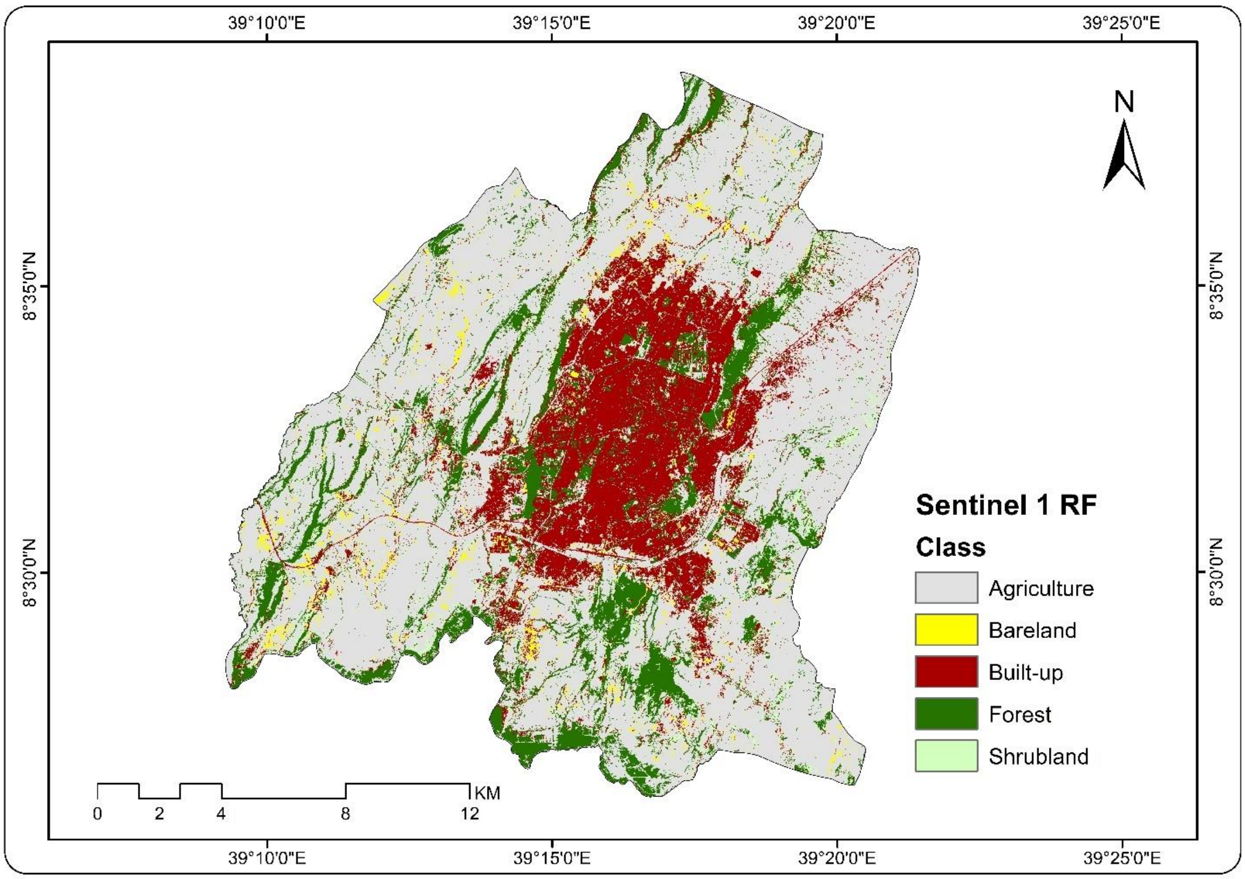

Figure 4-6: Sentinel 1 land use land cover classification using RF algorithm

Forest class area expanded significantly to 4,223.71 hectares (13.49%) over SVM predictions, which compensates for RF's ensemble tree structure biasing the forest class over existing radar signal conditions, which presumably include some of the edges of the agricultural or shrubland classes.

Shrubland area fell to 1,736.11 hectares (5.55%), which compensates for RF's propensity to blur this edge class with other dominant classes such as Forest or Agriculture. Lastly, Bareland was allocated to 647.5 hectares (2.07%), higher than the SVM output, due to RF's behavior of classifying open, low-backscatter areas more intensively. The results indicate RF's special character of processing radar information such that its application of an ensemble of many decision trees sometimes results in overgeneralization

Table 4-4: Classification Area difference between the two algorithms for Sentinel 1 SAR

	SVM		RF	
Class	Area	Percentage	Area	Percentage
Built-up	5417.89	17.31	5757.74	18.39
Agriculture	19810.27	63.28	18939.14	60.50
Forest	3362.42	10.74	4223.71	13.49
Shrubland	2322.7	7.42	1736.11	5.55
Bareland	390.92	1.25	647.5	2.07
Total	31304.2	100	31304.2	100

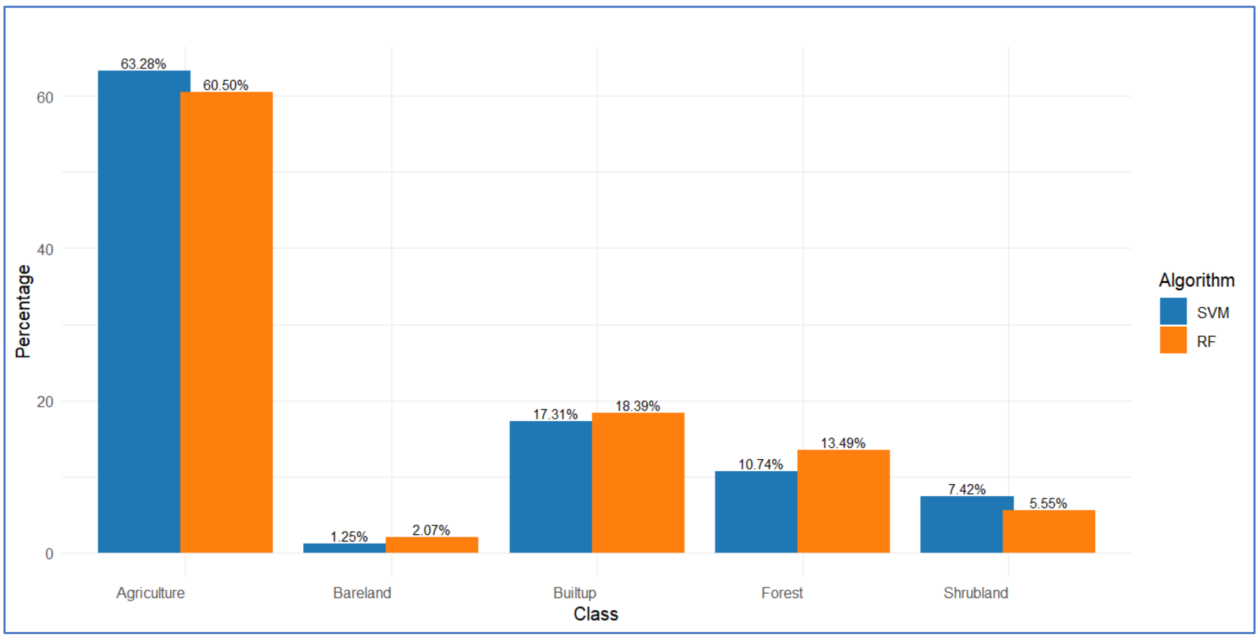

Figure 4-7: RF and SVM algorithms Land cover classification difference for Sentinel 1 SAR Data

4.3.3. Accuracy assessment for Sentinel 1A

Accuracy assessment of Sentinel-1A SAR classification using Random Forest (RF) algorithm (see Table 4-5) reveals a very good overall performance.

The categorization had an Overall Accuracy (OA) of 85% and a Kappa coefficient of 0.81, indicating high agreement between the classified output and reference data and a negligible effect of random chance. At class level too, the Built-up area was good with Producer's Accuracy (PA) being 89.19% and User's Accuracy (UA) being 86.84%, thus demonstrating that the RF model is capable of distinguishing between urban features in SAR data correctly. The Agriculture class too was healthy, with PA and UA both being 86.11%, showing good mapping for this broad land cover class. The Forest class had a PA of 78.79% and UA of 81.25%, showing excellent classification performance considering the intrinsic difficulties in radar backscatter change of forest canopies.

Shrubland was accurately classified with a PA of 87.88% and UA of 85.29%, showing RF's capability in detecting transitional vegetation belts. In addition, the Bareland class also achieved a PA of 82.14% and UA of 85.19%, once more attributing to the strength of the model in identifying non-vegetated, open surfaces correctly. The result in general bears testament to the ability of the Random Forest algorithm in handling an uncertain number of land cover classes in radar databases, balancing on the thin edge of accuracy between vegetated and non-vegetated classes in an equal ratio.

Table 4-5: Sentinel 1 SAR RF classification accuracy assessment result

	Built-up	Agriculture	Forest	Shrubland	Bareland	Total	PA
Built-up	33	2	0	2	0	37	89.19
Agriculture	2	31	2	0	1	36	86.11
Forest	2	1	26	1	3	33	78.79
Shrubland	1	0	3	29	0	33	87.88
Bareland	0	2	1	2	23	28	82.14
Total	38	36	32	34	27	167	
UA	86.84	86.11	81.25	85.29	85.19		
OA	0.85						
Kappa	0.81						

Sentinel-1A SAR image SVM classification in Table 4-6 yielded good performance but somewhat inferior to RF. Sentinel-1A SAR image SVM classification in Table 4-6 yielded good performance but somewhat inferior to RF. OA was 75% with a Kappa of 0.68, which reflects moderate agreement with reference and which reflects SVM struggled more with the radar-based class discrimination than RF. In class-wise accuracy, Built-up class achieved PA = 76.47% and UA = 74.29%, falling slightly short of RF model because of ambiguity between urban ground and spectrally similar bare or road surfaces in radar images. Agriculture class achieved a PA = 70.73%

and a UA = 76.32% and showed fair but poor performance, possibly because agricultural fields are heterogeneous in radar backscatter. Forest class was 78.79% PA and 72.22% UA, suggesting SVM could differentiate forest areas but with less certainty than RF. Shrubland was the worst class, with PA = 69.70% and UA = 74.19%, showing significant misclassification rates probably into Forest or Agriculture, a common issue for radar-based shrubland classification. Bareland was improved, with PA of 80.77% and UA of 77.78%, which emphasized SVM's capability in classifying open and surface surfaces. As a whole, although SVM overall was fine for classes, RF was more stable and reliable for Sentinel-1 SAR land cover classification.

Table 4-6: Sentinel 1 SAR SVM classification accuracy assessment result

	Built-up	Agriculture	Forest	Shrubland	Bareland	Total	PA
Built-up	26	2	4	2	0	34	76.47
Agriculture	6	29	2	3	1	41	70.73
Forest	2	1	26	1	3	33	78.79
Shrubland	1	4	3	23	2	33	69.70
Bareland	0	2	1	2	21	26	80.77
Total	35	38	36	31	27	167	
UA	74.29	76.32	72.22	74.19	77.78		
OA	0.75						
Kappa	0.68						

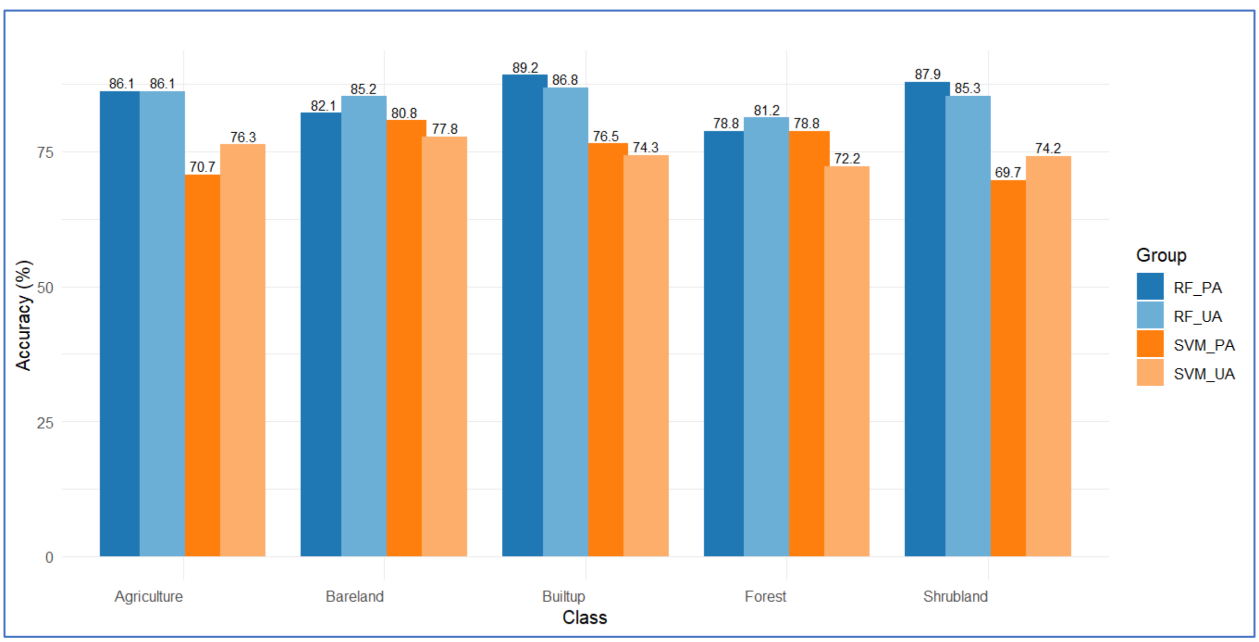

Figure 4-8: Accuracy assessments comparison between SVM and RF classifications for Sentinel 1 SAR

4.4.Combined classifications

4.4.1. Combined using SVM classification

Classification of the merged Sentinel-1A SAR and Sentinel-2 MSI data using the Support Vector Machine (SVM) algorithm produced a heterogenous land cover pattern distribution, both retrieving the strengths and weaknesses of SVM processing multi-source data. As Table 4-7 shows, the Built-up class was mapped onto 17.31% (5,417.89 hectares) of the study area. The ratio is plausible in light of the strong reflectance of city surfaces over Sentinel-2's near-infrared and visible bands, and the increased radar backscatter of built-up buildings in Sentinel-1 images. Nevertheless, the lower estimate of built-up areas compared to that of the RF classifier is attributable to the hyperplane-based approach of SVM classification, which tends to classify borderline or edge pixels more cautionally—especially where spectral ambiguity encompasses built-up areas and other comparable land covers, such as bareland.

Agricultural land was the dominant class in the SVM classification, at 63.28% (19,810.27 hectares). This bias may mean that SVM overgeneralizes spectrally heterogeneous but homogeneously distributed vegetated zones. Several radar and spectral signatures of croplands, grasslands, and sparsely vegetated zones can lead to overclassification, especially when training data sets for these classes overlap in feature space.

Forest zones were classified at 10.74% (3,362.42 hectares). While forests typically have distinct signatures—high NDVI and low SAR backscatter due to canopy structure—SVM may underestimate them, particularly forest edges where gradual changes towards shrubland or agricultural land make classification ambiguous. Because radar response is texture-dependent in forest canopy, SVM decision boundaries may strip transitional or mixed pixels from the forest class unless they are near the algorithm's support vectors.

Shrubland accounted for 7.42% (2,322.7 hectares) of classified output. The relatively higher percentage compared to RF signals SVM's sensitivity to small variations in spectral and radar traits common in shrubland communities. Since these categories of areas are often heterogeneously spatial and spectral, SVM can identify them more loosely, especially if there is overlap among class features.

Lastly, bareland was the worst-represented category at 1.25% (390.92 hectares). This sparsely mapped plot illustrates SVM's conservative approach in classifying thinly covered or recently disturbed surfaces. These units habitually resemble built-up regions or dry croplands in both optical and radar data, and since they have weak and inconsistently strong spectral identity, they will be less often classified with certainty as bareland unless clearly different in training data.

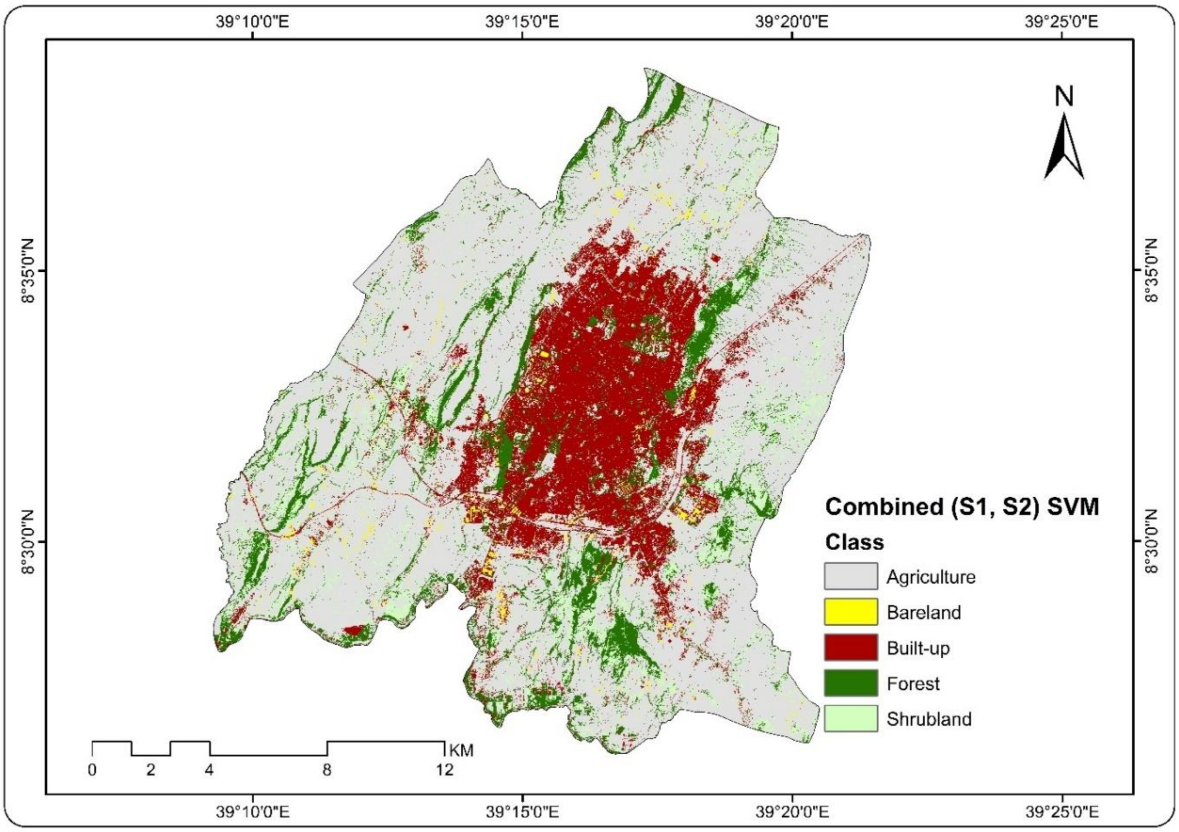

Figure 4-9: Combined land use land cover classification using SVM algorithm

4.4.2. Combined using RF classification

Random Forest (RF) classification of combined Sentinel-1A SAR and Sentinel-2 MSI produced a more balanced and seemingly realistic land cover mix, reflective of the strength of the algorithm in addressing nonlinear relationships and composite data sources. According to Table 4-7, Built-up area covered 18.39% (5,757.74 ha), a nearly greater percentage than the SVM output. That makes sense considering RF's ensemble approach, which relies on aggregating decisions from numerous decision trees, allowing it to better delineate the scattered urban area from spectrally or texturally adjacent classes such as bareland or dry cropland. Structural sensitivity of radar combined with Sentinel-2's spectral data most likely helped RF detect hard surfaces like rooftops, roads, and concrete strongly, which are likely to confuse other algorithms (Belgiu & Drăguţ, 2016).

The agriculture class was predicted as 60.50% (18,939.14 ha), slightly lower than that predicted by SVM. RF's lower value here is an indication of its greater capacity to pick up finer inter-class relationships, especially for vegetation. Agricultural fields, being structurally and seasonally variable, typically spectrally intersect with forest and shrubland, but RF can more comfortably deal with such ambiguities by using a variety of predictors and bootstrapped samples to minimize bias, preventing overgeneralization from SVM (Rodríguez-Galiano et al., 2012).

For Forest fields, RF accurately predicted 13.49% (4,223.71 ha) — far larger than the result from SVM. This expansion shows RF performed better to recognize forested regions accurately, perhaps due to its capacity to leverage both dense canopy's invariant spectral signature within Sentinel-2 and the salient radar backscatter features in Sentinel-1. RF's random choice of features at training also contributes to misclassification minimization by producing diverse trees that are specialists in subsets of features such that the ensemble can effectively find forests in even spectrally mixed areas (Cutler et al., 2007).

Shrubland received a lesser proportion of 5.55% (1,736.11 ha) compared to SVM. RF's decrease in this category is due to its ensemble voting strategy, which reduces overestimation in transition zones — a common pitfall of SVM because of overlapping margins of classes. Shrubland's mixed cover type and density make misclassifications with forest or agriculture more likely, but RF, using a majority voting system, reduces the likelihood of such misclassifications.

Bareland was more extensively classified with RF: 2.07% (647.5 ha), nearly double SVM's estimation. This improvement indicates RF's ability in distinguishing low-vegetation or open ground classes, especially when joined radar backscatter and optical reflectance signatures give certain evidences of non-vegetated covers. RF's ability in handling nonlinear and high-dimensional data allows it to delineate finer between bareland and early-stage agricultural land or sparsely vegetated shrubland, where SVM is cautious.

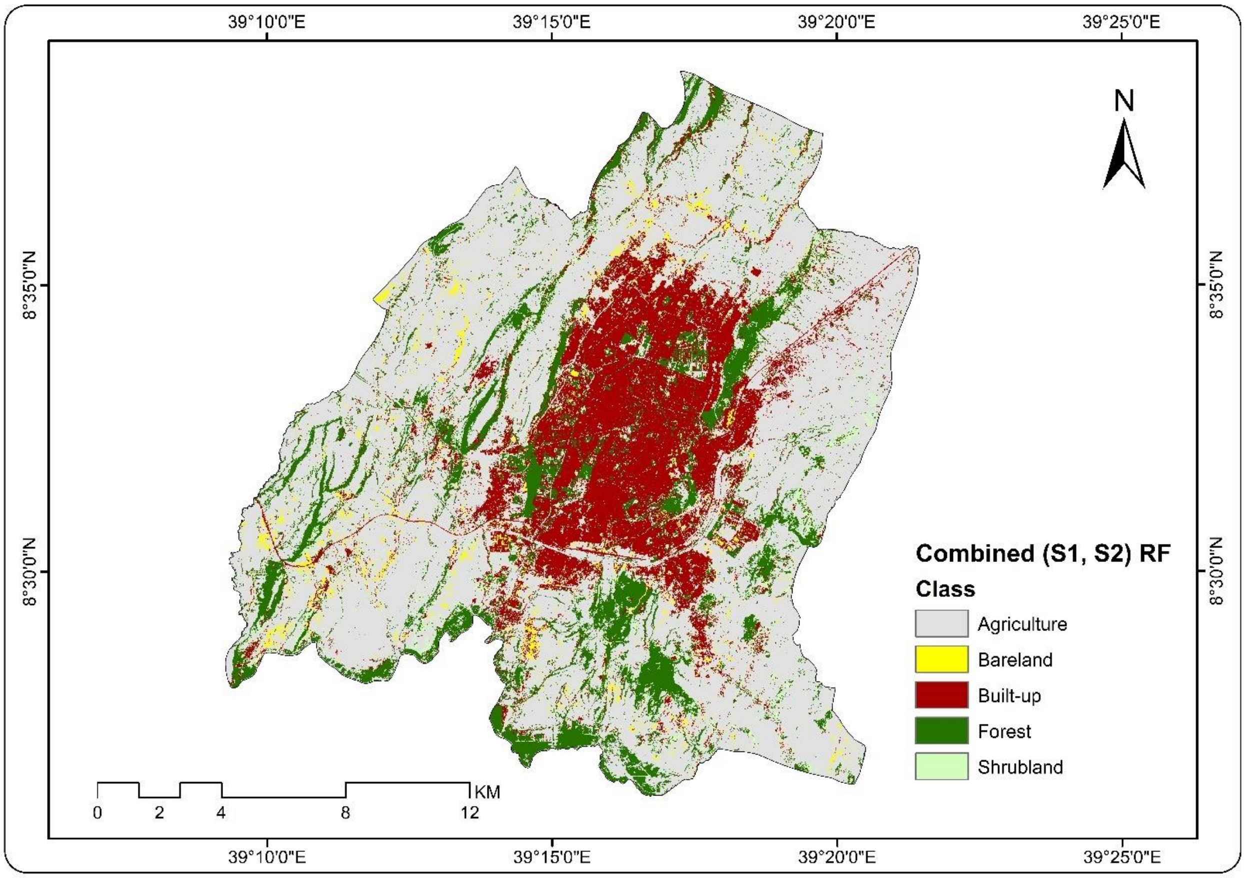

Figure 4-10: Combined land use land cover classification using RF algorithm

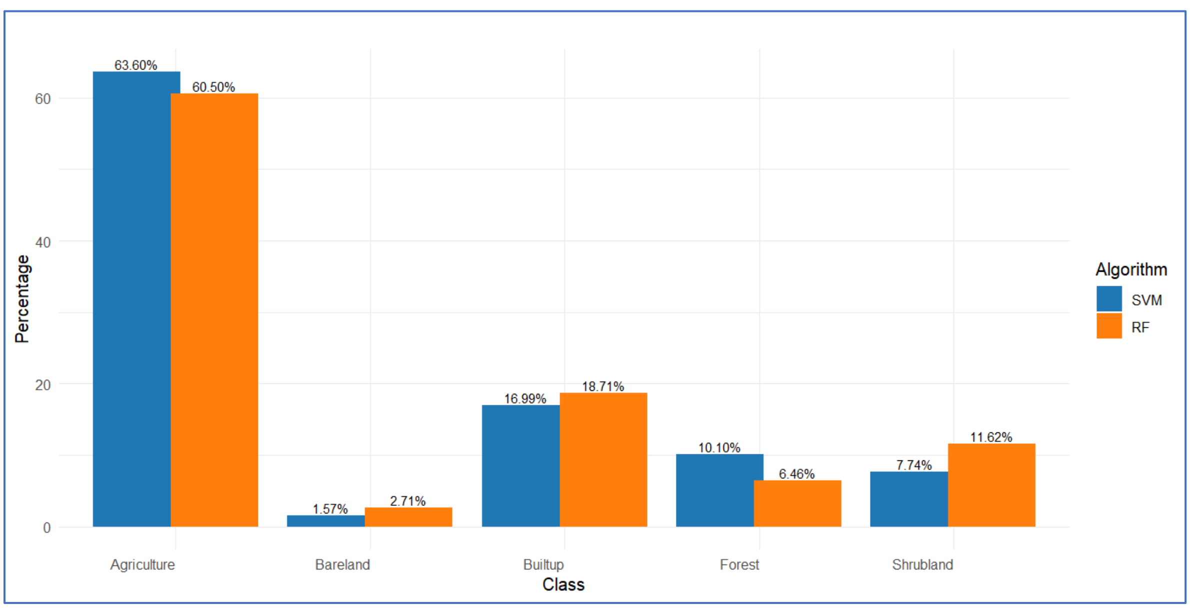

Figure 4-11: RF and SVM algorithms Land cover classification difference for combined data

Table 4-7: Classification Area difference between the two algorithms for combined Satellite data

	SVM		RF	
Class	Area	Percentage	Area	Percentage
Built-up	5417.89	17.31	5757.74	18.39
Agriculture	19810.27	63.28	18939.14	60.50
Forest	3362.42	10.74	4223.71	13.49
Shrubland	2322.7	7.42	1736.11	5.55
Bareland	390.92	1.25	647.5	2.07
Total	31304.2	100	31304.2	100

4.4.3. Accuracy assessment for the Combined classification using RF

The Random Forest (RF) classification of the combined Sentinel 1A SAR and Sentinel 2 MSI dataset demonstrates robust performance across most land use and land cover (LULC) classes. With an Overall Accuracy (OA) of 83% and a Kappa coefficient of 0.78, the RF algorithm effectively utilized the complementary strengths of both radar and optical data, achieving strong classification results.

For built-up areas, RF showed a high Producer's Accuracy (PA) of 86.11%, which indicates that the algorithm was successful in correctly identifying urban regions. The User's Accuracy (UA) of 83.78% also reflects the model's efficiency in minimizing misclassifications of non-urban areas as built-up, showcasing RF's capability in distinguishing urban landscapes from other land cover types, particularly with the aid of distinct structural features captured by SAR data.

When classifying agriculture, RF performed well with a PA of 76.92%, indicating that it successfully identified most agricultural areas. The UA of 85.71% reveals that RF was able to accurately classify agricultural land, with fewer misclassifications into other categories. However, the relatively lower PA suggests that there may have been some confusion between agricultural areas and other land covers, particularly where agricultural fields may overlap with shrubland or bareland.

The forest class saw a very strong classification performance with a PA of 87.50%, signaling that RF effectively identified forested regions, utilizing both SAR data (for forest structure) and optical data (for vegetation indices). The UA of 80.00% further confirms the algorithm's ability to minimize misclassification, although some forest areas may have been confused with agricultural or shrubland regions, particularly in areas where vegetation cover transitions occur.

For shrubland, RF showed a PA of 80.65% and a UA of 75.76%, indicating that while it could reliably identify shrubland areas, there was some ambiguity in distinguishing shrubland from similar vegetation types like forest or agriculture. These lower values might reflect the mixed nature of shrubland areas and their proximity to other land cover types, making classification more challenging.

Finally, bareland was classified with a PA of 82.76% and a UA of 88.89%, showing that RF had strong performance in identifying sparsely vegetated or cleared areas. The high UA suggests that RF successfully identified bareland areas with minimal misclassification, leveraging both the radar and optical data's ability to distinguish non-vegetated surfaces from other land types.

Table 4-8: Combined Satellite data classification accuracy assessment result using RF

	Built-up	Agriculture	Forest	Shrubland	Bareland	Total	PA
Built-up	31	2	1	2	0	36	86.11
Agriculture	3	30	2	3	1	39	76.92
Forest	2	1	28	1	0	32	87.50
Shrubland	1	0	3	25	2	31	80.65
Bareland	0	2	1	2	24	29	82.76
Total	37	35	35	33	27	167	
UA	83.78	85.71	80.00	75.76	88.89		
OA	0.83						
Kappa	0.78						

4.4.4. Accuracy assessment for the Combined classification using SVM

The Support Vector Machine (SVM) classification of the combined Sentinel 1A SAR and Sentinel 2 MSI dataset, while still yielding good results, had lower overall accuracy than RF. The Overall Accuracy (OA) of 77% and Kappa coefficient of 0.71 indicate moderate agreement between the classified results and the reference data. These results suggest that SVM had more difficulty with the complexities of combining SAR and optical data, particularly in handling transitional land covers.

For built-up areas, SVM achieved a PA of 85.71%, which is slightly lower than RF's performance. However, the UA of 88.24% indicates that SVM was fairly reliable in identifying urban regions, with fewer false positives. SVM performed relatively well with built-up areas, likely due to the clear boundaries and distinctive features of urban environments, which both SAR and optical data can easily identify.

In the case of agriculture, SVM produced a PA of 71.79% and a UA of 75.68%, which is lower than RF's performance. This suggests that SVM struggled more to accurately differentiate agricultural areas, possibly due to spectral overlap with other land cover types like shrubland or bareland. The lower PA reflects the difficulty of accurately capturing all agricultural areas, particularly in regions where farming activities are less distinct or transitioning.

For forest, SVM achieved a PA of 80.00%, which is comparable to RF's performance, but the UA of 70.59% suggests that SVM had more difficulty accurately identifying all forested regions. SVM tends to be less flexible when class boundaries are not well-defined, and forest areas, especially those transitioning into other types of vegetation, can present challenges in terms of spectral and radar data separability.

SVM performed moderately well for shrubland, achieving a PA of 73.68% and UA of 73.68%. These values reflect the algorithm's struggle to classify shrubland accurately, likely due to the spectral and radar data overlap with forest and agricultural areas. The lower classification performance for shrubland could also be a result of SVM's rigid boundary definitions, which may not be ideal for identifying intermediate land cover types like shrubland.

For bareland, SVM achieved a PA of 74.19%, reflecting moderate success in classifying non-vegetated or sparsely vegetated areas. However, the UA of 76.67% suggests that SVM correctly identified many bareland regions, but there were still some misclassifications into adjacent land cover types, possibly due to subtle transitions between bareland and nearby land uses like agriculture or built-up areas.

The greatest performance divergence between RF and SVM is how they differ in their approach to classification. RF is an ensemble learning algorithm that aggregates the vote of numerous decision trees such that it can better deal with high, nonlinear relationships between features. This gives RF a competitive edge in handling the varied and complex radar and spectral signatures of land cover classes, particularly in transitional or mixed pixels like agriculture and shrubland.

On the other hand, SVM is based on finding the optimally separating hyperplane between classes in feature space. SVM is effective where classes are separable and distinct but fails when there are overlapping land cover classes or transitional classes. This is confirmed by SVM having reduced accuracy when processing more complicated categories such as agriculture and shrubland, where spectral and radar data overlap occurs more often. In the case of Overall Accuracy (OA), RF is superior to SVM since RF is capable of handling non-linear relationships and is more flexible in classifying more complex land cover types.

Table 4-9: Combined Satellite data classification accuracy assessment result using SVM

	Built-up	Agriculture	Forest	Shrubland	Bareland	Total	PA
Built-up	30	2	1	2	0	35	85.71
Agriculture	3	28	2	5	1	39	71.79
Forest	0	1	24	1	4	30	80.00
Shrubland	1	4	3	28	2	38	73.68
Bareland	0	2	4	2	23	31	74.19
Total	34	37	34	38	30	173	
UA	88.24	75.68	70.59	73.68	76.67		
OA	0.77						
Kappa	0.71						

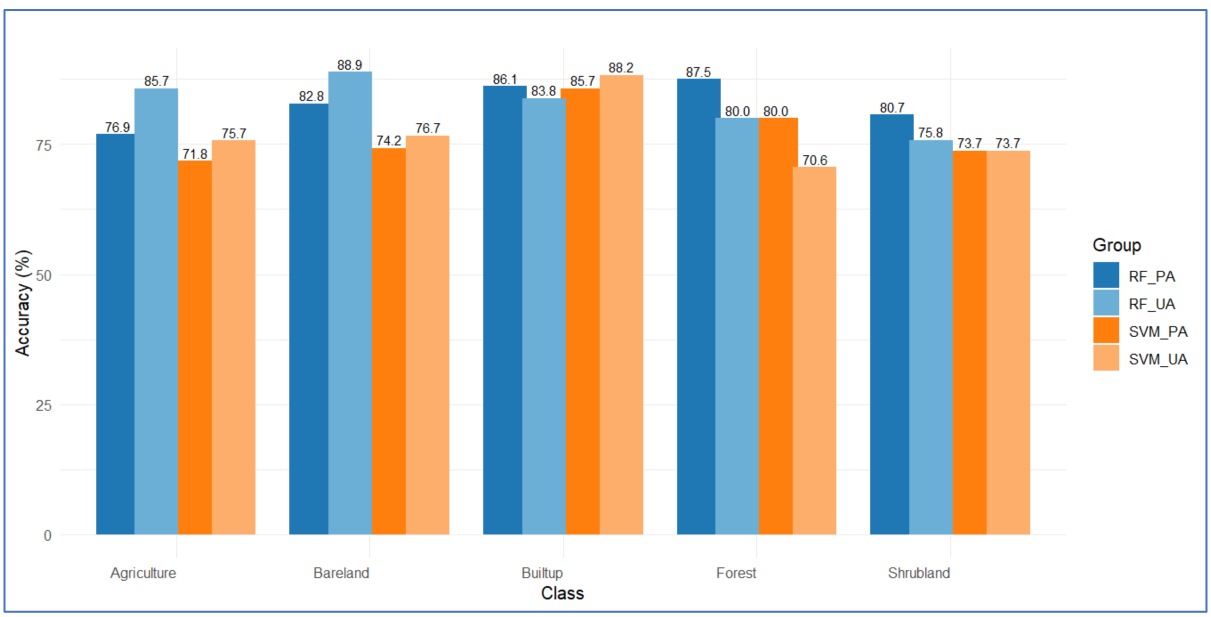

Figure 4-12: Accuracy assessments comparison between SVM and RF classifications for combined satellite data

4.4.5. Analysis of Land Use and Land Cover Change (2015–2025) in Adama City

The analysis of land use and land cover (LULC) change for Adama City between 2015 and 2025 reveals significant transformations in the spatial distribution of urban, agricultural, and natural landscapes, reflecting the city's rapid urbanization and land pressure over the decade.

The most striking change is observed in the Built-up category. As shown in Table 4-10, the built-up area expanded dramatically from 1,679.38 hectares (5.36% of the total area) in 2015 to 5,364.57 hectares (17.14%) in 2025. This represents a net increase of 3,685.19 hectares an extraordinary 219.37% growth rate (Table 4-11). This sharp increase illustrates the rapid urban expansion driven by population growth, industrial development, and infrastructure projects in Adama City, which has emerged as a key urban center in Ethiopia's Oromia Region. The conversion of surrounding agricultural and natural lands into residential, commercial, and industrial uses is likely the primary driver of this expansion, reflecting both urban sprawl and densification trends.

In contrast, agricultural land showed a modest decline over the decade, shrinking from 21,742.77 hectares (69.46%) to 21,235.69 hectares (67.84%). The decrease of 507.08 hectares corresponds to a -2.33% rate of change. This relatively small reduction indicates that while urban development is encroaching on farmland, agriculture still remains a dominant land use in the peri-urban and rural zones around Adama, albeit under increasing pressure from expanding urban areas.

The forest cover experienced a significant reduction from 5,201.93 hectares (16.62%) in 2015 to 2,569.65 hectares (8.21%) in 2025 a loss of 2,632.28 hectares, which translates to a -50.61% rate of change. This sharp decline highlights the vulnerability of forest ecosystems to human-induced disturbances, particularly urban encroachment, agricultural expansion, and possible deforestation for fuelwood or construction materials. Such a large reduction signals not only environmental degradation but also the loss of ecosystem services like carbon sequestration, biodiversity support, and soil stabilization.

Similarly, shrubland areas declined from 2,592.54 hectares (8.28%) to 1,743.46 hectares (5.57%), marking a loss of 849.08 hectares or -32.75% over the study period. The conversion of shrubland into either built-up land or cleared for other human activities reflects the growing demand for space within and around the urban periphery. In contrast to the declining trends of forest and shrubland, bareland showed a sharp increase from 87.58 hectares (0.28%) to 390.83 hectares (1.25%) — a 303.25 hectare increase or an impressive 346.18% rate of change. The expansion of bareland could be linked to land clearance for construction, industrial projects, or even resource extraction activities, which tend to leave areas temporarily or permanently devoid of vegetation.

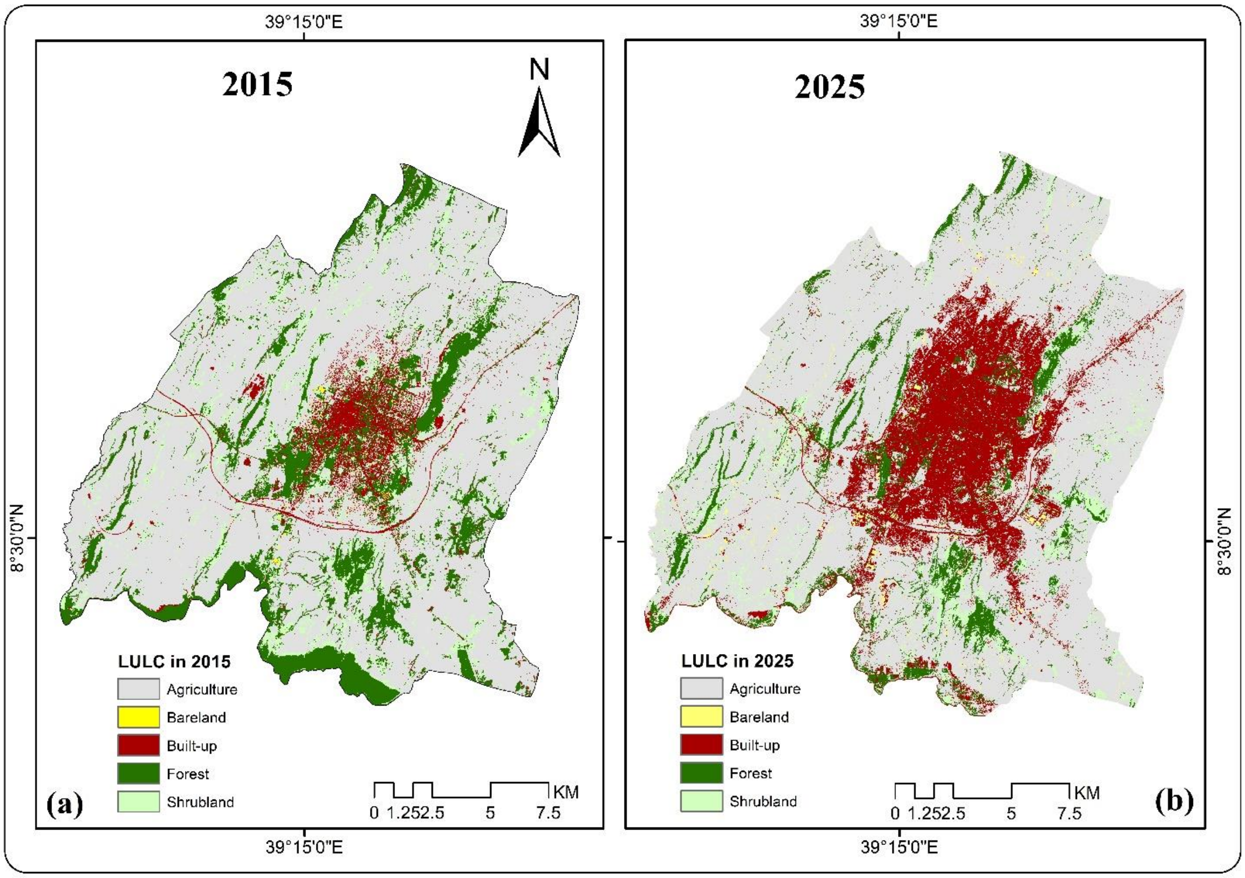

Figure 4-13: Land use land cover change between 2015-2025 in Adama City

Table 4-10: Land use land cover area changes between 2015-2025 in the Adama city

		2015		2025	
SN	Class	Area	Percentage	Area	Percentage
1	Built-up	1679.38	5.36	5364.57	17.14
2	Agriculture	21742.77	69.46	21235.69	67.84
3	Forest	5201.93	16.62	2569.65	8.21
4	Shrubland	2592.54	8.28	1743.46	5.57
5	Bareland	87.58	0.28	390.83	1.25
6	Total	31304.2	100	31304.2	100

The result of the land use and land cover change study in Adama City between 2015 and 2025 is a general trend of urban sprawl typical of most of the fast-growing cities, particularly in sub-Saharan

Africa. With more and more expanding cities naturally due to population growth and as a consequence of rural-urban migration, there is more pressure to provide land for housing, construction of infrastructure, and economic growth. This rising demand typically generates the conversion of land to agriculture, shrubland, and forest to urban built-up land (Seto et al., 2012; United Nations, 2018). The wild expansion of Adama's urban land by more than 219% in the past ten years — is a well-reflected representation of the type of urban growth, prompted by the government's industrialization policy and socio-economic reforms like infrastructural development in the form of road construction and railway lines connecting Adama to Addis Ababa and other urban areas (Woldegerima et al., 2017; Gebre and Gebremedhin, 2019).

The rapid loss of forest and shrubland cover is a problem that represents the environmental price paid for rushed urbanization. Forest cover, are irreplaceable ecological assets that serve as carbon sinks, microclimatic regulators, and home to biodiversity, are generally among the first to be destroyed as the city expands outward (Lambin & Meyfroidt, 2011). For Adama, forest cover reduced by over 50% in the course of a decade, presumably due to both direct deforestations to obtain wood and charcoal, common in urbanizing towns of Ethiopia, as well as for the purpose of developing land to be utilized for either housing or commercial developments (Tsegaye et al., 2010). Shrublands, acting as ecological buffers around forest patches and transitional zones between wild and cultivated landscapes, also saw a substantial reduction, supporting the notion that peri-urban areas are increasingly being claimed for human settlement and expansion (Mengistu & Salami, 2007). The increase in bareland further supports this observation, as barelands often indicate areas under active construction, recently cleared land, or sites awaiting development, which is a common feature of urbanizing landscapes (Herold et al., 2003).

The modest but notable decline in agricultural land (-2.33%) highlights another typical urbanization impact: the encroachment of cities into arable, productive lands. As Adama's urban footprint grows, fertile agricultural zones on the city's periphery are increasingly at risk of being converted into non-agricultural uses, including residential estates, commercial complexes, and road networks. This phenomenon has been observed across many African cities, where urban expansion often competes directly with food production spaces, posing long-term risks to urban food security and local livelihoods (Angel et al., 2011; Bren d'Amour et al., 2017).

Table 4-11: Rate of change between 2015-2025

SN	Class	Area 2015 (ha)	Area 2025 (ha)	Change (ha)	Rate of Change (%)
1	Built-up	1679.38	5364.57	3685.19	219.37%
2	Agriculture	21742.77	21235.69	-507.08	-2.33%
3	Forest	5201.93	2569.65	-2632.28	-50.61%
4	Shrubland	2592.54	1743.46	-849.08	-32.75%
5	Bareland	87.58	390.83	303.25	346.18%

4.5.Change detection between 2015-2025

The change detection matrix well illustrates the dynamic land use and land cover (LULC) class changes in Adama City between 2015 and 2025, with the extent of urbanization and remapping. The most striking finding of the matrix is the extensive conversion of agricultural and forest land into built-up land; a characteristic feature of urban sprawl.

Starting with agriculture, out of the total 21,854.07 hectares as agricultural land in 2015, approximately 2,527.72 hectares (11.56%) were converted into built-up area by 2025. This significant land conversion shows how rapidly urban development has encroached on previously cultivated zones, which aligns with global trends where the growth of cities predominantly consumes peri-urban agricultural land (Seto et al., 2012). This type of conversion is typical in Ethiopia's urbanizing centers, where government infrastructure initiatives, population growth, and private real estate developments contribute to the loss of farmland (Gebre & Gebremedhin, 2019).

The forest class also experienced substantial change. Out of 5,191.07 hectares of forest area recorded in 2015, only 2,040.30 hectares remained unchanged by 2025. A total of 1,056.06 hectares transitioned to built-up land, representing a direct loss of forest due to urban expansion, and a further 1,727.33 hectares were converted to agriculture, which reflects both formal and informal processes of land clearance. Forest degradation in urban surroundings is often driven by logging, charcoal production, and land clearance for settlement, and the data here confirms that Adama is not an exception to this pattern (Lambin & Meyfroidt, 2011).

Shrubland areas also saw heavy conversion. Out of 2,513.67 hectares originally classified as shrubland, only 297.08 hectares remained stable. A significant portion was absorbed by agricultural land (1,655.77 hectares) and built-up zones (333.48 hectares). This reveals the transitional nature of shrublands in urban expansion dynamics: they are often the first to be cleared or degraded when a city expands outward, serving as an intermediate stage between wilderness and development (Mengistu & Salami, 2007).

In contrast, bareland, although relatively small in absolute value, also shifted more radically. Although 79.45 hectares comprised bareland in 2015, 21.75 hectares of bareland and 55.96 hectares of built-up area were present in 2025. This is a reasonable trend, as barelands — often because they have been disturbed earlier or empty lots — are usually employed as staging grounds for development and urbanization (Herold et al., 2003).

Finally, the overall class experienced spectacular growth, from 1,657.35 hectares in 2015 to 5,370.66 hectares in 2025, a dramatic reflection of Adama's urban land growth. To a significant degree, it was driven by the conversion of arable land, forest, and scrubland, reflecting the competitive pressure of urbanization on natural and semi-natural land covers.

In short, this matrix captures not just Adama's land use transformation in physical land terms but also the socio-economic drivers of the transformations: real estate pressure, migration, industrial policy, and population growth. It needs sustainable urbanization and harmonized land use planning interventions to counter growth with environmental sustainability and food security (Angel et al., 2011; UN-Habitat, 2020).

Table 4-12: Change detection matrix between 2015-2025

		2025					
		Agriculture	Bareland	Built-up	Forest	Shrubland	Grand Total
2015	Agriculture	17820.25	286.16	2527.72	240.35	979.59	21854.07
	Bareland	1.57	21.75	55.96	0.12	0.04	79.45
	Built-up	183.22	22.42	1397.45	32.19	22.07	1657.35
	Forest	1727.33	13.84	1056.06	2040.30	353.54	5191.07
	Shrubland	1655.77	17.84	333.48	209.51	297.08	2513.67
	Grand Total	21388.14	362.01	5370.66	2522.47	1652.32	31295.60

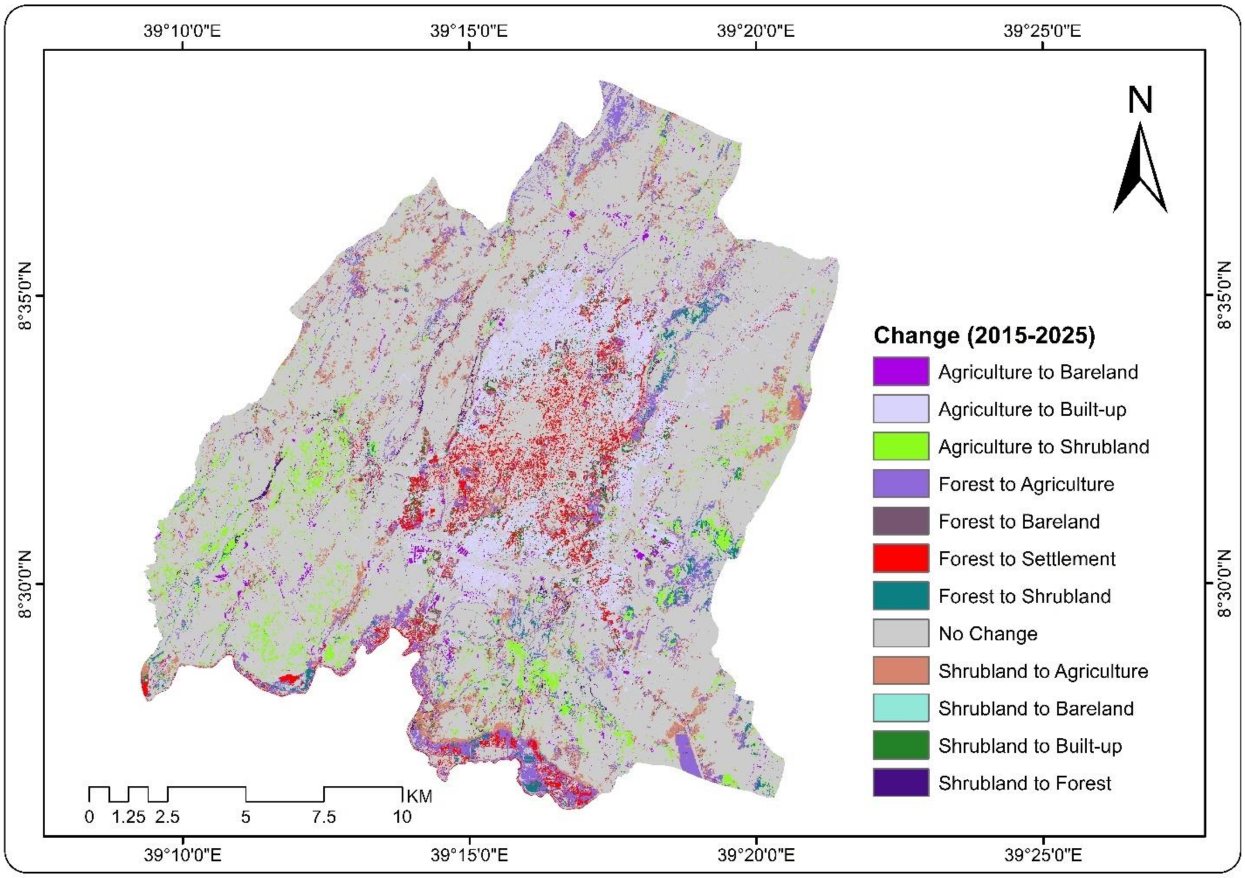

Figure 4-14: Change detection between 2015-2025

4.6.Discussion

This research attempted to independently classify Sentinel-2 MSI and Sentinel-1A SAR satellite images by utilizing the Random Forest (RF) and Support Vector Machine (SVM) algorithms in order to examine their applicability to Adama City urban land cover mapping. The results confirmed Sentinel-2 MSI, which captures multi-spectral reflectance data within the optical range, achieved higher total classification accuracy than Sentinel-1A SAR when classified separately. This finding is in accordance with earlier studies that reported multispectral Sentinel-2 data, owing to the large spectral variability, high performance for discriminating land cover classes, especially types of vegetation, urban areas, and exposed lands (Immitzer, Vuolo, & Atzberger, 2016).

With the application of RF classifier to Sentinel-2 MSI data, it recorded high overall and class-wise accuracies compared to SVM, especially in urban conditions. This is because RF's ensemble technique relies on the use of multiple decision trees, which is less susceptible to overfitting but still provides strong generalization power, especially in areas with high population density in cities where patterns of reflectance are highly mixed and variable (Belgiu & Drăguţ, 2016). RF's non-parametric method provides it with more capacity to handle outliers, noise, and non-linear relationships than most other classifiers, especially when handling high-dimensional remote sensing data.

Nonetheless, when Sentinel-1A SAR data were classified separately with individual classifiers, each of the individual classifiers struggled with the kind of radar backscatter data. Radar systems measure physical and geometric surface characteristics, such that in the majority of situations, they cause overlapping track records of backscatter values for classes such as built-up land, bare land, and shrublands (Joshi et al., 2016). But RF performed better than SVM even on SAR data too, a result repeated previously in literature — that RF's capacity to handle noisy, redundant, and correlated features offers a special edge in classifying SAR images (Pelletier et al., 2016). SVM, while theoretically robust by virtue of its maximum margin hyperplane approach, is susceptible to time-consuming kernel and parameter tuning, which can restrict its performance in very variable urban SAR data unless domain expertise is employed to manually tune the model (Mountrakis, Im, & Ogole, 2011).

Sentinel-2 MSI provides spectral richness within the visible, near-infrared, and shortwave-infrared bands that is highly effective at discriminating between surface materials according to their spectral signatures. Sentinel-1A SAR, however, is cloud-invariant and provides textural and structural data through microwave backscatter that can identify surface roughness, geometry, and moisture content (Zhao et al., 2019). Together, the two complementary data types overcome the long-standing issue of remote sensing — the spectral ambiguity normally encountered in mixed urban environments. Fusion of optical and radar data has been shown to alleviate such ambiguity, improve class separability, and offer better and more reliable classification, especially when urban growth and land cover change are observed (Joshi et al., 2016; Huang et al., 2018).

The fusion approach in this study conforms to findings by Zhang et al. (2018), where they noted that through combining multi-sensor data, landscape interpretation improves as several diverse but complementary sources of information are integrated. In cities like Adama where new development, vegetation, and exposed soil are intermixed within limited spatial sections, such diversity in input is particularly beneficial. The fusion method also helps to counter particular weaknesses of each sensor type. For example, Sentinel-1 SAR backscattering confusion of urban and bareland classes was countered by most cases by the distinct spectral signatures recorded in Sentinel-2 MSI data. Likewise, Sentinel-2's inability to distinguish between urban and shadowed vegetation was clarified by the geometric data contained within SAR datasets. As such, the fusion methodology not only enhanced overall accuracy in classification but also class performance for individual classes, particularly transitional or hybrid classes like shrubland and built-up land. Such a result justifies growing evidence that multi-sensor fusion is an optimal practice for LULC mapping operations with high complexities (Huang et al., 2018; Ban et al., 2020).

The comparative evaluation of RF and SVM classifiers across individual data sets as well as combined data sets has been done in this research with specific focus on their performance for urban land cover mapping. The study showed that RF performed better than SVM in all conditions both when applied to individual satellite data sets and with the combined data set of Sentinel-1 and Sentinel-2. This RF performance enhancement can be attributed to a great extent to its ensemble nature, which makes it more stable, less overfitting-prone, and shows more consistent performance over imbalanced class distributions, which are the norm in urban studies (Belgiu & Drăguţ, 2016). The RF algorithm performs well with regard to both handling high-dimensional data and noise tolerance, two of the most prominent satellite image characteristics, especially when sensor types are diverse. SVM, while theoretically optimal for finding the best class boundaries, is weaker without accurate parameter adjustment and kernel selection, especially when feature distributions overlap (Mountrakis et al., 2011).

This study's finding that RF yielded greater kappa coefficients and overall accuracies in combined datasets is consistent with results of other studies, such as Pelletier et al. (2016), demonstrating RF's stability when applied to large, high-resolution satellite image time series. The ease with which RF can be interpreted with feature importance values also gives it another pragmatic advantage over SVM, especially in real-world urban planning and policy contexts, where model decision understandability is a concern.

If the combined dataset was employed, performance for both was improved, but RF still had an edge. This finding is corroborated by other research: classifier performance is improved when input data describe complementary physical characteristics of the terrain, and RF excels at leveraging this diversity due to its ensemble-based decision strategy (Zhao et al., 2019).

The findings of the current research, derived from land use/land cover (LULC) mapping using Sentinel-1A SAR and Sentinel-2 MSI data combined with machine learning algorithms (Random Forest and Support Vector Machine), are of immense importance to most global policy mechanisms addressing urbanization, land resource management, and sustainable environmental monitoring. Specifically, these findings are consistent with the United Nations Sustainable Development Goals (SDGs), the New Urban Agenda (NUA), the Sendai Framework for Disaster Risk Reduction, and the Global Urban Observatory (GUO) principles of UN-Habitat. The observed rapid urban expansion in Adama City, as detected from change detection analysis, is directly concerned with SDG 11 Sustainable Cities and Communities. This objective fosters inclusive, safe, resilient, and sustainable city. Appropriate LULC classification and change detection are necessary inputs in achieving objectives such as reducing the per capita adverse environmental impact of cities (Goal Target 11.6) and providing public access to green and public spaces (Goal Target 11.7). The transformation of massive tracts of agricultural land, forest, and shrubland into urbanized areas underscores the need to pursue sustainable urban planning that balances development with the protection of the environment (United Nations, 2015). The New Urban Agenda (NUA) that was adopted during the UN Habitat III summit in 2016 encourages the use of geospatial technologies and evidence-based planning to facilitate more enlightened urban governance.

Your research particularly the combined use of Sentinel imagery and machine learning algorithms are an example of the "evidence-based and integrated urban and territorial planning" policy advocated by the NUA (United Nations, 2017). With urban centers like Adama in the Global South expanding unchecked, and underutilized spatial data fusion and advanced classification algorithms allow urban planners to possess decision-making resources that can guide sustainable infrastructure development, optimize land resource use, and prevent encroachment of urban sprawl into ecologically fragile habitats. Urbanization into forest and shrubland lands that were previously vegetated, as your research shows, has a tendency of increasing the city's vulnerability to natural calamities such as floods, soil erosion, and heatwaves. The Sendai Framework encourages the use of spatial data and emerging technologies, including satellite-based Earth Observation, to further risk-informed development and resilient urban planning (UNDRR, 2015).

CHAPTER FIVE

5. CONCLUSION AND RECOMMENDATION

5.1.Conclusion

This study examined the dynamic urbanization of Adama City's landscape through sophisticated remote sensing techniques of fusion of Sentinel-2 MSI optical and Sentinel-1A SAR radar data and application of two most widely used machine learning classifiers, i.e., Random Forest (RF) and Support Vector Machine (SVM). It was found in the research that the two classifiers were both able to acquire meaningful land cover data, but each with strengths based on the nature of input data as well as the complexity levels in the land cover classes. The Sentinel-2 MSI high spectral resolution images were particularly beneficial for identification and mapping of vegetation-related land covers such as agriculture, forest, and shrublands, whose vegetation condition and structure heterogeneity can be best explained by optical reflectance traits. On the other hand, Sentinel-1A SAR images — being more resistant to atmospheric condition and cloud effects — offered distinct advantages in discrimination of urban and exposed ground areas, especially in urban landscapes where information on surface structure and texture would be more dominant over spectral variation. Following the integration of the two data sets, the fusion resulted in much superior classification accuracy, supporting the argument that combining radar and optical data enhances reliability and robustness of land cover mapping. Fused output data allowed RF and SVM algorithms to harness each sensor's strengths, to better discriminate all land use classes. Random Forest still offered the best overall performance, however, through its capacity to maintain over vast data amounts, non-linear interactions, and high-dimensional feature space without overfitting. SVM performed well too, especially under hard boundary conditions as well as under the same class spectra, further cementing its robustness where class boundaries are poorly defined or class distributions overlap. Temporal analysis depicted a clear trend of urban sprawl of Adama, with developed area increased significantly during 2015-2025 at the expense of forests, shrublands, and cropland to some extent. This is typical for urban expansion in the world for the majority of fastest-growing cities, particularly in sub-Saharan Africa, where rural-to-urban migration, industrialization, and advancement in infrastructure drive massive landscape transformation. These alterations not only redefine the map but also emphasize the call for innovative urban planning for the future on a sustainable platform, which has to be founded upon correct and timely information regarding land cover.

5.2.Recommendations

Based on the findings of this study, which examined land use and land cover dynamics in Adama City using Sentinel-1A SAR and Sentinel-2 MSI data classified by Random Forest (RF) and Support Vector Machine (SVM), the following recommendations are proposed:

- Adopt Multi-Sensor Data Integration for Urban Land Monitoring: The integration of Sentinel-1 SAR and Sentinel-2 MSI data significantly improves classification accuracy and should be utilized by municipal authorities and urban planners for more accurate land use monitoring, supporting evidence-based decisions.
- Implement Land Use Policies that Balance Urban Expansion and Ecosystem Preservation: Given the rapid urban expansion at the expense of agricultural land and forests, it is essential to develop land use policies that protect natural resources while accommodating urban growth, following international frameworks like the UN Sustainable Development Goals.
- Promote the Use of Machine Learning Algorithms for Sustainable Land Management: Machine learning algorithms, particularly Random Forest, should be employed by local and national agencies for accurate and consistent land cover classification to support effective land management and sustainable development planning.

5.3.Implications for future research

Future research should focus on enhancing machine learning algorithms like Random Forest and Support Vector Machines, optimizing them for complex urban landscapes and considering the potential of deep learning and ensemble methods for better classification accuracy. Long-term monitoring using time-series satellite data could provide valuable insights into dynamic land cover changes, particularly in rapidly urbanizing areas, and could help assess the long-term impacts of urban expansion. Additionally, advancing data fusion techniques, integrating multispectral, hyperspectral, and radar data, can further improve the robustness of land cover classification models. It would also be beneficial to explore how climate change and environmental factors affect land use dynamics, integrating climate models with remote sensing data for more accurate predictions. Finally, applying these methodologies to other urban centers across diverse geographical contexts would help assess the global applicability of the findings, providing insights for more proactive land use planning worldwide.

References

Abass, K., Afriyie, K., & Gyasi, R. M. (2019). From green to grey: the dynamics of land use/land cover change in urban Ghana. *Landscape Research*, *44*(8), 909–921. https://doi.org/10.1080/01426397.2018.1552251

Alexander, C. (2020). Normalised difference spectral indices and urban land cover as indicators of land surface temperature (LST). *International Journal of Applied Earth Observation and Geoinformation*, *86*, 102013. https://doi.org/10.1016/J.JAG.2019.102013

Amani, M., Ghorbanian, A., Ahmadi, S. A., Kakooei, M., Moghimi, A., Mirmazloumi, S. M., Moghaddam, S. H. A., Mahdavi, S., Ghahremanloo, M., Parsian, S., Wu, Q., & Brisco, B. (2020). Google Earth Engine Cloud Computing Platform for Remote Sensing Big Data Applications: A Comprehensive Review. *IEEE Journal of Selected Topics in Applied Earth Observations and Remote Sensing*, *13*, 5326–5350. https://doi.org/10.1109/JSTARS.2020.3021052

Amiri, A. M., Nadimi, N., Khalifeh, V., & Shams, M. (2021). GIS-based crash hotspot identification: a comparison among mapping clusters and spatial analysis techniques. *International Journal of Injury Control and Safety Promotion*, *28*(3), 325–338. https://doi.org/10.1080/17457300.2021.1925924

Arsanjani, J. J., Helbich, M., Kainz, W., & Boloorani, A. D. (2013). Integration of logistic regression, Markov chain and cellular automata models to simulate urban expansion. *International Journal of Applied Earth Observation and Geoinformation*, *21*(1), 265–275. https://doi.org/10.1016/J.JAG.2011.12.014

Avelar, S., Zah, R., & Tavares-Corrêa, C. (2009). Linking socioeconomic classes and land cover data in Lima, Peru: Assessment through the application of remote sensing and GIS. *International Journal of Applied Earth Observation and Geoinformation*, *11*(1), 27–37. https://doi.org/10.1016/j.jag.2008.05.001

Azzari, G., & Lobell, D. B. (2017). Landsat-based classification in the cloud: An opportunity for a paradigm shift in land cover monitoring. *Remote Sensing of Environment*, *202*, 64–74. https://doi.org/10.1016/J.RSE.2017.05.025

Bajocco, S., De Angelis, A., Perini, L., Ferrara, A., & Salvati, L. (2012). The impact of Land Use/Land Cover Changes on land degradation dynamics: A Mediterranean case study. *Environmental Management*, *49*(5), 980–989. https://doi.org/10.1007/s00267-012-9831-8

Balzter, H., Cole, B., Thiel, C., & Schmullius, C. (2015). Mapping CORINE land cover from Sentinel-1A SAR and SRTM digital elevation model data using random forests. *Remote Sensing*, *7*(11), 14876–14898. https://doi.org/10.3390/rs71114876

Ban, Y., & Jacob, A. (2013). Object-based fusion of multitemporal multiangle ENVISAT ASAR and HJ-1B multispectral data for urban land-cover mapping. *IEEE Transactions on Geoscience and Remote Sensing*, *51*(4), 1998–2006. https://doi.org/10.1109/TGRS.2012.2236560

Bao, Y., Lin, L., Wu, S., Kwal Deng, K. A., & Petropoulos, G. P. (2018). Surface soil moisture retrievals over partially vegetated areas from the synergy of Sentinel-1 and Landsat 8 data using a modified water-cloud model. *International Journal of Applied Earth Observation and Geoinformation*, *72*, 76–85. https://doi.org/10.1016/j.jag.2018.05.026

Becker, W. R., Ló, T. B., Johann, J. A., & Mercante, E. (2021). Statistical features for land use and land cover classification in Google Earth Engine. *Remote Sensing Applications: Society and Environment*, *21*. https://doi.org/10.1016/j.rsase.2020.100459

Belgiu, M., & Drăgu, L. (2016). Random forest in remote sensing: A review of applications and future directions. *ISPRS Journal of Photogrammetry and Remote Sensing*, *114*, 24–31. https://doi.org/10.1016/J.ISPRSJPRS.2016.01.011

Bengston, D. N., Fletcher, J. O., & Nelson, K. C. (2004). Public policies for managing urban growth and protecting open space: policy instruments and lessons learned in the United States. *Landscape and Urban Planning*, *69*(2–3), 271–286. https://doi.org/10.1016/J.LANDURBPLAN.2003.08.007

Bibri, S. E. (2018). The IoT for smart sustainable cities of the future: An analytical framework for sensor-based big data applications for environmental sustainability. *Sustainable Cities and Society*, *38*, 230–253. https://doi.org/10.1016/J.SCS.2017.12.034

Billah, M., Islam, A. K. M. S., Mamoon, W. Bin, & Rahman, M. R. (2023). Random forest classifications for landuse mapping to assess rapid flood damage using Sentinel-1 and Sentinel-2 data. *Remote Sensing Applications: Society and Environment*, *30*, 100947. https://doi.org/10.1016/J.RSASE.2023.100947

Blaschke, T. (2010). Object based image analysis for remote sensing. *ISPRS Journal of Photogrammetry and Remote Sensing*, *65*(1), 2–16. https://doi.org/10.1016/J.ISPRSJPRS.2009.06.004

Blaschke, T., Hay, G. J., Kelly, M., Lang, S., Hofmann, P., Addink, E., Queiroz Feitosa, R., van der Meer, F., van der Werff, H., van Coillie, F., & Tiede, D. (2014). Geographic Object-Based Image Analysis – Towards a new paradigm. *ISPRS Journal of Photogrammetry and Remote Sensing*, *87*, 180–191. https://doi.org/10.1016/J.ISPRSJPRS.2013.09.014

Bowler, D. E., Buyung-Ali, L., Knight, T. M., & Pullin, A. S. (2010). Urban greening to cool towns and cities: A systematic review of the empirical evidence. *Landscape and Urban Planning*, *97*(3), 147–155. https://doi.org/10.1016/J.LANDURBPLAN.2010.05.006

Breiman. (2001). Random forests. *Random Forests*, 5–32. https://doi.org/10.1201/9780429469275-8

Cai, J., Huang, B., & Song, Y. (2017). Using multi-source geospatial big data to identify the structure of polycentric cities. *Remote Sensing of Environment*, *202*, 210–221. https://doi.org/10.1016/J.RSE.2017.06.039

Cao, X., Gao, X., Shen, Z., & Li, R. (2020). Expansion of Urban Impervious Surfaces in Xining City Based on GEE and Landsat Time Series Data. *IEEE Access*, *8*, 147097–147111. https://doi.org/10.1109/ACCESS.2020.3013640

Carter, J. G., Cavan, G., Connelly, A., Guy, S., Handley, J., & Kazmierczak, A. (2015). Climate change and the city: Building capacity for urban adaptation. *Progress in Planning*, *95*, 1–66. https://doi.org/10.1016/j.progress.2013.08.001

Castillo, J. A. A., Apan, A. A., Maraseni, T. N., & Salmo, S. G. (2017). Estimation and mapping of above-ground biomass of mangrove forests and their replacement land uses in the Philippines using Sentinel imagery. *ISPRS Journal of Photogrammetry and Remote Sensing*, *134*, 70–85. https://doi.org/10.1016/j.isprsjprs.2017.10.016

Cerbelaud, A., Roupioz, L., Blanchet, G., Breil, P., & Briottet, X. (2021). A repeatable change detection approach to map extreme storm-related damages caused by intense surface runoff based on optical and SAR remote sensing: Evidence from three case studies in the South of France. *ISPRS Journal of Photogrammetry and Remote Sensing*, *182*, 153–175. https://doi.org/10.1016/J.ISPRSJPRS.2021.10.013

Chakhar, A., Hernández-López, D., Ballesteros, R., & Moreno, M. A. (2021). Improving the accuracy of multiple algorithms for crop classification by integrating sentinel-1 observations with sentinel-2 data. *Remote Sensing*, *13*(2), 1–21. https://doi.org/10.3390/rs13020243

Chen, J., Gao, J., & Chen, W. (2016). Urban land expansion and the transitional mechanisms in Nanjing, China. *Habitat International*, *53*, 274–283. https://doi.org/10.1016/j.habitatint.2015.11.040

Chen, Z., & Zhao, S. (2022). Automatic monitoring of surface water dynamics using Sentinel-1 and Sentinel-2 data with Google Earth Engine. *International Journal of Applied Earth Observation and Geoinformation*, *113*, 103010. https://doi.org/10.1016/J.JAG.2022.103010

Chowdhury, M. S. (2024). Comparison of accuracy and reliability of random forest, support vector machine, artificial neural network and maximum likelihood method in land use/cover classification of urban setting. *Environmental Challenges*, *14*. https://doi.org/10.1016/j.envc.2023.100800

Chowdhury, S., Peddle, D. R., Wulder, M. A., Heckbert, S., Shipman, T. C., & Chao, D. K. (2021). Estimation of land-use/land-cover changes associated with energy footprints and other disturbance agents in the Upper Peace Region of Alberta Canada from 1985 to 2015 using Landsat data. *International Journal of Applied Earth Observation and Geoinformation*, *94*, 102224. https://doi.org/10.1016/J.JAG.2020.102224

Cleve, C., Kelly, M., Kearns, F. R., & Moritz, M. (2008). Classification of the wildland-urban interface: A comparison of pixel- and object-based classifications using high-resolution aerial photography. *Computers, Environment and Urban Systems*, *32*(4), 317–326. https://doi.org/10.1016/j.compenvurbsys.2007.10.001

Colson, D., Petropoulos, G. P., & Ferentinos, K. P. (2018). Exploring the Potential of Sentinels-1 & 2 of the Copernicus Mission in Support of Rapid and Cost-effective Wildfire Assessment. *International Journal of Applied Earth Observation and Geoinformation*, *73*, 262–276. https://doi.org/10.1016/j.jag.2018.06.011

Cortes, C., Vapnik, V., & Saitta, L. (1995). Support-Vector Networks Editor. In *Machine Leaming* (Vol. 20). Kluwer Academic Publishers.

Cutler, A. (2012). Ensemble Machine Learning. In *Ensemble Machine Learning* (2011th ed.). Springer International Publishing. https://doi.org/10.1007/978-1-4419-9326-7

Demers, A. M., Banks, S. N., Pasher, J., Duffe, J., & Laforest, S. (2015). A comparative analysis of object-based and pixel-based classification of RADARSAT-2 C-band and optical satellite data for mapping shoreline types in the canadian arctic. *Canadian Journal of Remote Sensing*, *41*(1), 1–19. https://doi.org/10.1080/07038992.2015.1020361

Deng, C., & Wu, C. (2013). Examining the impacts of urban biophysical compositions on surface urban heat island: A spectral unmixing and thermal mixing approach. *Remote Sensing of Environment*, *131*, 262–274. https://doi.org/10.1016/J.RSE.2012.12.020

Dewan, A. M., & Yamaguchi, Y. (2009a). Land use and land cover change in Greater Dhaka, Bangladesh: Using remote sensing to promote sustainable urbanization. *Applied Geography*, *29*(3), 390–401. https://doi.org/10.1016/j.apgeog.2008.12.005

Dewan, A. M., & Yamaguchi, Y. (2009b). Land use and land cover change in Greater Dhaka, Bangladesh: Using remote sensing to promote sustainable urbanization. *Applied Geography*, *29*(3), 390–401. https://doi.org/10.1016/J.APGEOG.2008.12.005

Diesing, M., Green, S. L., Stephens, D., Lark, R. M., Stewart, H. A., & Dove, D. (2014). Mapping seabed sediments: Comparison of manual, geostatistical, object-based image analysis and machine learning approaches. *Continental Shelf Research*, *84*, 107–119. https://doi.org/10.1016/j.csr.2014.05.004

Drusch, M., Del Bello, U., Carlier, S., Colin, O., Fernandez, V., Gascon, F., Hoersch, B., Isola, C., Laberinti, P., Martimort, P., Meygret, A., Spoto, F., Sy, O., Marchese, F., & Bargellini, P. (2012). Sentinel-2: ESA's Optical High-Resolution Mission for GMES Operational Services. *Remote Sensing of Environment*, *120*, 25–36. https://doi.org/10.1016/J.RSE.2011.11.026

El Garouani, A., Mulla, D. J., El Garouani, S., & Knight, J. (2017). Analysis of urban growth and sprawl from remote sensing data: Case of Fez, Morocco. *International Journal of Sustainable Built Environment*, *6*(1), 160–169. https://doi.org/10.1016/J.IJSBE.2017.02.003

Erinjery, J. J., Singh, M., & Kent, R. (2018). Mapping and assessment of vegetation types in the tropical rainforests of the Western Ghats using multispectral Sentinel-2 and SAR Sentinel-1 satellite imagery. *Remote Sensing of Environment*, *216*, 345–354. https://doi.org/10.1016/j.rse.2018.07.006

Esch, T., Asamer, H., Bachofer, F., Balhar, J., Boettcher, M., Boissier, E., d'Angelo, P., Gevaert, C. M., Hirner, A., Jupova, K., Kurz, F., Kwarteng, A. Y., Mathot, E., Marconcini, M., Marin, A., Metz-Marconcini, A., Pacini, F., Paganini, M., Permana, H., … Zeidler, J. N. (2020). Digital world meets urban planet–new prospects for evidence-based urban studies arising from joint exploitation of big earth data, information technology and shared knowledge. *International Journal of Digital Earth*, *13*(1), 136–157. https://doi.org/10.1080/17538947.2018.1548655

Faehnle, M., Bäcklund, P., Tyrväinen, L., Niemelä, J., & Yli-Pelkonen, V. (2014). How can residents' experiences inform planning of urban green infrastructure? Case Finland. *Landscape and Urban Planning*, *130*(1), 171–183. https://doi.org/10.1016/j.landurbplan.2014.07.012

Fakhri, F., & Gkanatsios, I. (2021). Integration of Sentinel-1 and Sentinel-2 data for change detection: A case study in a war conflict area of Mosul city. *Remote Sensing Applications: Society and Environment*, *22*, 100505. https://doi.org/10.1016/J.RSASE.2021.100505

Fibæk, C. S., Keßler, C., & Arsanjani, J. J. (2021). A multi-sensor approach for characterising human-made structures by estimating area, volume and population based on sentinel data and deep learning. *International Journal of Applied Earth Observation and Geoinformation*, *105*, 102628. https://doi.org/10.1016/J.JAG.2021.102628

Fu, J., Xiao, G., & Wu, C. (2020). Urban green transformation in Northeast China: A comparative study with Jiangsu, Zhejiang and Guangdong provinces. *Journal of Cleaner Production*, *273*, 122551. https://doi.org/10.1016/J.JCLEPRO.2020.122551

Gascon, M., Cirach, M., Martínez, D., Dadvand, P., Valentín, A., Plasència, A., & Nieuwenhuijsen, M. J. (2016). Normalized difference vegetation index (NDVI) as a marker of surrounding greenness in epidemiological studies: The case of Barcelona city. *Urban Forestry & Urban Greening*, *19*, 88–94. https://doi.org/10.1016/J.UFUG.2016.07.001

Ghosh, S., Kumar, D., & Kumari, R. (2022). Cloud-based large-scale data retrieval, mapping, and analysis for land monitoring applications with Google Earth Engine (GEE). *Environmental Challenges*, *9*, 100605. https://doi.org/10.1016/J.ENVC.2022.100605

Goetz, A. F. H. (2009). Three decades of hyperspectral remote sensing of the Earth: A personal view. *Remote Sensing of Environment*, *113*(SUPPL. 1). https://doi.org/10.1016/j.rse.2007.12.014

Goldstein, B. A., Hubbard, A. E., Cutler, A., & Barcellos, L. F. (2010). An application of Random Forests to a genome-wide association dataset: Methodological considerations and new findings. *BMC Genetics*, *11*. https://doi.org/10.1186/1471-2156-11-49

Gomes, V. C. F., Queiroz, G. R., & Ferreira, K. R. (2020). An overview of platforms for big earth observation data management and analysis. In *Remote Sensing* (Vol. 12, Issue 8). MDPI AG. https://doi.org/10.3390/RS12081253

Gómez-Limón, J. A., Arriaza, M., & Guerrero-Baena, M. D. (2020). Building a composite indicator to measure environmental sustainability using alternative weighting methods. *Sustainability (Switzerland)*, *12*(11). https://doi.org/10.3390/su12114398

Gong, P., Wang, J., Yu, L., Zhao, Y., Zhao, Y., Liang, L., Niu, Z., Huang, X., Fu, H., Liu, S., Li, C., Li, X., Fu, W., Liu, C., Xu, Y., Wang, X., Cheng, Q., Hu, L., Yao, W., … Chen, J. (2013). Finer resolution observation and monitoring of global land cover: First mapping results with Landsat TM and ETM+ data. *International Journal of Remote Sensing*, *34*(7), 2607–2654. https://doi.org/10.1080/01431161.2012.748992

Gorelick, N., Hancher, M., Dixon, M., Ilyushchenko, S., Thau, D., & Moore, R. (2017). Google Earth Engine: Planetary-scale geospatial analysis for everyone. *Remote Sensing of Environment*, *202*, 18–27. https://doi.org/10.1016/j.rse.2017.06.031

Grafius, D. R., Corstanje, R., Warren, P. H., Evans, K. L., Hancock, S., & Harris, J. A. (2016). The impact of land use/land cover scale on modelling urban ecosystem services. *Landscape Ecology*, *31*(7), 1509–1522. https://doi.org/10.1007/s10980-015-0337-7

Grêt-Regamey, A., Altwegg, J., Sirén, E. A., van Strien, M. J., & Weibel, B. (2017). Integrating ecosystem services into spatial planning—A spatial decision support tool. *Landscape and Urban Planning*, *165*, 206–219. https://doi.org/10.1016/j.landurbplan.2016.05.003

Gunawardena, K. R., Wells, M. J., & Kershaw, T. (2017). Utilising green and bluespace to mitigate urban heat island intensity. *Science of the Total Environment*, *584–585*, 1040–1055. https://doi.org/10.1016/j.scitotenv.2017.01.158

Haas, J., & Ban, Y. (2017). Sentinel-1A SAR and sentinel-2A MSI data fusion for urban ecosystem service mapping. *Remote Sensing Applications: Society and Environment*, *8*, 41–53. https://doi.org/10.1016/J.RSASE.2017.07.006

Hafner, S., Ban, Y., & Nascetti, A. (2022). Unsupervised domain adaptation for global urban extraction using Sentinel-1 SAR and Sentinel-2 MSI data. *Remote Sensing of Environment*, *280*, 113192. https://doi.org/10.1016/J.RSE.2022.113192

Hansen, M. C., & Loveland, T. R. (2012). A review of large area monitoring of land cover change using Landsat data. In *Remote Sensing of Environment* (Vol. 122, pp. 66–74). https://doi.org/10.1016/j.rse.2011.08.024

Hassan, M. M. (2017a). Monitoring land use/land cover change, urban growth dynamics and landscape pattern analysis in five fastest urbanized cities in Bangladesh. *Remote Sensing Applications: Society and Environment*, *7*, 69–83. https://doi.org/10.1016/j.rsase.2017.07.001

Hassan, M. M. (2017b). Monitoring land use/land cover change, urban growth dynamics and landscape pattern analysis in five fastest urbanized cities in Bangladesh. *Remote Sensing Applications: Society and Environment*, *7*, 69–83. https://doi.org/10.1016/J.RSASE.2017.07.001

Heiden, U., Heldens, W., Roessner, S., Segl, K., Esch, T., & Mueller, A. (2012). Urban structure type characterization using hyperspectral remote sensing and height information. *Landscape and Urban Planning*, *105*(4), 361–375. https://doi.org/10.1016/J.LANDURBPLAN.2012.01.001

Herold, M., Goldstein, N. C., & Clarke, K. C. (2003a). The spatiotemporal form of urban growth: Measurement, analysis and modeling. *Remote Sensing of Environment*, *86*(3), 286–302. https://doi.org/10.1016/S0034-4257(03)00075-0

Herold, M., Goldstein, N. C., & Clarke, K. C. (2003b). The spatiotemporal form of urban growth: Measurement, analysis and modeling. *Remote Sensing of Environment*, *86*(3), 286–302. https://doi.org/10.1016/S0034-4257(03)00075-0

Herold, M., Roberts, D. A., Gardner, M. E., & Dennison, P. E. (2004). Spectrometry for urban area remote sensing—Development and analysis of a spectral library from 350 to 2400 nm. *Remote Sensing of Environment*, *91*(3–4), 304–319. https://doi.org/10.1016/J.RSE.2004.02.013

Herold, M., Scepan, J., & Clarke, K. C. (2002). The use of remote sensing and landscape metrics to describe structures and changes in urban land uses. *Environment and Planning A*, *34*(8), 1443–1458. https://doi.org/10.1068/a3496

Hu, B., Xu, Y., Huang, X., Cheng, Q., Ding, Q., Bai, L., & Li, Y. (2021). Improving urban land cover classification with combined use of sentinel-2 and sentinel-1 imagery. *ISPRS International Journal of Geo-Information*, *10*(8). https://doi.org/10.3390/ijgi10080533

Hu, B., Xu, Y., Wan, B., Wu, X., & Yi, G. (2018). Hydrothermally altered mineral mapping using synthetic application of Sentinel-2A MSI, ASTER and Hyperion data in the Duolong area, Tibetan Plateau, China. *Ore Geology Reviews*, *101*, 384–397. https://doi.org/10.1016/j.oregeorev.2018.07.017

Hu, Y., Zhang, Q., Zhang, Y., & Yan, H. (2018). A deep convolution neural network method for land cover mapping: A case study of Qinhuangdao, China. *Remote Sensing*, *10*(12). https://doi.org/10.3390/rs10122053

Huang, C. W., McDonald, R. I., & Seto, K. C. (2018). The importance of land governance for biodiversity conservation in an era of global urban expansion. *Landscape and Urban Planning*, *173*, 44–50. https://doi.org/10.1016/j.landurbplan.2018.01.011

Huang, H., Roy, D. P., Boschetti, L., Zhang, H. K., Yan, L., Kumar, S. S., Gomez-Dans, J., & Li, J. (2016). Separability analysis of Sentinel-2A Multi-Spectral Instrument (MSI) data for burned area discrimination. *Remote Sensing*, *8*(10). https://doi.org/10.3390/rs8100873

Hunt, M. L., Blackburn, G. A., Carrasco, L., Redhead, J. W., & Rowland, C. S. (2019). High resolution wheat yield mapping using Sentinel-2. *Remote Sensing of Environment*, *233*, 111410. https://doi.org/10.1016/J.RSE.2019.111410

Ienco, D., Interdonato, R., Gaetano, R., & Ho Tong Minh, D. (2019). Combining Sentinel-1 and Sentinel-2 Satellite Image Time Series for land cover mapping via a multi-source deep learning architecture. *ISPRS Journal of Photogrammetry and Remote Sensing*, *158*, 11–22. https://doi.org/10.1016/J.ISPRSJPRS.2019.09.016

Ines, A. V. M., Das, N. N., Hansen, J. W., & Njoku, E. G. (2013). Assimilation of remotely sensed soil moisture and vegetation with a crop simulation model for maize yield prediction. *Remote Sensing of Environment*, *138*, 149–164. https://doi.org/10.1016/j.rse.2013.07.018

Izakovičová, Z., Mederly, P., & Petrovič, F. (2017). Long-term land use changes driven by urbanisation and their environmental effects (example of Trnava City, Slovakia). *Sustainability (Switzerland)*, *9*(9). https://doi.org/10.3390/su9091553

Jiang, H., & Eastman, J. R. (2000). Application of fuzzy measures in multi-criteria evaluation in GIS. *International Journal of Geographical Information Science*, *14*(2), 173–184. https://doi.org/10.1080/136588100240903

Johnson, B. A. (2013). High-resolution urban land-cover classification using a competitive multi-scale object-based approach. *Remote Sensing Letters*, *4*(2), 131–140. https://doi.org/10.1080/2150704X.2012.705440

Kabisch, N., Selsam, P., Kirsten, T., Lausch, A., & Bumberger, J. (2019). A multi-sensor and multi-temporal remote sensing approach to detect land cover change dynamics in heterogeneous urban landscapes. *Ecological Indicators*, *99*, 273–282. https://doi.org/10.1016/J.ECOLIND.2018.12.033

Kamel Boulos, M. N., Resch, B., Crowley, D. N., Breslin, J. G., Sohn, G., Burtner, R., Pike, W. A., Jezierski, E., & Chuang, K.-Y. S. (2011). *Crowdsourcing, citizen sensing and sensor web technologies for public and environmental health surveillance and crisis management: trends, OGC standards and application examples*. http://www.ij-healthgeographics.com/content/10/1/67

Khan, S., Ayaz, M., Ghazi, S. R., Khan, I. U., & Khan, N. (2017). Impact of Parents' Occupation on Students Self-Concept at Secondary Level. *International Journal of Academic Research in Business and Social Sciences*, *7*(1), 46. https://doi.org/10.6007/IJARBSS/v7-i1/2615

Lau, B. P. L., Marakkalage, S. H., Zhou, Y., Hassan, N. U., Yuen, C., Zhang, M., & Tan, U. X. (2019). A survey of data fusion in smart city applications. *Information Fusion*, *52*, 357–374. https://doi.org/10.1016/J.INFFUS.2019.05.004

Laurin, G. V., Liesenberg, V., Chen, Q., Guerriero, L., Del Frate, F., Bartolini, A., Coomes, D., Wilebore, B., Lindsell, J., & Valentini, R. (2013). Optical and SAR sensor synergies for forest and land cover mapping in a tropical site in West Africa. *International Journal of Applied Earth Observation and Geoinformation*, *21*(1), 7–16. https://doi.org/10.1016/J.JAG.2012.08.002

Lehmler, S., Förster, M., & Frick, A. (2023). Modelling Green Volume Using Sentinel-1, -2, PALSAR-2 Satellite Data and Machine Learning for Urban and Semi-Urban Areas in Germany. *Environmental Management*, *72*(3), 657–670. https://doi.org/10.1007/s00267-023-01826-9

Li, F., Yigitcanlar, T., Nepal, M., Nguyen, K., & Dur, F. (2023). Machine learning and remote sensing integration for leveraging urban sustainability: A review and framework. *Sustainable Cities and Society*, *96*, 104653. https://doi.org/10.1016/J.SCS.2023.104653

Li, M., Guo, J., Xu, C., Lei, Y., & Li, J. (2018). Identifying climatic factors and circulation indices related to apple yield variation in main production areas of China. *Global Ecology and Conservation*, *16*. https://doi.org/10.1016/j.gecco.2018.e00478

Li, X., & Shao, G. (2014). Object-based land-cover mapping with high resolution aerial photography at a county scale in midwestern USA. *Remote Sensing*, *6*(11), 11372–11390. https://doi.org/10.3390/rs61111372

Li, Y., Zhang, F., Li, R., Yu, H., Chen, Y., & Yu, H. (2024). Comprehensive Ecological Functional Zoning: A Data-Driven Approach for Sustainable Land Use and Environmental Management—A Case Study in Shenzhen, China. *Land*, *13*(9), 1413. https://doi.org/10.3390/land13091413

Liang, D., Guo, H., Zhang, L., Cheng, Y., Zhu, Q., & Liu, X. (2021). Time-series snowmelt detection over the Antarctic using Sentinel-1 SAR images on Google Earth Engine. *Remote Sensing of Environment*, *256*, 112318. https://doi.org/10.1016/J.RSE.2021.112318

Liu, J., Liu, W., Allechy, F. B., Zheng, Z., Liu, R., & Kouadio, K. L. (2024). Machine learning-based techniques for land subsidence simulation in an urban area. *Journal of Environmental Management*, *352*, 120078. https://doi.org/10.1016/J.JENVMAN.2024.120078

Liu, T., & Yang, X. (2015). Monitoring land changes in an urban area using satellite imagery, GIS and landscape metrics. *Applied Geography*, *56*, 42–54. https://doi.org/10.1016/J.APGEOG.2014.10.002

Liu, Y., Chen, X., Peng, H., & Wang, Z. (2017). Multi-focus image fusion with a deep convolutional neural network. *Information Fusion*, *36*, 191–207. https://doi.org/10.1016/J.INFFUS.2016.12.001

Liu, Y., Jing, W., Wang, Q., & Xia, X. (2020). Generating high-resolution daily soil moisture by using spatial downscaling techniques: a comparison of six machine learning algorithms. *Advances in Water Resources*, *141*, 103601. https://doi.org/10.1016/j.advwatres.2020.103601

Lu, D., & Weng, Q. (2006). Use of impervious surface in urban land-use classification. *Remote Sensing of Environment*, *102*(1–2), 146–160. https://doi.org/10.1016/J.RSE.2006.02.010

Lv, Q., Dou, Y., Niu, X., Xu, J., Xu, J., & Xia, F. (2015). Urban land use and land cover classification using remotely sensed sar data through deep belief networks. *Journal of Sensors*, *2015*. https://doi.org/10.1155/2015/538063

Ma, L., Li, M., Ma, X., Cheng, L., Du, P., & Liu, Y. (2017). A review of supervised object-based land-cover image classification. *ISPRS Journal of Photogrammetry and Remote Sensing*, *130*, 277–293. https://doi.org/10.1016/J.ISPRSJPRS.2017.06.001

Ma, Y., Wu, H., Wang, L., Huang, B., Ranjan, R., Zomaya, A., & Jie, W. (2015). Remote sensing big data computing: Challenges and opportunities. *Future Generation Computer Systems*, *51*, 47–60. https://doi.org/10.1016/j.future.2014.10.029

Maclachlan, A., Roberts, G., Biggs, E., & Boruff, B. (2017). Subpixel land-cover classification for improved urban area estimates using landsat. *International Journal of Remote Sensing*, *38*(20), 5763–5792. https://doi.org/10.1080/01431161.2017.1346403

Mahdianpari, M., Salehi, B., Mohammadimanesh, F., Homayouni, S., & Gill, E. (2019). The first wetland inventory map of newfoundland at a spatial resolution of 10 m using sentinel-1 and sentinel-2 data on the Google Earth Engine cloud computing platform. *Remote Sensing*, *11*(1). https://doi.org/10.3390/rs11010043

Majidi Nezhad, M., Nastasi, B., Groppi, D., Lamagna, M., Piras, G., & Astiaso Garcia, D. (2021). Green Energy Sources Assessment Using Sentinel-1 Satellite Remote Sensing. In *Frontiers in Energy Research* (Vol. 9). Frontiers Media S.A. https://doi.org/10.3389/fenrg.2021.649305

Maulik, U., & Chakraborty, D. (2017). Remote Sensing Image Classification: A survey of support-vector-machine-based advanced techniques. In *IEEE Geoscience and Remote Sensing Magazine* (Vol. 5, Issue 1, pp. 33–52). Institute of Electrical and Electronics Engineers Inc. https://doi.org/10.1109/MGRS.2016.2641240

Mboga, N., Grippa, T., Georganos, S., Vanhuysse, S., Smets, B., Dewitte, O., Wolff, E., & Lennert, M. (2020). Fully convolutional networks for land cover classification from historical panchromatic aerial photographs. *ISPRS Journal of Photogrammetry and Remote Sensing*, *167*, 385–395. https://doi.org/10.1016/j.isprsjprs.2020.07.005

McPhearson, T., Hamstead, Z. A., & Kremer, P. (2014). Urban ecosystem services for resilience planning and management in New York City. *Ambio*, *43*(4), 502–515. https://doi.org/10.1007/s13280-014-0509-8

Mertes, C. M., Schneider, A., Sulla-Menashe, D., Tatem, A. J., & Tan, B. (2015). Detecting change in urban areas at continental scales with MODIS data. *Remote Sensing of Environment*, *158*, 331–347. https://doi.org/10.1016/J.RSE.2014.09.023

Morabito, M., Crisci, A., Guerri, G., Messeri, A., Congedo, L., & Munafò, M. (2021). Surface urban heat islands in Italian metropolitan cities: Tree cover and impervious surface influences. *Science of the Total Environment*, *751*. https://doi.org/10.1016/j.scitotenv.2020.142334

Muñoz-Marí, J., Bovolo, F., Gómez-Chova, L., Bruzzone, L., & Camp-Valls, G. (2010). Semisupervised one-class support vector machines for classification of remote sensing data. *IEEE Transactions on Geoscience and Remote Sensing*, *48*(8), 3188–3197. https://doi.org/10.1109/TGRS.2010.2045764

Myint, S. W., Gober, P., Brazel, A., Grossman-Clarke, S., & Weng, Q. (2011). Per-pixel vs. object-based classification of urban land cover extraction using high spatial resolution imagery. *Remote Sensing of Environment*, *115*(5), 1145–1161. https://doi.org/10.1016/J.RSE.2010.12.017

Myneni, R. B., Hoffman, S., Knyazikhin, Y., Privette, J. L., Glassy, J., Tian, Y., Wang, Y., Song, X., Zhang, Y., Smith, G. R., Lotsch, A., Friedl, M., Morisette, J. T., Votava, P., Nemani, R. R., & Running, S. W. (2002). Global products of vegetation leaf area and fraction absorbed PAR from year one of MODIS data. *Remote Sensing of Environment*, *83*(1–2), 214–231. https://doi.org/10.1016/S0034-4257(02)00074-3

Olofsson, A., & Ohman, S. (2006). *Environment and Behavior GENERAL BELIEFS AND ENVIRONMENTAL CONCERN Transatlantic Comparisons*.

Ottinger, M., & Kuenzer, C. (2020). Spaceborne L-Band synthetic Aperture Radar Data for geoscientific analyses in coastal land applications: A review. In *Remote Sensing* (Vol. 12, Issue 14). MDPI AG. https://doi.org/10.3390/rs12142228

Ouma, Y. O. (2016). Advancements in medium and high resolution Earth observation for land-surface imaging: Evolutions, future trends and contributions to sustainable development. *Advances in Space Research*, *57*(1), 110–126. https://doi.org/10.1016/j.asr.2015.10.038

Pahlevan, N., Sarkar, S., Franz, B. A., Balasubramanian, S. V., & He, J. (2017). Sentinel-2 MultiSpectral Instrument (MSI) data processing for aquatic science applications: Demonstrations and validations. *Remote Sensing of Environment*, *201*, 47–56. https://doi.org/10.1016/J.RSE.2017.08.033

Pal, M., Maxwell, A. E., & Warner, T. A. (2013a). Kernel-based extreme learning machine for remote-sensing image classification. *Remote Sensing Letters*, *4*(9), 853–862. https://doi.org/10.1080/2150704X.2013.805279

Pal, M., Maxwell, A. E., & Warner, T. A. (2013b). Kernel-based extreme learning machine for remote-sensing image classification. *Remote Sensing Letters*, *4*(9), 853–862. https://doi.org/10.1080/2150704X.2013.805279

Pandey, P. C., Koutsias, N., Petropoulos, G. P., Srivastava, P. K., & Ben Dor, E. (2021). Land use/land cover in view of earth observation: data sources, input dimensions, and classifiers—a review of the state of the art. In *Geocarto International* (Vol. 36, Issue 9, pp. 957–988). Taylor and Francis Ltd. https://doi.org/10.1080/10106049.2019.1629647

Parece, T. E., & Campbell, J. B. (2015). Land use/land cover monitoring and geospatial technologies: An overview. In *Handbook of Environmental Chemistry* (Vol. 33, pp. 1–32). Springer Verlag. https://doi.org/10.1007/978-3-319-14212-8_1

Peng, M., Liu, Y., Khan, A., Ahmed, B., Sarker, S. K., Ghadi, Y. Y., Bhatti, U. A., Al-Razgan, M., & Ali, Y. A. (2024). Crop monitoring using remote sensing land use and land change data: Comparative analysis of deep learning methods using pre-trained CNN models. *Big Data Research*, *36*, 100448. https://doi.org/10.1016/J.BDR.2024.100448

Plank, S. (2014). Rapid damage assessment by means of multi-temporal SAR-A comprehensive review and outlook to Sentinel-1. In *Remote Sensing* (Vol. 6, Issue 6, pp. 4870–4906). MDPI AG. https://doi.org/10.3390/rs6064870

Pu, J., Zhao, X., Dong, P., Wang, Q., & Yue, Q. (2021). Extracting information on rocky desertification from satellite images: A comparative study. *Remote Sensing*, *13*(13). https://doi.org/10.3390/rs13132497

Richards, J. A. (2009). *The Imaging Radar System* (pp. 1–10). https://doi.org/10.1007/978-3-642-02020-9_1

Roteta, E., Bastarrika, A., Padilla, M., Storm, T., & Chuvieco, E. (2019). Development of a Sentinel-2 burned area algorithm: Generation of a small fire database for sub-Saharan Africa. *Remote Sensing of Environment*, *222*, 1–17. https://doi.org/10.1016/j.rse.2018.12.011

Ruzza, G., Guerriero, L., Grelle, G., Guadagno, F. M., & Revellino, P. (2019). Multi-method tracking of monsoon floods using Sentinel-1 imagery. In *Water (Switzerland)* (Vol. 11, Issue 11). MDPI AG. https://doi.org/10.3390/w11112289

Saadat, H., Adamowski, J., Bonnell, R., Sharifi, F., Namdar, M., & Ale-Ebrahim, S. (2011). Land use and land cover classification over a large area in Iran based on single date analysis of satellite imagery. *ISPRS Journal of Photogrammetry and Remote Sensing*, *66*(5), 608–619. https://doi.org/10.1016/J.ISPRSJPRS.2011.04.001

Sahin, E. K. (2020). Assessing the predictive capability of ensemble tree methods for landslide susceptibility mapping using XGBoost, gradient boosting machine, and random forest. *SN Applied Sciences*, *2*(7). https://doi.org/10.1007/s42452-020-3060-1

Sano, E. E., Ferreira, L. G., Asner, G. P., & Steinke, E. T. (2007). Spatial and temporal probabilities of obtaining cloud-free Landsat images over the Brazilian tropical savanna. *International Journal of Remote Sensing*, *28*(12), 2739–2752. https://doi.org/10.1080/01431160600981517

Schadt, E. E., Linderman, M. D., Sorenson, J., Lee, L., & Nolan, G. P. (2010). Computational solutions to large-scale data management and analysis. In *Nature Reviews Genetics* (Vol. 11, Issue 9, pp. 647–657). https://doi.org/10.1038/nrg2857

Schneider, A. (2012a). Monitoring land cover change in urban and peri-urban areas using dense time stacks of Landsat satellite data and a data mining approach. *Remote Sensing of Environment*, *124*, 689–704. https://doi.org/10.1016/j.rse.2012.06.006

Schneider, A. (2012b). Monitoring land cover change in urban and peri-urban areas using dense time stacks of Landsat satellite data and a data mining approach. *Remote Sensing of Environment*, *124*, 689–704. https://doi.org/10.1016/J.RSE.2012.06.006

Schulz, K., & Siriwardane, R. (2016). The risk frontier: Perceiving social transformations in rural and peri-urban West Africa through a territorial lens. In *Adaptation to Climate Change and Variability in Rural West Africa* (pp. 171–190). Springer International Publishing. https://doi.org/10.1007/978-3-319-31499-0_10

Schumann, G. J. P., Neal, J. C., Mason, D. C., & Bates, P. D. (2011). The accuracy of sequential aerial photography and SAR data for observing urban flood dynamics, a case study of the UK summer 2007 floods. *Remote Sensing of Environment*, *115*(10), 2536–2546. https://doi.org/10.1016/J.RSE.2011.04.039

Seto, K. C., Fragkias, M., Güneralp, B., & Reilly, M. K. (2011). A meta-analysis of global urban land expansion. *PLoS ONE*, *6*(8). https://doi.org/10.1371/journal.pone.0023777

Seto, K. C., Güneralp, B., & Hutyra, L. R. (2012). Global forecasts of urban expansion to 2030 and direct impacts on biodiversity and carbon pools. *Proceedings of the National Academy of Sciences of the United States of America*, *109*(40), 16083–16088. https://doi.org/10.1073/pnas.1211658109

Shelestov, A., Lavreniuk, M., Kussul, N., Novikov, A., & Skakun, S. (2017). Exploring Google earth engine platform for big data processing: Classification of multi-temporal satellite imagery for crop mapping. *Frontiers in Earth Science*, *5*, 1–10. https://doi.org/10.3389/feart.2017.00017

Shrestha, S., Sattar, H., Khattak, M. S., Wang, G., & Babur, M. (2020). Evaluation of adaptation options for reducing soil erosion due to climate change in the Swat River Basin of Pakistan. *Ecological Engineering*, *158*. https://doi.org/10.1016/j.ecoleng.2020.106017

Sidhu, N., Pebesma, E., & Câmara, G. (2018). Using Google Earth Engine to detect land cover change: Singapore as a use case. *European Journal of Remote Sensing*, *51*(1), 486–500. https://doi.org/10.1080/22797254.2018.1451782

Singh, K. K., & Frazier, A. E. (2018). A meta-analysis and review of unmanned aircraft system (UAS) imagery for terrestrial applications. *International Journal of Remote Sensing*, *39*(15–16), 5078–5098. https://doi.org/10.1080/01431161.2017.1420941

Sivarajah, U., Kamal, M. M., Irani, Z., & Weerakkody, V. (2017). Critical analysis of Big Data challenges and analytical methods. *Journal of Business Research*, *70*, 263–286. https://doi.org/10.1016/j.jbusres.2016.08.001

Solórzano, J. V., Mas, J. F., Gao, Y., & Gallardo-Cruz, J. A. (2021a). Land use land cover classification with U-net: Advantages of combining sentinel-1 and sentinel-2 imagery. *Remote Sensing*, *13*(18). https://doi.org/10.3390/rs13183600

Solórzano, J. V., Mas, J. F., Gao, Y., & Gallardo-Cruz, J. A. (2021b). Land use land cover classification with U-net: Advantages of combining sentinel-1 and sentinel-2 imagery. *Remote Sensing*, *13*(18). https://doi.org/10.3390/rs13183600

Steinhausen, M. J., Wagner, P. D., Narasimhan, B., & Waske, B. (2018). Combining Sentinel-1 and Sentinel-2 data for improved land use and land cover mapping of monsoon regions. *International Journal of Applied Earth Observation and Geoinformation*, *73*, 595–604. https://doi.org/10.1016/J.JAG.2018.08.011

Talukdar, S., Singha, P., Mahato, S., Shahfahad, Pal, S., Liou, Y. A., & Rahman, A. (2020). Land-use land-cover classification by machine learning classifiers for satellite observations-A review. In *Remote Sensing* (Vol. 12, Issue 7). MDPI AG. https://doi.org/10.3390/rs12071135

Tamiminia, H., Salehi, B., Mahdianpari, M., Quackenbush, L., Adeli, S., & Brisco, B. (2020a). Google Earth Engine for geo-big data applications: A meta-analysis and systematic review. In *ISPRS Journal of Photogrammetry and Remote Sensing* (Vol. 164, pp. 152–170). Elsevier B.V. https://doi.org/10.1016/j.isprsjprs.2020.04.001

Tamiminia, H., Salehi, B., Mahdianpari, M., Quackenbush, L., Adeli, S., & Brisco, B. (2020b). Google Earth Engine for geo-big data applications: A meta-analysis and systematic review. *ISPRS Journal of Photogrammetry and Remote Sensing*, *164*, 152–170. https://doi.org/10.1016/J.ISPRSJPRS.2020.04.001

Tang, J., Liu, D., Shang, C., & Niu, J. (2024). Impacts of land use change on surface infiltration capacity and urban flood risk in a representative karst mountain city over the last two decades. *Journal of Cleaner Production*, *454*, 142196. https://doi.org/10.1016/J.JCLEPRO.2024.142196

Tassi, A., & Vizzari, M. (2020). Object-oriented lulc classification in google earth engine combining snic, glcm, and machine learning algorithms. *Remote Sensing*, *12*(22), 1–17. https://doi.org/10.3390/rs12223776

Torres, R., Snoeij, P., Geudtner, D., Bibby, D., Davidson, M., Attema, E., Potin, P., Rommen, B. Ö., Floury, N., Brown, M., Traver, I. N., Deghaye, P., Duesmann, B., Rosich, B., Miranda, N., Bruno, C., L'Abbate, M., Croci, R., Pietropaolo, A., … Rostan, F. (2012). GMES Sentinel-1 mission. *Remote Sensing of Environment*, *120*, 9–24. https://doi.org/10.1016/J.RSE.2011.05.028

Tsokas, A., Rysz, M., Pardalos, P. M., & Dipple, K. (2022). SAR data applications in earth observation: An overview. *Expert Systems with Applications*, *205*, 117342. https://doi.org/10.1016/J.ESWA.2022.117342

Van de Voorde, T., Jacquet, W., & Canters, F. (2011). Mapping form and function in urban areas: An approach based on urban metrics and continuous impervious surface data. *Landscape and Urban Planning*, *102*(3), 143–155. https://doi.org/10.1016/j.landurbplan.2011.03.017

Vanacker, V., Molina, A., Govers, G., Poesen, J., & Deckers, J. (2007). Spatial variation of suspended sediment concentrations in a tropical Andean river system: The Paute River, southern Ecuador. *Geomorphology*, *87*(1–2), 53–67. https://doi.org/10.1016/j.geomorph.2006.06.042

Verburg, P. H., Neumann, K., & Nol, L. (2011). Challenges in using land use and land cover data for global change studies. In *Global Change Biology* (Vol. 17, Issue 2, pp. 974–989). https://doi.org/10.1111/j.1365-2486.2010.02307.x

Villeneuve, P. J., Ysseldyk, R. L., Root, A., Ambrose, S., Dimuzio, J., Kumar, N., Shehata, M., Xi, M., Seed, E., Li, X., Shooshtari, M., & Rainham, D. (2018). Comparing the normalized difference vegetation index with the google street view measure of vegetation to assess associations between greenness, walkability, recreational physical activity, and health in Ottawa, Canada. *International Journal of Environmental Research and Public Health*, *15*(8). https://doi.org/10.3390/ijerph15081719

Vizzari, M. (2022). PlanetScope, Sentinel-2, and Sentinel-1 Data Integration for Object-Based Land Cover Classification in Google Earth Engine. *Remote Sensing*, *14*(11). https://doi.org/10.3390/rs14112628

Voogt, J. A., & Oke, T. R. (2003). Thermal remote sensing of urban climates. *Remote Sensing of Environment*, *86*(3), 370–384. https://doi.org/10.1016/S0034-4257(03)00079-8

Waleed, M., & Sajjad, M. (2023). On the emergence of geospatial cloud-based platforms for disaster risk management: A global scientometric review of google earth engine applications. *International Journal of Disaster Risk Reduction*, *97*, 104056. https://doi.org/10.1016/J.IJDRR.2023.104056

Walker, W. S., Kellndorfer, J. M., Kirsch, K. M., Stickler, C. M., Nepstad, D. C., Stickler, C. M., & Nepstad, D. C. (2010). Large-Area Classification and Mapping of Forest and Land Cover in the Brazilian Amazon: A Comparative Analysis of ALOS/PALSAR and Landsat Data Sources. *IEEE Journal of Selected Topics in Applied Earth Observations and Remote Sensing*, *3*(4), 594–604. https://doi.org/10.1109/JSTARS.2010.2076398

Wang, D., Wan, B., Qiu, P., Su, Y., Guo, Q., Wang, R., Sun, F., & Wu, X. (2018). Evaluating the performance of Sentinel-2, Landsat 8 and Pléiades-1 in mapping mangrove extent and species. *Remote Sensing*, *10*(9). https://doi.org/10.3390/rs10091468

Wang, L., Diao, C., Xian, G., Yin, D., Lu, Y., Zou, S., & Erickson, T. A. (2020). A summary of the special issue on remote sensing of land change science with Google earth engine. In *Remote Sensing of Environment* (Vol. 248). Elsevier Inc. https://doi.org/10.1016/j.rse.2020.112002

Wang, R., Zhao, X., Qiu, H., Cheng, X., & Liu, X. (2024). Uncovering urban water consumption patterns through time series clustering and entropy analysis. *Water Research*, *262*, 122085. https://doi.org/10.1016/J.WATRES.2024.122085

Wang, Z. N., Yuan, J. S., Pang, B., & Huang, L. (2022). The interpretation and highlights on mitigation of climate change in IPCC AR6 WGIII report. *Climate Change Research*, *18*(5), 531–537. https://doi.org/10.12006/j.issn.1673-1719.2022.123

Weng, Q. (2012a). Remote sensing of impervious surfaces in the urban areas: Requirements, methods, and trends. *Remote Sensing of Environment*, *117*, 34–49. https://doi.org/10.1016/j.rse.2011.02.030

Weng, Q. (2012b). Remote sensing of impervious surfaces in the urban areas: Requirements, methods, and trends. *Remote Sensing of Environment*, *117*, 34–49. https://doi.org/10.1016/j.rse.2011.02.030

Weng, Q. (2012c). Remote sensing of impervious surfaces in the urban areas: Requirements, methods, and trends. *Remote Sensing of Environment*, *117*, 34–49. https://doi.org/10.1016/J.RSE.2011.02.030

Wheater, H., & Evans, E. (2009). Land use, water management and future flood risk. *Land Use Policy*, *26*(SUPPL. 1), S251–S264. https://doi.org/10.1016/J.LANDUSEPOL.2009.08.019

Whiteside, T. G., Boggs, G. S., & Maier, S. W. (2011). Comparing object-based and pixel-based classifications for mapping savannas. *International Journal of Applied Earth Observation and Geoinformation*, *13*(6), 884–893. https://doi.org/10.1016/J.JAG.2011.06.008

Wulder, M. A., Masek, J. G., Cohen, W. B., Loveland, T. R., & Woodcock, C. E. (2012). Opening the archive: How free data has enabled the science and monitoring promise of Landsat. *Remote Sensing of Environment*, *122*, 2–10. https://doi.org/10.1016/j.rse.2012.01.010

Wurm, M., Taubenböck, H., Schardt, M., Esch, T., & Dech, S. (2011). Object-based image information fusion using multisensor earth observation data over urban areas. *International Journal of Image and Data Fusion*, *2*(2), 121–147. https://doi.org/10.1080/19479832.2010.543934

Yan, K., Park, T., Yan, G., Liu, Z., Yang, B., Chen, C., Nemani, R. R., Knyazikhin, Y., & Myneni, R. B. (2016). Evaluation of MODIS LAI/FPAR product collection 6. Part 2: Validation and intercomparison. *Remote Sensing*, *8*(6). https://doi.org/10.3390/rs8060460

Yang, L., Driscol, J., Sarigai, S., Wu, Q., Chen, H., & Lippitt, C. D. (2022). Google Earth Engine and Artificial Intelligence (AI): A Comprehensive Review. In *Remote Sensing* (Vol. 14, Issue 14). MDPI. https://doi.org/10.3390/rs14143253

Yin, J., Dong, J., Hamm, N. A. S., Li, Z., Wang, J., Xing, H., & Fu, P. (2021). Integrating remote sensing and geospatial big data for urban land use mapping: A review. *International Journal of Applied Earth Observation and Geoinformation*, *103*, 102514. https://doi.org/10.1016/J.JAG.2021.102514

Yin, J., Yin, Z., Zhong, H., Xu, S., Hu, X., Wang, J., & Wu, J. (2011). Monitoring urban expansion and land use/land cover changes of Shanghai metropolitan area during the transitional economy (1979-2009) in China. *Environmental Monitoring and Assessment*, *177*(1–4), 609–621. https://doi.org/10.1007/s10661-010-1660-8

Zhang, H., Li, J., Wang, T., Lin, H., Zheng, Z., Li, Y., & Lu, Y. (2018). A manifold learning approach to urban land cover classification with optical and radar data. *Landscape and Urban Planning*, *172*, 11–24. https://doi.org/10.1016/j.landurbplan.2017.12.009

Zhang, X., Chang, L., Wang, M., & Stein, A. (2023). Measuring polycentric urban development with multi-temporal Sentinel-1 SAR imagery: A case study in Shanghai, China. *International Journal of Applied Earth Observation and Geoinformation*, *121*, 103340. https://doi.org/10.1016/J.JAG.2023.103340

Zhou, D.-X., & Jetter, K. (2006). Approximation with polynomial kernels and SVM classifiers. In *Advances in Computational Mathematics* (Vol. 25). Springer.

Teressa Chamada

Plagiarism Report

Checker 3

GIS

Arsi University

Document Details

Submission ID

trn:oid:::1:3256069835

Submission Date

May 21, 2025, 5:07 AM GMT+1

Download Date

May 21, 2025, 5:11 AM GMT+1

File Name

Teresa_Thesis_Final_Version_2025_S.docx

File Size

4.8 MB

96 Pages

27,569 Words

163,934 Characters

13% Overall Similarity

The combined total of all matches, including overlapping sources, for each database.

Filtered from the Report

- Bibliography
- Quoted Text

Match Groups

233 Not Cited or Quoted 9%
Matches with neither in-text citation nor quotation marks

122 Missing Quotations 4%
Matches that are still very similar to source material

0 Missing Citation 0%
Matches that have quotation marks, but no in-text citation

0 Cited and Quoted 0%
Matches with in-text citation present, but no quotation marks

Top Sources

6% Internet sources
12% Publications
0% Submitted works (Student Papers)

Integrity Flags

0 Integrity Flags for Review

No suspicious text manipulations found.

Our system's algorithms look deeply at a document for any inconsistencies that would set it apart from a normal submission. If we notice something strange, we flag it for you to review.

A Flag is not necessarily an indicator of a problem. However, we'd recommend you focus your attention there for further review.